Supplementary Information (SI) for Polymer Chemistry.
This journal is © The Royal Society of Chemistry 2025

Immunostimulatory pH-responsive Nanogels Derived from Poly(oxanorbornene) Precursor Polymers

– Supporting Information –

Johannes Kockelmann,[a] Lutz Nuhn [a]

[a] Chair of Macromolecular Chemistry, Center of Polymers for Life, Department of Chemistry and Pharmacy, Julius-Maximilians-Universität Würzburg, 97074 Würzburg, Germany.

Content

1. General Instrumentation

Nuclear Magnetic Resonance (NMR)

Nuclear magnetic resonance spectra were recorded on a Bruker Avance 300 (300 MHz for ^{1}H and 75 MHz for ^{13}C), or a Bruker Avance III HD 400 (400 MHz for ^{1}H, 101 MHz for ^{13}C and 376 MHz for ^{19}F). Chemical shifts were referenced from the chemical shifts of residual solvent peaks (*Organometallics* 2010, 29, 9, 2176–2179). NMR spectra were processed with TopSpin 4.2.0 and MestReNova 14.2.0.

Size exclusion chromatography (SEC)

SEC analyses were carried out on a SECurity^2 instrument with a SECcurtity^2 isocratic pump, a solvent degasser, an autosampler, a column thermostat, set to 40 °C, a UV- and RI-detector. HFIP containing 3 g/L potassium trifluoroacetate was used as eluent at a flow rate of 0.8 ml/min. The polymers were separated by two columns (PSS PFG pore size: 100 Å bead size: 7 µm, PSS PFG pore size: 1000 Å bead size: 7 µm). Calibration was performed with poly(methyl methacrylate) standards, purchased from PSS, Mainz. Polymer samples were prepared at 1 mg/mL and filtered through PTFE syringe filters (0.2 µm pore size) before measurements.

Ultraviolet-Visible Spectroscopy (UV-Vis)

IMDQ loading was measured using a Cary Series UV-Vis-NIR Spectrophotometer manufactured by Agilent Technologies with heating control. Fluorescence spectroscopy and absorbance read-out of RAW-blue and MTT assays was measured using a Tecan Spark 20M Multimode Microplate-Reader was used.

Flow Cytometry

Flow cytometric analysis was performed on a BD Accuri C6 (BD Biosciences), equipped with two light scattering detectors and the following fluorescence-excitation and -detection channels:

Exitation wavelength	Detection Channel	Optical Filter
488 nm	533 nm	30 nm
	585 nm (“Cy3-Channel”)	40 nm
	670 nm (“FRET-Channel”)	LP
640 nm	670 nm (“Cy5-Channel”)	LP

The obtained data were analyzed with FlowJo_v10.10.0 by BD Biosciences.

Dynamic Light Scatteing by Zetasizer Nano

Dynamic light scattering measurements were performed using a Malvern Z Nano instrument equipped with a He-Ne-Laser (λ= 632.8) using ZetaSizer Software 7.12. Measurements were performed in triplicates at 25°C or 37°C at a detection angle of 173°.

Dynamic Light Scattering by Multi Angle Dynamic Light Scattering

Multi Angle Dynamic Light Scattering (MADLS) measurements were performed with an ALV CGS-3 Multi detection goniometry system (ALV, Langen, Germany), equipped with a He-Ne laser (22 mW at λ= 632.8) and an infrared-laser (70mW at λ= 785 nm) for investigation of dye labeled nanogels. Detection was achieved with eight fiber optic detection units, including eight simultaneously working APD avalanche diodes. The measurements were conducted at scattering angles from 20° to 140° in steps of 5°. The samples were thermostated in a cell with temperature stability of ±0.1°C. The samples were filtered through syringe filters (PVDF-membrane, 0.2 µm) before measuring. The measurements were carried out in appropriately cut NMR-tubes (⌀ = 5mm).

2. Syntheses

7-Oxanorbornene-2-carboxylic acid

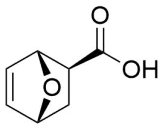

The procedure was adapted from literature[1]. Freshly distilled furan (95 mL, 1.316 mol, 2.7 equiv.) is added to a round bottom flask, charged with freshly distilled acryloyl chloride (43 g, 0.475 mol, 1.0 equiv.). The mixture is then protected from light and stirred at room temperature. After 3 days, the majority of unreacted furan and acryloyl chloride is removed at -17°C under vacuum. The brownish residue (76 g) was then transferred to a dropping funnel and diluted with THF to dissolve a precipitate, which formed at low temperatures. This solution is then slowly added to an ice-cooled suspension of $NaHCO_3$ (70 g) in H_2O (150 mL). The resulting basic (pH=10), brown solution is then extracted with Et_2O (1x 250 mL, 2x 100 mL). The aqueous layer is then neutralized with conc. HCl and concentrated to 170 mL under reduced pressure at 25°C. The solution is then acidified with conc. HCl to pH=2 and extracted with Et_2O (1x 250 mL, 17x 100 mL, 14x, 50 mL). The combined organic layers from the acidic extraction were dried over MgSO4 and the solvent removed under reduced pressure. The crude product was obtained as a brown solid material (50 g, ca.75% purity, *endo*/*exo* 1:1.67).

Purification of the exo-derivative via iodolactonisation:

The procedure was adapted from literature[2]. The crude acid (50 g) was dissolved in aqueous $NaHCO_3$. To this solution, 175 mL of an aqueous mixture of I_2 (0.72 M) and KI (2.32 M) were added slowly at room temperature, while the reaction was monitored by TLC. During the addition, a brown oil separated from the aqueous layer and a solid, inorganic material precipitated. The insoluble solid was removed by filtration and washed with Et_2O. Excess Iodine is then reacted with a 10%-NaS_2O_3-solution. The mixture is then transferred to a separatory funnel and extracted with Et_2O (1x250 mL, 2x150 mL), while maintaining pH=10. After a few days standing open to the air, crystals consisting of the iodolactone, separated from the organic layer. The aqueous layer is then neutralized with conc. HCl and concentrated under reduced pressure. The resulting solution is then further acidified to pH=2 with conc. HCl and then extracted with Et_2O (1 x 250 mL, 10 x 150 mL). After removal of the solvent, a brown oil is obtained, which crystalized quickly and exothermally after addition of a seed crystal. The crude product (32.5 g) melted under 35 °C. Residual acrylic acid and the majority of the colored side products were removed *in vacuo.* This led to a crude, yellow solid (20.84 g). Further recrystallization from petroleum ether/ Et_2O 2:1 yielded the pure *exo*-acid as colorless, needles (14.57 g, 104 mmol, 22%)

mp. = 84.0 – 84.9 °C (petroleum ether/diethyl ether 2.5:1 v/v)

IR (ATR)**:** n [cm^{-1}] = 3013, 1698, 1421, 1314, 1280, 1237, 1168, 1092, 1011, 925, 869, 807, 754, 713, 701, 586.

^{1}H-NMR (400 MHz, $CDCl_3$): δ [ppm] = 9.48 (bs, 1H, O***H***), 6.41 (dd, J = 5.8, 1.6 Hz, 1H, ***H***-6), 6.36 (dd, J = 5.8, 1.7 Hz, 1H, ***H***-5), 5.23 (dd, J = 1.7, 0.8 Hz, 1H, ***H***-1), 5.11 (ddd, J = 4.6, 1.7, 0.8 Hz, 1H, ***H***-4), 2.48 (dd, J = 8.5, 3.9 Hz, 1H, ***H***-2), 2.17 (dt, J = 11.6, 4.2 Hz, 1H, ***H***-3-*exo*), 1.60 (dd, J = 11.6, 8.5 Hz, 1H, ***H***-3-*endo*).

^{13}C-NMR (100 MHz, $CDCl_3$): δ [ppm] = 179.84 (*C*O_2H), 137.30 (***C***-6), 134.65 (***C***-5), 81.07 (***C***-1), 78.17 (***C***-4), 42.77 (***C***-2), 29.13 (***C***-3).

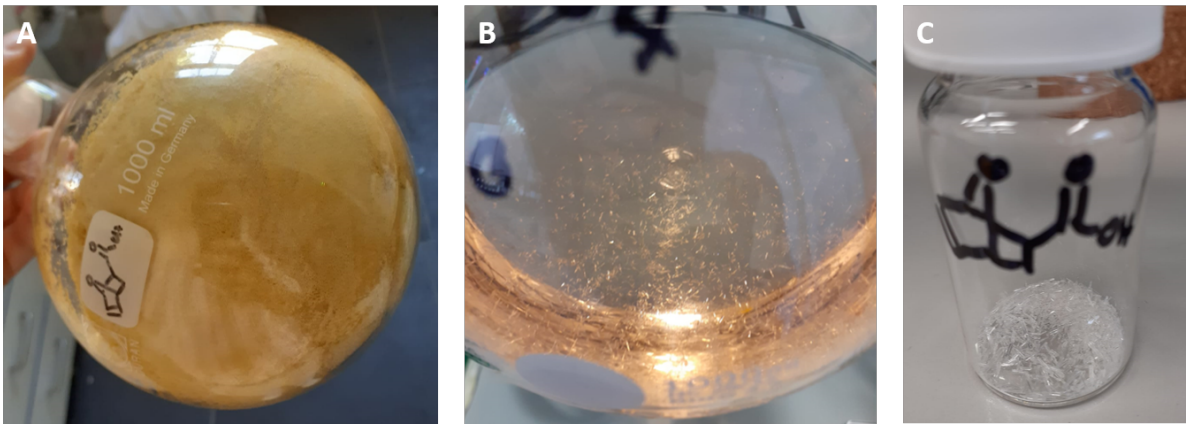

Fig.S 1: **A)** Lyophilized, crude *exo*-acid after iodolactonisation and separation from the endo-iodolacton. **B)** Initiation of crystallization of the pure exo-acid from a mixture of petroleum ether and diethyl ether. **C)** Pure exo-acid crystals.

7-Oxanorbornene-2-carboxylic acid pentafluorophenyl ester

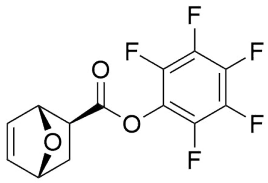

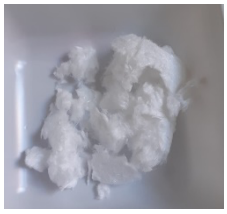

The procedure was adapted from literature[3]. *Exo*-7-oxabicyclo[2.2.1]hept-5-ene-2-carboxylic acid (1.00 g, 7.14 mmol, 1.0 equiv.), pentafluorophenol (1.71 g, 9.28 mmol, 1.3 equiv.) and DMAP (0.07 g, 0.57 mmol, 0.08 equiv.) are dissolved in dry dichloromethane (15 mL) and cooled to 0°C. After stirring for 15 minutes, a suspension of EDC-HCl (1.64 g, 8.57 mmol, 1.2 equiv.) in DCM (15 mL) was added dropwise during 15 min. The reaction mixture was stirred for 15 h and allowed to warm to room temperature. The solvent was then removed under reduced pressure and the residue (5.82 g) was chromatographed (SiO_2, ^{c}Hex/EtOAc 10:1->EtOAc). The product was then crystallized from heptane (-20°C) to provide the pure product as colorless, woolly fibers (1.65 g, 5.40 mmol, 76%).

Mp. = 60.3 – 60.7 °C (heptane)

R_f = 0.47 (^{c}Hex/EtOAc 5:1 v/v; $KmnO_4$, UV)

IR (ATR)**:** n [cm^{-1}] = 1776, 1517, 1351, 1318, 1120, 1031, 1012, 993, 871, 712

^{1}H NMR (400 MHz, $CDCl_3$) δ [ppm] = 6.49 (dd, *J* = 5.8, 1.6 Hz, 1H, *H*-6), 6.43 (dd, *J* = 5.8, 1.7 Hz, 1H, *H*-5), 5.35 (dd, *J* = 1.8, 0.8 Hz, 1H, *H*-1), 5.18 (ddd, *J* = 4.6, 1.7, 0.8 Hz, 1H, *H*-4), 2.79 (dd, *J* = 8.5, 3.9 Hz, 1H, *H*-2), 2.29 (ddd, *J* = 11.8, 4.7, 4.0, 1H, H-3 *exo*), 1.75 (dd, *J* = 11.7, 8.5 Hz, 1H, H-3 *endo*).

^{13}C-NMR (100 MHz, $CDCl_3$): δ [ppm] = 170.15 (*C*O_2Pfp), 141.28 (dm, *J* = 252.1 Hz, *C*-2-Pfp), 139.58 (dm, *J* = 253.1 Hz, *C*-3-Pfp), 138.01 (dm, *J* = 252.1 Hz, C-4-Pfp), 137.72 (*C*-6), 134.57 (*C*-5), 125.3 (m, *C*-1-Pfp), 81.12 (*C*-1), 78.29 (*C*-4), 42.70 (*C*-2), 29.76 (*C*-3)

^{19}F NMR (376 MHz, $CDCl_3$) δ [ppm] = -152.78 – -153.00 (m, 2F), -157.87 (t, *J* = 21.7 Hz, 1F), -161.77 – -162.64 (m, 2F).

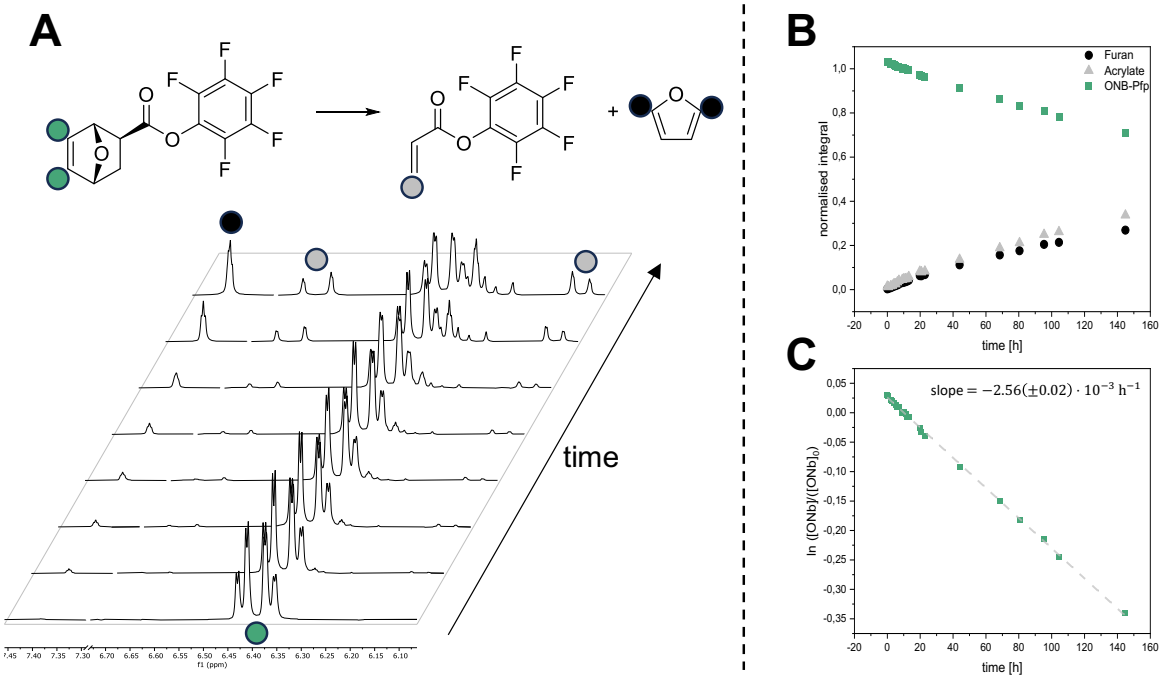

Fig.S 2: **A)** Reaction scheme of the retro-Diels-Alder reaction of ONB-PFP and the corresponding ^{1}H-NMR spectra of the reaction. **B)** Plot of the intensities versus time. **C)** Plot of ln([ONB-PFP]/[ONB-PFP]$_0$) versus time.

NMR peak assignment for the pentafluorophenyl ester monomer

For correctly assigning the peaks in the oxanorbornene carboxylic acid, 2D-spectra were recorded. The vicinity to the electron withdrawing carboxylic acid causes H-1 to be shifted more downfield, compared to H-4. The assignment of H3-exo and H3-endo however is rationalized with the help of the ^{1}H^{13}C-HSQC and ^{1}H^{1}H-COSY spectra. Clearly, the protons attached to carbon C3 can be assigned apart from ^{1}H-chemical shift, as C3 is the only carbon with two hydrogens, as provided by the HSQC. In the COSY spectrum, a clear coupling is observable between proton H4 and one of the protons, attached to C3. Because only one coupling between H4 and the two H3 protons is visible, this must be the coupling to a proton in *exo*-position at C3. If a coupling to the endo-proton would be visible, also a coupling between H1 and the proton in endo-position of C-2 would be visible. Because there is no such signal in the COSY spectrum, it can be concluded that neither H1-H2 nor H4-H3-endo coupling is strong. This is also supported by looking at the 3D-structure of the molecule and the respective dihedral angles of the coupling partners. Here, the angles between H1-C1-C2-H2 and H4-C4-C3-H3endo are close to 90°, whereas the dihedral angle of H4-C4-C3-H3exo is closer to 40° and therefore a higher coupling constant is expected taken the Karplus equation into account.

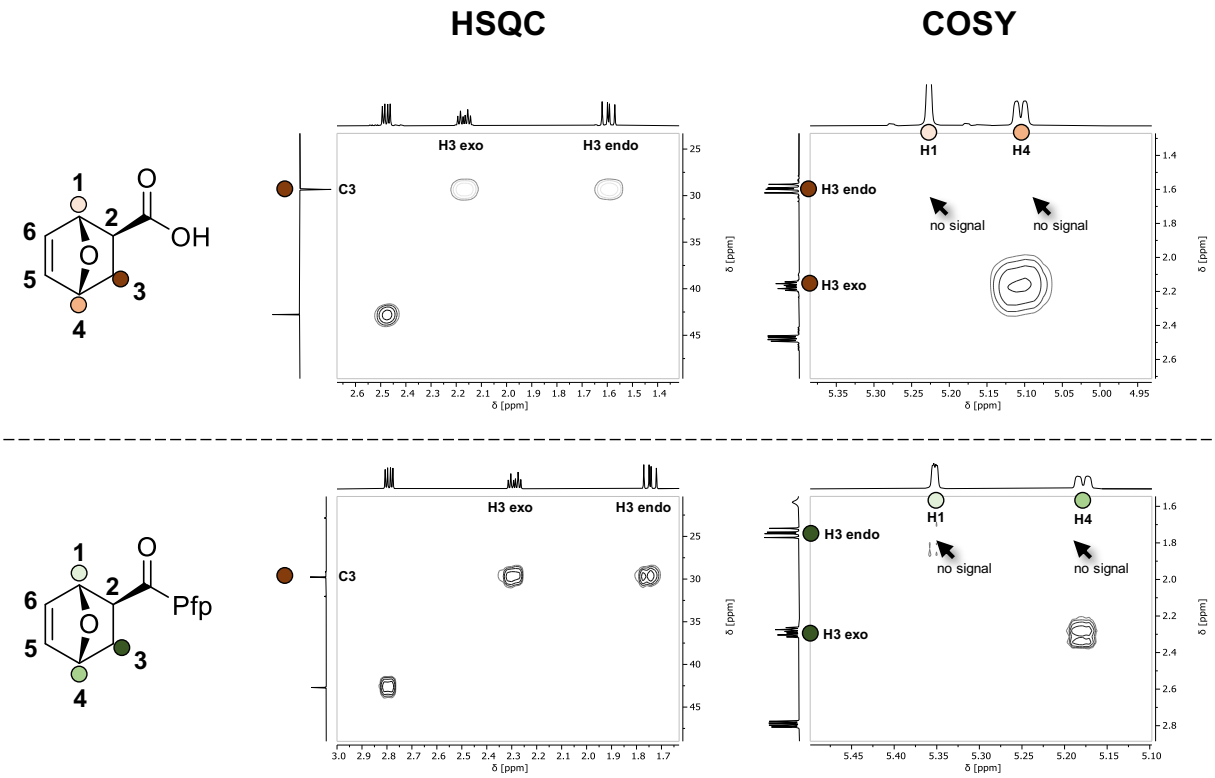

Fig.S 3: Relevant regions of the HSQC- and COSY-spectra for the peak assignment of the protons H3-exo and H3-endo of the exo-oxanorbornene-2-carboxylic acid (top) and the exo-oxanorbornene-2-carboxylic acid pentafluorophenyl ester (bottom). Because there is no signal (COSY) observable between H1 and H3 and only one observable coupling of H4 to H3, the more downfield signal (2.29 ppm for the Pfp-ester and 2.17 ppm for the acid) is assigned to the *exo*-positioned proton, H3-exo.

Methoxytriethylene glycol tosylate

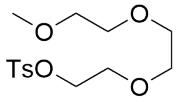

The procedure was adapted from literature[4]. Triethylene glycol (10.0 g 60.9 mmol, 1.0 equiv.) was dissolved in THF (120 mL) and NaOH (3.64 g, 91.0 mmol, 1.5 equiv.) was added as a solution in 20 mL water. The mixture was then cooled to 0°C and a solution of tosyl chloride (12.77 g, 67.0 mmol, 1.1 equiv.) in THF (20 mL) was slowly added via a dropping funnel. After 4 h, the reaction mixture was poured into ice-water and THF was removed under reduced pressure. The residual aqueous phase was then extracted with DCM (4x 100 mL). The combined organic layers were dried over $MgSO_4$ and the solvent removed under reduced pressure to yield the tosylate as a colorless, viscous oil (18.7 g, 58.7 mmol, 96%).

R_f = 0.51 (^{c}Hex/EtOAc 1:2 v/v; $KmnO_4$, UV)

^{1}H NMR (300 MHz, $CDCl_3$) δ [ppm] = 7.78 (d, J = 8.3 Hz, 2H, Ts), 7.33 (d, J = 8.1 Hz, 2H, Ts), 4.15 (t, J = 4.8 Hz, 2H, TsOC***H***$_2$CH$_2$), 3.67 (t, J = 5.0 Hz, 2H, TsOCH$_2$C***H***$_2$), 3.62 – 3.56 (m, 6H, OC***H***$_2$C*H*$_2$OC***H***$_2$CH$_2$OCH$_3$), 3.54 – 3.49 (m, 2H, C***H***$_2$OCH$_3$), 3.36 (s, 2H, OC***H***$_3$), 2.43 (s, 3H, Ts).

^{13}C-NMR (101 MHz, $CDCl_3$): δ [ppm] = 144.91 (*C*1 Ts), 133.06 (***C***4 Ts), 129.92 (***C***3 Ts), 128.08 (***C***2 Ts), 71.99 (***C***H$_2$OCH$_3$), 70.83, 70.65, 70.63, 69.34 (TsO***C***H$_2$), 68.76 (TsOCH$_2$***C***H$_2$), 59.14 (O***C***H$_3$), 21.75 (Ts-***C***H$_3$).

Methoxytriethylene glycol azide

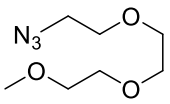

Triethylene glycol tosylate (5.0 g, 15.7 mmol, 1.0 equiv.) is dissolved in DMF (10 mL) and NaN_3 (3.06 g, 47.1 mmol, 3.0 equiv.) is added. The mixture is then heated to 60°C. After 24 hours, the mixture is diluted with water (50 mL) and the product is extracted with EtOAc (3x 100 mL). The combined organic layer is washed with 10% LiCl-solution (5 mL) and dried over $MgSO_4$. The crude product (4.99 g) is then chromatographed on SiO_2 (^{c}Hex/EtOAc 1:2) to yield the product as a colorless oil (2.86 g, 16.96 mmol, 95%)

R_f = 0.63 (^{c}Hex/EtOAc 1:2 v/v; $KmnO_4$, PPh_3/Ninhydrin)

^{1}H NMR (400 MHz, $CDCl_3$) δ [ppm] = 3.69 – 3.60 (m, 8H, C***H***$_2$OC***H***$_2$C***H***$_2$OC***H***$_2$), 3.57 – 3.49 (m, 2H, C***H***$_2$OCH$_3$), 3.42 – 3.32 (m, 5H, C*H*$_3$O, N_3C***H***$_2$CH$_2$).

^{13}C NMR (101 MHz, $CDCl_3$) δ [ppm] = 71.98 (CH_3O***C***H$_2$), 70.75 (O***C***H$_2$), 70.72 (O***C***H$_2$), 70.67 (O***C***H$_2$), 70.10 (O***C***H$_2$), 59.09 (***C***H$_3$O) , 50.73 (CH$_2$***C***H$_2$N$_3$).

Methoxytriethylene glycol amine

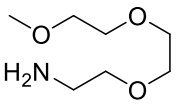

The procedure was adapted from literature[5]. Methoxy-triethylene glycol azide (1.5 g, 7.93 mmol, 1.0 equiv.) was dissolved in 20 mL THF. To this solution, PPh_3 (2.3 g, 8.75 mmol, 1.1 equiv.) was added and the mixture was stirred for 5 minutes at room temperature. Then, H_2O (1 mL) was added, and the reaction mixture was stirred overnight. Then, the solvent was removed by rotary evaporation and the crude, yellow product (1.3 g) was Kugelrohr-destilled to yield the methoxy-triethyleneglycol amine as a colorless oil (1.13 g, 6.92 mmol, 88%).

R_f = 0.44 ($CHCl_3$/MeOH/TEA 10:1:0.1 v/v; Ninhydrin)

^{1}H NMR (400 MHz, $CDCl_3$) δ [ppm] = 3.63 – 3.54 (m, 6H, OC***H***$_2$C***H***$_2$OC***H***$_2$), 3.53 – 3.48 (m, 2H, C***H***$_2$OCH$_3$), 3.45 (t, *J* = 5.3 Hz, 2H, H$_2$NCH$_2$C***H***$_2$), 3.33 (s, 3H, OC***H***$_3$), 2.79 (t, *J* = 5.3 Hz, 2H, H$_2$NC***H***$_2$CH$_2$), 1.35 (m, 2H, N***H***$_2$).

^{13}C NMR (101 MHz, $CDCl_3$) δ [ppm] = 73.98 (H$_2$NCH$_2$***C***H$_2$O), 72.33 (***C***H$_2$OCH$_3$), 70.91 (O***C***H$_2$***C***H$_2$O***C***H$_2$), 70.81 (O***C***H$_2$***C***H$_2$O***C***H$_2$), 70.68 (O***C***H$_2$***C***H$_2$O***C***H$_2$), 59.01(O***C***H$_3$), 42.29 (H$_2$N***C***H$_2$CH$_2$).

7-Oxanorbornene-2,3-*exo*-dicarboximide

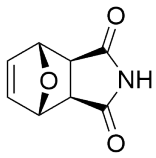

The procedure was adapted from literature[6]. Maleimide (2.0 g, 20.6 mmol, 1.0 equiv.) and freshly distilled furan (15 mL, 207.1 mmol, 10 equiv.) were placed in a closed vessel. The reaction mixture was then heated to 90°C for 12 h. After the mixture has cooled to room temperature, excess furan was removed under vacuum and the solid residue was dissolved in hot ethyl acetate. Minor insoluble precipitates were removed via hot filtration. The ethyl acetate solution was then slowly cooled to yield the product as colorless rhombic crystals (2.15 g, 13.2 mmol, 63%).

m.p. = 159°C (EtOAc, decomposition)

^{1}H NMR (400 MHz, DMSO-d6) δ [ppm] = 11.13 (s, 1H, N*H*), 6.53 (s, 2H, ***H***C=C***H***), 5.11 (s, 2H, OC***H***-bridgehead), 2.85 (s, 2H, αC***H***).

^{13}C NMR (101 MHz, DMSO-d6) δ [ppm] = 177.89 (Carbonyl), 136.50 (***C***=***C***), 80.35 (***C***-bridgehead), 48.46 (α***C***).

***N*-(triethylene glycol)-7-oxanorborn-5-ene-2,3-dicarboximide**

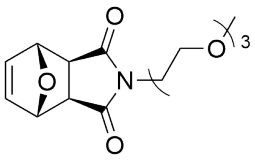

The procedure was adapted from literature[7]. 7-oxanorbornene-2,3-*exo*-dicarboximide (372 mg, 2.25 mmol, 1.1 equiv.) and methoxy-triethyleneglycol tosylate (651 mg, 2.04 mmol, 1.0 equiv.) were dissolved in ACN (10 mL) and Cs_2CO_3 (1.27 g, 3.9 mmol, 1.7 equiv.) was added. The reaction mixture was stirred at room temperature for 5 days. Then, the solvent was removed under reduced pressure and the residue was taken up in DCM (30 mL). The mixture was then washed with water and the organic layer was dried over $MgSO_4$. The solvent was removed under reduced pressure and the crude product was purified via chromatography on SiO_2 (^{c}Hex/EtOAc 2:1→1:2) to give the product as a colorless oil (600 mg, 1.93 mmol, 94%)

$\mathbf{R_f}$ = 0.59 ($CHCl_3$/MeOH 10:1 v/v, $KMnO_4$)

^{1}H NMR (400 MHz, $CDCl_3$) δ [ppm] = 6.49 (t, J = 1.0 Hz, 2H, ***H***C=C***H***), 5.24 (t, J = 1.0 Hz, 2H, OC***H***-bridgehead), 3.67 (td, J = 5.6, 1.2 Hz, 2H, NC***H***$_2$CH$_2$), 3.64 – 3.56 (m, 9H), 3.54 – 3.48 (m, 2H, C***H***$_2$OCH$_3$), 3.35 (s, 3H, OC***H***$_3$), 2.84 (s, 2H αC***H***).

^{13}C NMR (101 MHz, $CDCl_3$) δ [ppm] = 176.22 (carbonyl), 136.66 (***C***=***C***), 80.99 (O***C***-bridgehead), 72.04 (CH$_2$***C***H$_2$OCH$_3$), 70.68 (***C***H$_2$CH$_2$OCH$_3$), 70.64 (***C***H$_2$OCH$_2$CH$_2$OCH$_3$), 70.21 (NCH$_2$CH$_2$O***C***H$_2$), 67.22 (NCH$_2$***C***H$_2$O), 59.12 (O***C***H$_3$), 47.58 (α***C***), 38.31 (N***C***H$_2$CH$_2$).

3. Polymerizations

Catalyst synthesis G3

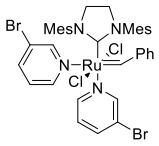

The procedure was adapted from literature[8]. 3-bromopyridine (0.2 mL, 324 mg, 2.05 mmol, 30 equiv.)) was added to [(H_2IMes)(PCy_3)($Cl)_2$ Ru=CHPh] (52 mg, 61.3 µmol, 1.0 equiv.). The reaction was stirred for 5 minutes at room temperature. Pentane (3 mL) was layered on top of the green solution and the green product started to precipitate. The mixture was then stored at 4°C overnight. The precipitate was filtered, washed with pentane (3x 4 mL) and dried under vacuum to yield the product as a brightly green solid (35.8 mg, 40.5 µmol, 66%).

Homopolymers of 7-oxabicyclo [2.2.1] hept-5-ene-exo-2-carboxylic acid pentafluorophenyl ester:

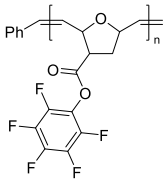

For a typical polymerization, the catalyst was dissolved in degassed, dry DCM to give a stock solution c = 3.3 mM. The monomer (ONB-PFP) was dissolved in degassed DCM to give a stock solution of a concentration of c = 200 mM. The monomer solution was then rapidly injected to the catalyst solution while stirring vigorously at -20°C (Ice/NaCl). After 40 min, the reaction was quenched with an excess of ethyl vinyl ether and the polymers were precipitated from hexane (3x). Finally, the polymers were dissolved in DCM and transferred to a 20 mL vial for storage. The solvent was removed by rotary evaporation to yield the polymers as brittle, brown to colorless films.

^{1}H NMR (400 MHz, CD_2Cl_2) δ [ppm] = 7.63 – 7.10 (m, Ph, 5H), 6.15 – 5.51 (m, olefin, *n*2H), 5.02 – 4.73 (m, allyl-cis, *n*2H), 4.69 – 4.32 (m, allyl-trans, *n*2H), 3.36 – 3.03 (*b*, C*H*COPFP, *n*1H), 2.70 – 2.40 (*b*, CH_2, *n*1H), 2.27 – 1.93 (*b*, CH_2, *n*1H).

Tab.S 1: Summary of the polymerization of **ONB-PFP**.

entry	P_n [a)]	% cis [a)]	M/Ru	M_n [b)] [kg/mol]	$Đ$ [b)]	yield [%]
1	15	49	10	3.1	1.17	25
2	35	54	30	5.6	1.18	quant.
3	63	56	50	9.3	1.23	quant.
4	90	56	70	15.2	1.16	quant.
5	111	55	100	19.9	1.16	quant.

a) determined via ^{1}H-NMR, **b)** determined via GPC (HFIP, PMMA-standard, UVD).

Homopolymers of *N*-(triethylene glycol)-7-oxanorborn-5-ene-2,3-dicarboximide

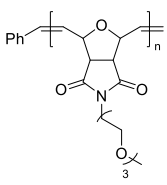

For a typical polymerization, the catalyst was dissolved in degassed, dry DCM to give a stock solution c = 3.3 mM. The monomer (ONB-TEG) was dissolved in degassed DCM to give a stock solution of a concentration of c = 200 mM. The monomer solution was then rapidly injected to the catalyst solution while stirring vigorously at -20°C (Ice/NaCl). After 40 min, the reaction was quenched with an excess of ethyl vinyl ether and the polymers were precipitated from Et_2O(3x). Finally, the polymers were dissolved in DCM and transferred to a 20 mL vial for storage. The solvent was removed by rotary evaporation to yield the polymers as brown to colorless films.

^{1}H NMR (400 MHz, $CDCl_3$) δ [ppm] = 7.41 – 7.14 (*m*, Ph, 5H), 5.97 – 5.80 (*m*, olefin-trans, *n*2H), 5.74 – 5.57 (*m*, olefin-cis, *n*2H), 4.87 – 4.63 (*m*, allyl-cis, *n*2H), 4.37 – 4.19 (*m*, allyl-trans, *n*2H), 3.54 – 3.06 (*m*, C*H*CON, CH_2CH_2O, *n*14H).

Tab.S 2: Summary of the polymerization of **ONB-TEG**.

entry	P_n [a)]	% cis [a)]	M/Ru	M_n [b)] [kg/mol]	$Đ$ [b)]	yield [%]
1	8	47	5	7.6	1.11	27
2	15	50	15	12.7	1.10	53
3	53	53	50	31.9	1.08	52
4	115	54	100	49.9	1.08	66

a) determined via ^{1}H-NMR, **b)** determined via GPC (HFIP, PMMA-standard, UVD).

Block copolymerization

The following describes a typical block copolymerization procedure. **G3** (6.2 mg, 7.0 µmol, 1.0 equiv.) was weighed into a flame dried Schlenck-tube. **ONB-PFP** (106.8 mg, 349 µmol, 50 equiv.) and **ONB-TEG** (44.6 mg, 143 µmol, 20 equiv.) were separately weighed into flame dried, 20-mL sized screw cap glass-vials with septums. The catalyst was then dissolved in dry, degassed DCM (3 mL) and cooled to -20°C with ice-NaCl cooling bath. The first monomer (ONB-PFP) was dissolved in DCM (0.5 mL) and rapidly injected into the catalyst solution under vigorous stirring. After about 40 minutes, TLC showed full conversion of the monomer. Then, the second monomer (ONB-TEG), dissolved in DCM (0.5 mL) was rapidly injected to the stirred solution of the first block. After one hour, TLC showed full conversion of the second monomer. The reaction was quenched by an excess amount of ethyl vinyl ether and stirred for 30 minutes, while the mixture was allowed to warm to room temperature. The block polymer was then precipitated from hexanes (3x) to give the product as a brown, clear film (126 mg, 84%).

M_n (HFIP-GPC, PMMA-standard) = 30.4 kDa

Đ = 1.09

^{1}H NMR (300 MHz, $CDCl_3$) δ [ppm] = 7.55 – 7.05 (m), 6.45 – 5.43 (m), 5.06 – 4.67 (m), 4.61 – 4.24 (m), 3.86 – 2.96 (m), 2.48 (m), 2.02 (m).

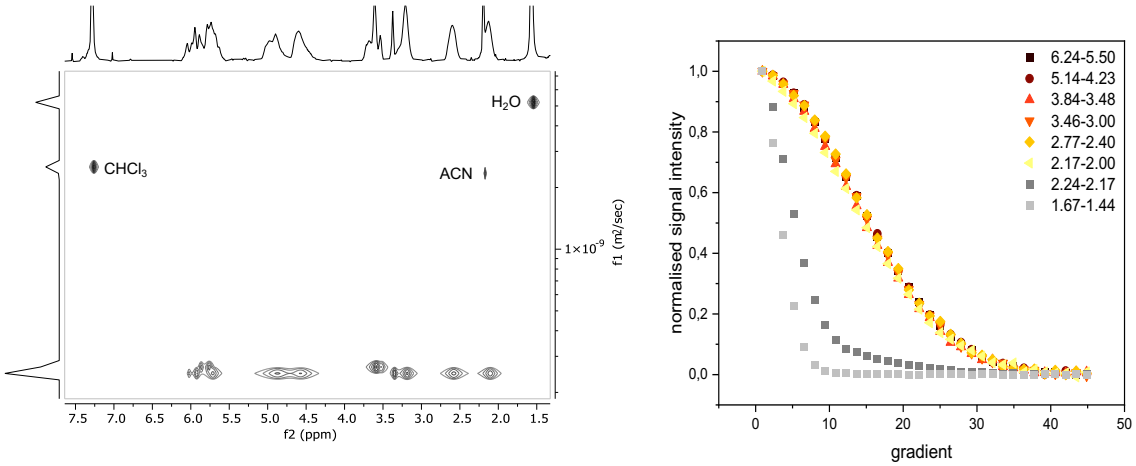

Fig.S 4: DOSY-NMR of the block copolymer Poly(ONB-PFP)-b-Poly(ONB-TEG). Left: 2D-DOSY depiction. Right: Corresponding normalized integral intensity of the different ^{1}H-signals against the gradient strength, applied during DOSY-measurement.

Determination of the number average repeating units for each block in the block copolymers

The repeating units for each block can be determined in reference to the signal from the phenyl-unit at the polymer end group, corresponding to 5 protons:

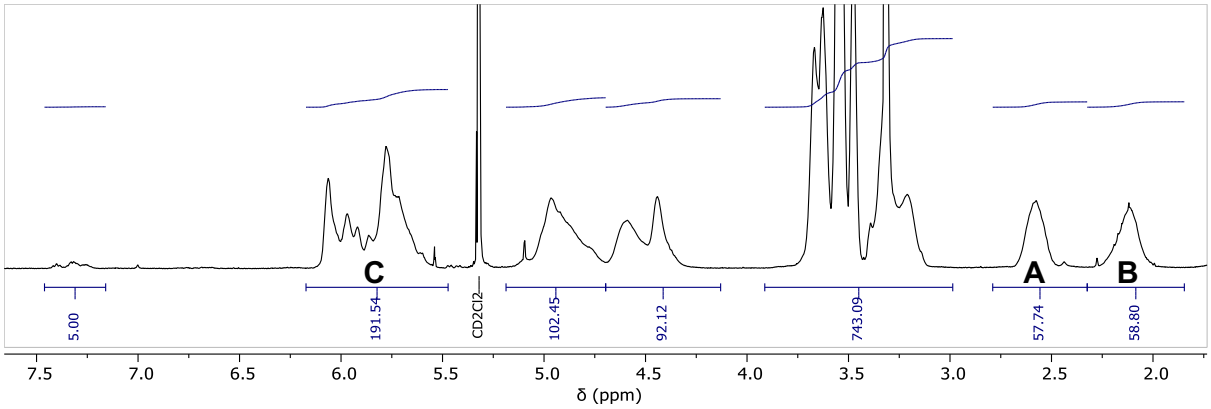

Fig.S 5: Exemplary NMR of BP-5 for the determination of the average degree of polymerization P_n.

The number average degree of polymerization for the PFP-containing block is derived from the two downfield signals A, and B:

$$P_n(\mathrm{ONB-PFP}) = \frac{A+B}{2}$$

The degree of polymerization for the TEG-containing block is then derived from the olefinic signals (C):

$$P_n(\mathrm{ONB-TEG}) = \frac{C - 2 \cdot P_\mathrm{n}(\mathrm{ONB-PFP})}{2}$$

4. Cy3- and Cy5-dye conjugation

In a flame-dried Schlenk-tube, the block polymer P(ONB-Pfp)$_{68}$-*b*-P(ONB-TEG)$_{23}$ (20 mg, 48.6 µmol PFP, 1.0 equiv.) was dissolved in dry dioxane (4 mL) and Cy3-amine (62 µL of a 10 mg/mL stock solution in DMSO, 0.73 µmol, 0.015 equiv.) was added, as well as DIPEA (0.5 µL, 2.9 µmol, 3.9 equiv.). To solubilize the dye in dioxane, anhydrous DMSO (1 mL) was added to the mixture. After reaction at room temperature overnight. The polymer were isolated by precipitation from hexane/EtOH (9:1, v/v). After removal of DMSO via this method, the polymer was redissolved in dioxane and 3 times precipitated from hexane to give the Cy-3-polymers as pink powders (20 mg, quant.).

$\boldsymbol{M}_n$ (HFIP-GPC, PMMA-standard) = 56.8 kDa

Đ = 1.16

The synthesis of Cy5-polymers was performed as described above. Instead of Cy3-amine, Cy5-amine (64µL of a 10 mg/mL stock solution in DMSO, 0.73 µmol, 0.015 equiv.) was used. The Cy5-polymer was received as a blue powder (20 mg, quant.).

$\boldsymbol{M}_n$ (HFIP-GPC, PMMA-standard) = 55.5 kDa

Đ = 1.19

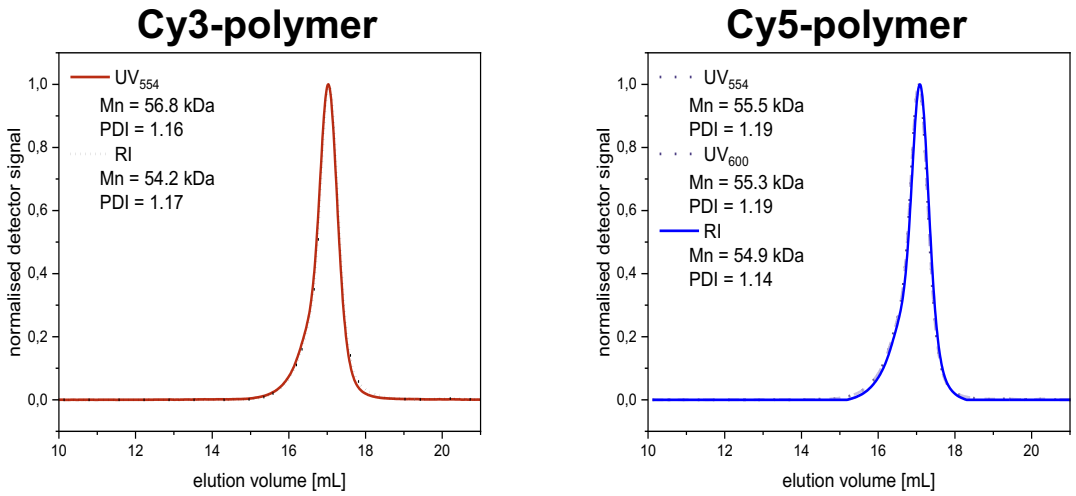

Fig.S 6: GPC-traces (HFIP) of the isolated Cy3-polymer (left) and Cy5-polymer (right).

5. Cloud-Point-Temperature of ONB-TEG and NB-TEG

The determination of the cloud point temperature (T_{cp}) was performed with aqueous solutions (1 mg/mL) of the different polymer samples by turbidity measurements (transmittance at 500 nm, heating rate of 1ºC/ min).

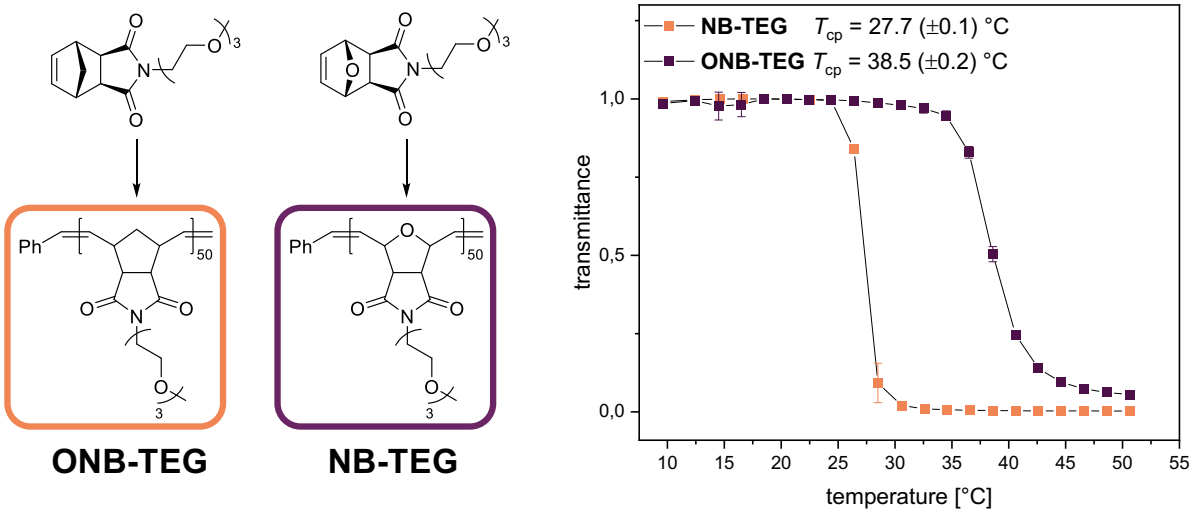

Fig.S 7: Measurements of the cloud point temperature (T_{cp}) via turbidimetry of a 1 mg/mL solution of the respective polymer in water at 500 nm.

6. Nanogel syntheses

6.1 Polymer self-assembly in DMSO

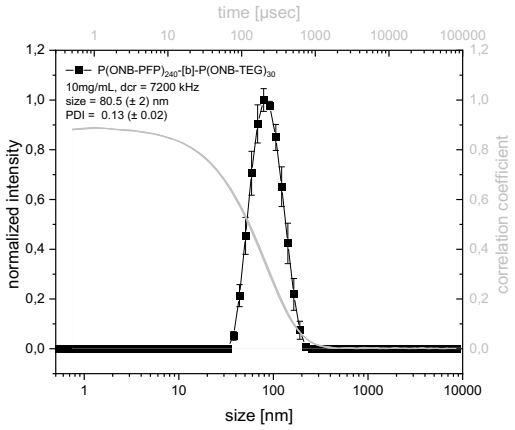

Fig.S 8: DLS results of BP-6 in DMSO. Only high amounts of **ONB-PFP** in the polymer lead to efficient self-assembly in DMSO.

6.2 Polymer self-assembly in water

For the self-assembly, the respective block copolymer was dissolved in acetone to give a concentration of 0.5 mg/mL. To induce self-assembly, water was slowly added, while stirring. The amount of water was adjusted, that the final concentration of the polymer is 1 mg/mL (after evaporation of acetone). Then, the acetone was removed via rotary evaporation (300 mbar→ 90 mbar, over 45 min). During this process, particle formation can be observed visually as the previous clear solution becomes highly opaque.

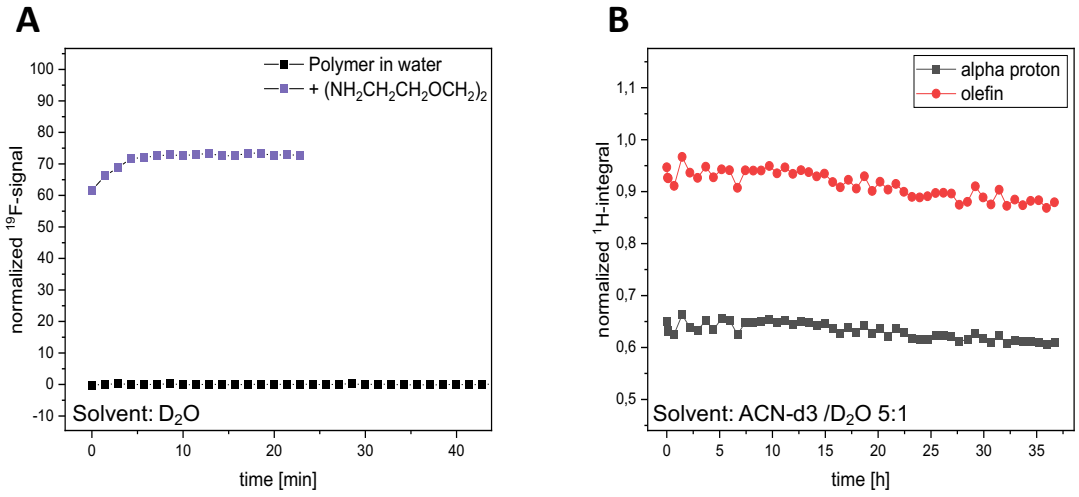

Fig.S 9: A) ^{19}F-NMR signals of the released pentafluorophenol during the reaction of a block copolymer with water (black) or a bisamine crosslinker (2,2′-(ethylenedioxy)-diethylamine – purple). B) ^{1}H-Signals of the backbone of the block copolymer during the reaction with water in a mixture of ACN-d3/D_2O.

6.3 Nanogel synthesis

To a stirred dispersion of the block copolymer in water (1 mg/mL, 1.0 equiv. PFP), either 2,2-di(2-aminoethoxy) propane for pH-responsive crosslinking (0.3 equiv.), or 2,2′-(ethylendioxy)-diethylamine for none-responsive crosslinking (0.3 equiv.) and DIPEA (0.65 equiv.) were added. The mixture was stirred for 20 minutes at room temperature. Then, 2-(2-(2-methoxyethoxy)ethoxy)-ethan-1-amine (2.0 equiv.) and DIPEA (2.0 equiv.) were added to fully convert all the remaining PFP-esters into hydropholic amides. Zhe mixture was stirred at room temperature overnight and then transferred into a dialysis tube (MWCO 10 kDa). It was dialyzed against 0.1%-NH_3-H_2O (3x 1L) and then filtered through a syringe filter (regenerated cellulose, 0.45µm pore size) before lyophilization yielding the nanogel particles as a colorless powder. By sonication they could be redispersed in respective buffers prior to use.

Tab.S 3: Summary of the DLS-measurements for D-NG and ND-NG

	D-NG (0.05 mg/mL, PBS)	ND-NG (0.05 mg/mL, PBS)
size	69.0 (± 1.6) nm	73.1 (± 0.2) nm
PDI	0.10 (± 0.04)	0.10 (± 0.03)

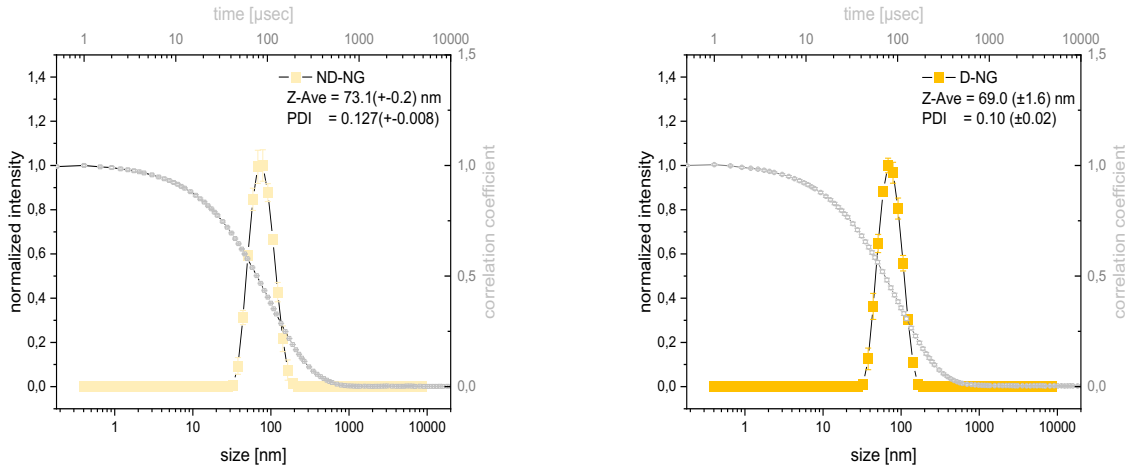

Fig.S 10: DLS-measurements of the ether-crosslinked **ND-NG** (left) and the ketal-crosslinked, **D-NG** (right). The normalized intensity distribution is shown in yellow and orange. The corresponding autocorrelation curve is shown in grey.

Tab.S 4: Overview of different prepared nanogels, from the block copolymers **BP1-6**

entry	Nanogel	P_n (ONB-PFP)	P_n (ONB-TEG)	Size [nm]	PDI
1	NG-BP1	14	15	86 (± 3)	0.39 (± 0.06)
2	NG-BP2[a)]	50	5	84 (± 1)	0.203 (± 0.003)
3	NG-BP3	55	28	64 (± 2)	0.01 (± 0.03)
4	NG-BP4	62	17	71.1 (± 0.2)	0.138 (± 0.003)
5	NG-BP5	58	38	93 (± 2)	0.304 (± 0.008)
6	NG-BP6[b)]	240	30	99 (± 3)	0.257 (± 0.006)

a) The nanogel prepared from BP-2 did not redissolve well after lyophilization. This is probably due to the very short (P_n= 5) hydrophilic block and subsequent aggregation of the particles after removal of the solvent. b) The nanogel prepared from BP-6 was synthesized by self-assembly in DMSO. Due to the high PFP-content the polymer was not dispersible in water.

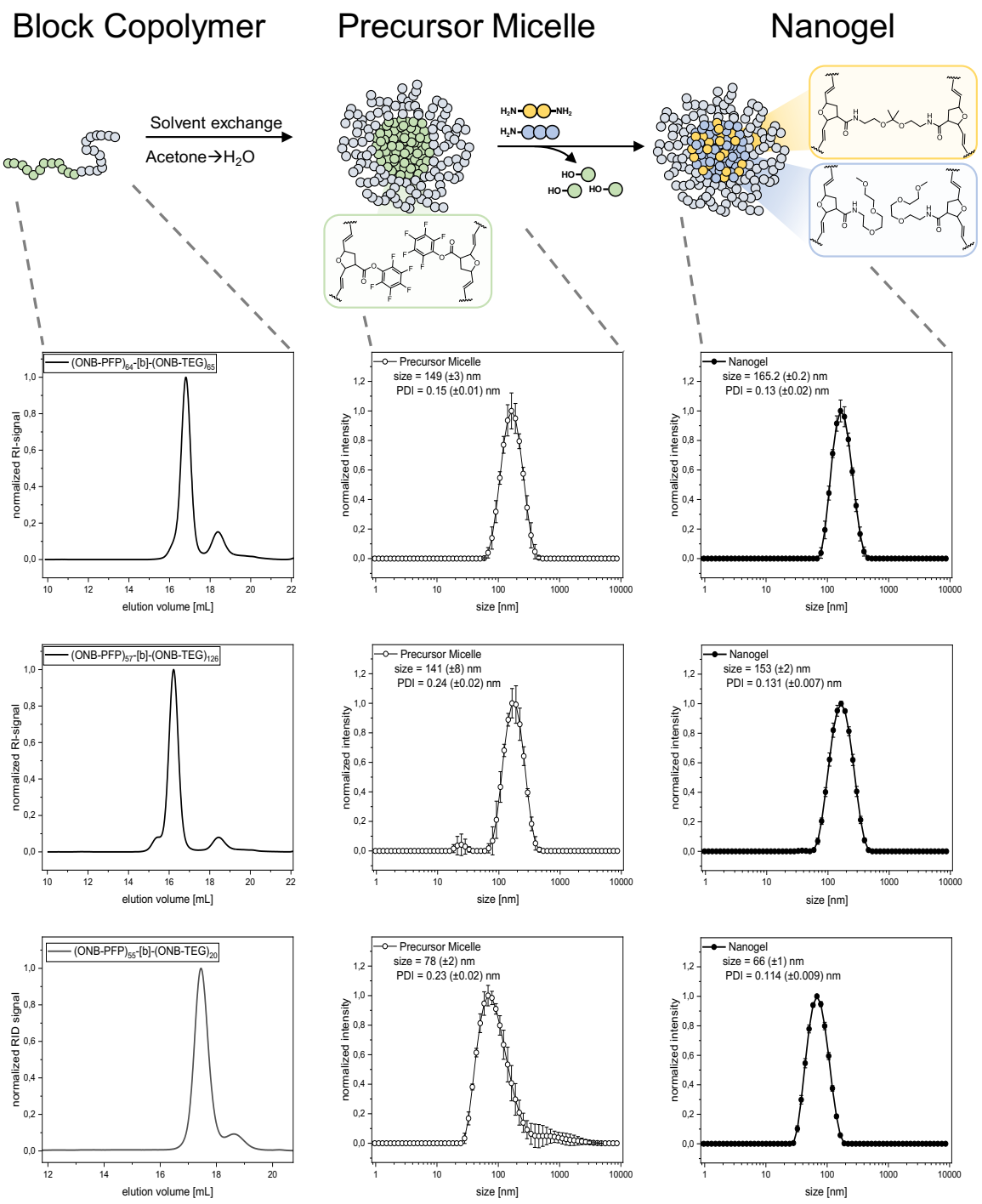

Fig.S 11: Overview on the preparation of nanogels from different polymers. The size of the resulting nanogels is determined by the size of the precursor micelles.

6.4 IMDQ-loaded nanogel syntheses

For the preparation of IMDQ-loaded nanogels, a stock solution of the polymer, assembled in water was prepared as described above. For the IMDQ conjugation, IMDQ was added as a stock-solution in DMSO (20.6 µL, 1.15 µmol, 0.15 equiv.). The cloudy mixture was then sonicated (10 min, at 25°C, to redisperse the precipitated IMDQ) and DIPEA (0.5 µL, 3.06 µmol, 0.4 equiv.) was added. The mixture was stirred for 20 minutes at room temperature. Then, ketal-crosslinker 2,2-bis(aminoethoxy)propane (0.37 µL, 2.29 µmol, 0.3 equiv.) and DIPEA (0.8 µL, 4.56 µmol, 0.6 equiv.) were added and the mixture was further stirred for 2 hours at room temperature. Finally, 2-(2-(2-methoxyethoxy)ethoxy)ethan-1-amine (2.50 µL, 15.3 µmol, 2.0 equiv.) and DIPEA (2.67 µL, 15.3 µmol, 2.0 equiv.) were added and the particle dispersion was stirred overnight. Then, the dispersion was transferred into a dialysis tube (MWCO 10 kDa) and dialyzed against 0.1% NH_3 in water (3x 1 L). The resulting ketal-crosslinked nanogels were then filtered through a syringe filter (regenerated cellulose filter, 0.45 µm pore size) and lyophilized. In analogy to the ketal-crosslinked nanogels, the non-degradable ether-crosslinked nanogels could be prepared by crosslinked with 2,2′-(ethylenedioxy)-diethylamine, too, as well as the non-crosslinked IMDQ-polymers that were obtained by conversoin with 2-(2-(2-methoxyethoxy)ethoxy)ethan-1-amine.

6.5 IMDQ determination

Covalent attachment of IMDQ to the nanogel was verified by UV-Vis spectroscopy. For this, the IMDQ particle was dispersed in 0.1% NH_3-H_2O at a concentration of 0.75 mg/mL. To determine the drug loading of the particles by UV-Vis spectroscopy, the contribution of scattered light to the spectrum should be determined first. In the absence of a suitable control particle, the scattering contribution is approximated by an empirical approach. The theoretical determination of the contribution to the intensity of scattered light is however difficult to achieve. For particles smaller than the wavelength of the incident light beam, wavelength dependent scattering intensity could be determined by the Raleigh theory ($I \propto \lambda^{-4}$). For larger particles, however, Mie-scattering becomes more important and, therefore, theoretical determination becomes more complicated. The polydispersity of the particles adds even further complexity to this. A more empirical approach finally provided us with the absorbance spectrum of the particles where a triexponential decay curve could be fitted through the areas of the spectrum, that do not show absorption due to chromophores [9]. The resulting absorbance at 337 nm was then taken for quantification of IMDQ based on a calibration curve from Fig.S 12:

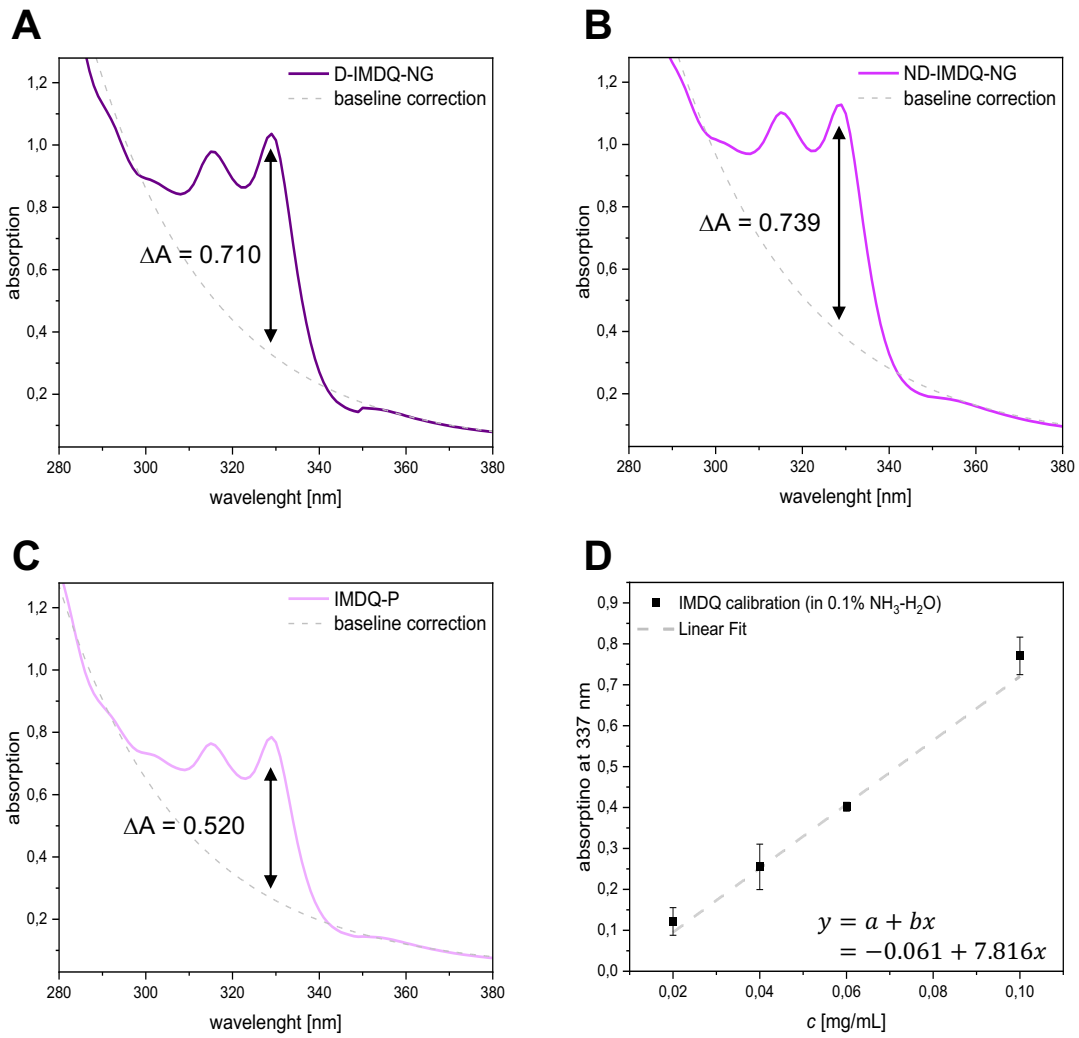

Fig.S 12: UV-Vis absorbance spectra of the IMDQ-loaded nanogels. **A**: D-IMDQ-NG; **B**: ND-IMDQ-NG; **C**: IMDQ-P; **D**: Calibration of IMDQ in 0.1% NH_3-H_2O, determined by the absorption values at 337 nm.

The concentration of IMDQ (c_{IMDQ}) and the drug loading (DL) was then determined by the derived absorbance of IMDQ at 337 nm (ΔA), the y-intercept (a) and the slope of the linear regression (b), according to the following formula:

$$C_{IMDQ} = \frac{\Delta A - a}{b}$$

Exemplary calculation for the degradable, IMDQ-loaded nanogel (D-IMDQ-NG):

$$\Rightarrow C_{IMDQ,D-NG} = \frac{0.710 + 0.061}{7.816\ \frac{\mathrm{mL}}{\mathrm{mg}}}$$

$$= 0.099 \frac{\mathrm{mg}}{\mathrm{mL}} = 99\ \frac{\mathrm{mg}}{\mathrm{L}}$$

$$DL = \frac{c_{IMDQ}}{c_{Part}}$$

$$\Rightarrow \frac{0.099\ \frac{\mathrm{mg}}{\mathrm{mL}}}{0.75\ \frac{\mathrm{mg}}{\mathrm{mL}}} = 0.13$$

The error of the IMDQ-concentration was then determined according to the following formula. The error is derived from the error of the linear calibration of free IMDQ in NH_3-H_2O. The error, due to the baseline correction method, explained above is however neglected:

$$\Delta c = \sqrt{\left(\frac{\partial c}{\partial a}\Delta a\right)^2 + \left(\frac{\partial c}{\partial b}\Delta b\right)^2} = \sqrt{\left(\frac{\Delta a}{b}\right)^2 + \left(\frac{(a - A)\Delta b}{b^2}\right)^2}$$

Exemplary error calculation for the degradable, IMDQ-loaded nanogel (D-IMDQ-NG):

$$\Rightarrow \Delta c_{D-IMDQ-NG} = \sqrt{\left(\frac{0.054}{7.816\ \frac{\mathrm{mL}}{\mathrm{mg}}}\right)^2 + \left(\frac{(-0.061 - 0.710) \cdot 0.906\ \frac{\mathrm{mL}}{\mathrm{mg}}}{\left(7.816\ \frac{\mathrm{mL}}{\mathrm{mg}}\right)^2}\right)^2}$$

$$= 0.013\ \frac{\mathrm{mg}}{\mathrm{mL}}$$

All determined concentrations and drug loadings are summarized in Tab.S 5. The drug loading (**DL**) of the nanogels was then determined by taking the mass of the investigated nanogels into account.

Tab.S 5: Summary of the IMDQ-determination of the particles via UV-Vis spectroscopy.

	ΔA	***c*** [mg/L]	**DL (wt%)**
D-IMDQ-NG	0.710	99 (±13)	13 (±2)
ND-IMDQ-NG	0.739	102 (±14)	13 (±2)
IMDQ-P	0.520	74 (±11)	10 (±1)

6.6 FRET nanogel synthesis

The synthesis of the dye-labeled particles for FRET-analysis was performed in analogy to the procedure described above. Cy3-polymer (1 mg) and Cy5-polymer (1 mg) were dissolved in acetone/water (6:1, v/v). Acetone was then slowly removed via rotary evaporation to give an aqueous dispersion of the block copolymers at a concentration of c = 1 mg/mL. For crosslinking with a degradable ketal-linker, 2,2-bis(aminoethoxy)propane (1.46 µL of a 1 M stock solution in DMSO, 1.46 µmol, 0.3 equiv.) and DIPEA (0.51 µL, 2.92 µmol, 0.6 equiv.) were added. The mixture was stirred for 1 hour at room temperature. Then, methoxy-triethyleneglycol amine (1.59 µL, 9.72 µmol, 2.0 equiv.) and DIPEA (1.70 µL, 9.72 µmol. 2.0 equiv.) were added. The mixture was stirred overnight. The resulting nanogel was then dialyzed against 0.1 % aqueous NH_3 (3x, 10 kDa MWCO) and lyophilized to yield the product as voluminous purple powder (1.5 mg).

6.7 DLS nanogel size determination

The size of IMDQ-loaded nanogels was determined using multiangle dynamic light scattering (MADLS). The obtained autocorrelation function was fitted with a bi-exponential decay function. Average diffusion coefficients were extrapolated to 0° to yield the apparent diffusion coefficient D_{app} of the particles in PBS buffer. The particle hydrodynamic radius R_H was then determined using the Stokes-Einstein equation:

$$R_H = \frac{k_B T}{6\pi\eta D_{app}}$$

With the Boltzmann-constant k_B, the temperature T (298.15 K) and the viscosity of water at room temperature η (1.00 cP), the hydrodynamic radii (R_H) could be determined:

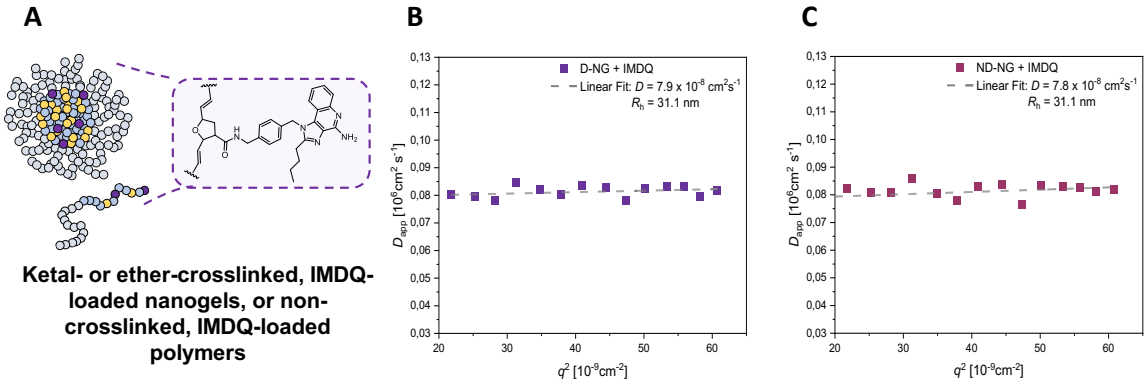

Fig.S 13: Multi-Angle-Dynamic-Light-Scattering (MADLS) of D-NG +IMDQ and ND-NG+ IMDQ

D-NG + IMDQ : R_H = 31.1 nm **ND-NG + IMDQ :** R_H = 31.1 nm

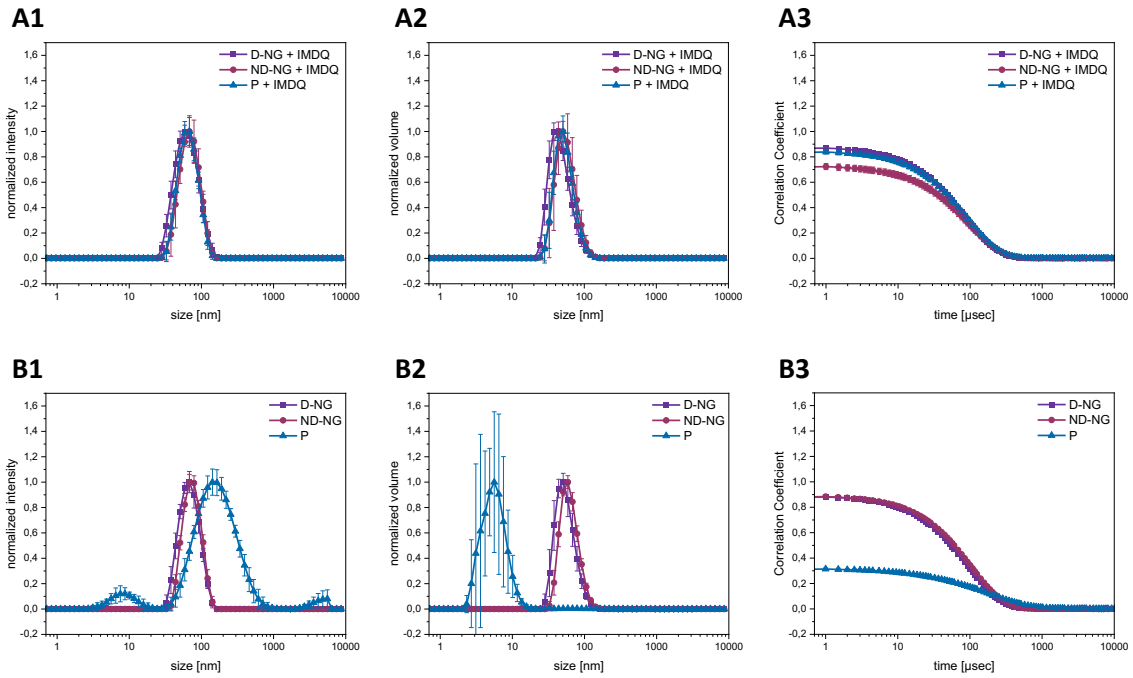

Fig.S 14: DLS measurements of D-NG, ND-NG and P. **A)** DLS measurements of D-NG, ND-NG and P, conjugated to IMDQ in H_2O at 0.1 mg/mL; and **B)** DLS measurements of D-NG, ND-NG and P, without IMDQ-conjugation in H_2O at 1 mg/mL (1: intensity size distribution, 2: volume distribution, 3: autocorrelation).

Tab.S 6: Summary of the sizes, measured by DLS of the TAMRA-labeled degradable, non-degradable and non-crosslinked nanogels with and without conjugation of IMDQ.

	+IMDQ		**-**	
	size [nm]	**PDI**	**size [nm]**	**PDI**
D-NG	58 ± 4	0.10 ± 0.02	64 ± 2	0.10 ± 0.03
ND-NG	65 ± 5	0.07 ± 0.03	71 ± 2	0.06 ± 0.02
P	62 ± 2	0.08 ± 0.02	12 ± 4[a)]	0.5 ± 0.1

a) *here, the size of the smaller intensity peak is used*

.

7. In vitro Experiments

Cell culture

RAW-Blue cells were cultured in DMEM-GlutaMAX™ medium, supplemented with 10% fetal bovine serum (FBS), 1% penicillin/streptomycin, 0.01% Zeocin®, 0.02% Normocin® at 37°C with 5% CO_2 saturation.

IMDQ-activation assay

TLR receptor stimulation was measured by NF-κB/AP-1 activation and subsequent secretion of embryonic alkaline phosphatase from RAW-Blue cells (InvivoGen). The cells were seeded into 96-well plates at a density of 90 000 cells/well in 180 µL culture medium (DMEM-GlutaMAX™, supplemented with 10% fetal bovine serum, 1% penicillin/streptomycin, 0.01% Zeocin®, 0.02% Normocin® at 37°C with 5% CO_2 saturation. After 24 hours, each well was treated with 20 µL of a 10x concentrated sample solution. After 24 hours incubation, 50 µL of the supernatant from each well was collected and tested for secreted embryonic alkaline phosphatase (SEAP) using the QUANTI-Blue™ assay (InvivoGen). Quanti-Blue™ (150 µL) was added to each supernatant and incubated at 37 °C for 2 hours. SEAP levels were determined by an increase in absorbance at 615 nm using a microplate reader. The activity was determined relative to PBS as a negative control and soluble IMDQ as the positive control. All experiments were conducted at n = 4.

3-(4,5-Dimethylthiazol-2-yl)-2,5-diphenyltetrazolium Bromide (MTT) Assay

3-(4,5-Dimethylthiazol-2-yl)-2,5-diphenyltetrazolium bromide (MTT) (30 µL, 2 mg/mL in PBS buffer) was added to the remaining RAW-blue cells and incubated for 2-3 hours at 37°C. The formed formazan crystals were redissolved by addition of a 10% m/v SDS solution in 0.01 M HCl and incubation at 37°C overnight. Quantification was performed by measuring the absorbance at 570 nm. As positive control, cells incubated with PBS were used and as a negative control, cells incubated with soluble DMSO were applied. Viability was determined in relation to PBS as the positive and DMSO as the negative control.

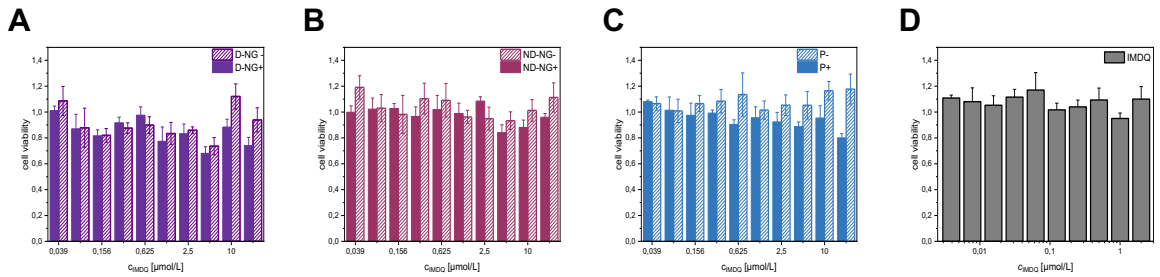

Fig.S 15: Cell viability of IMDQ-conjugated and empty nanogels, as well as soluble IMDQ, assessed via MTT assay. **(A)** Cell viability of D-NG (acid-labile nanogels) with and without IMDQ conjugation. **(B)** Cell viability of ND-NG (stable nanogels) with and without IMDQ conjugation. **(C)** Cell viability of P (non-crosslinked polymers) with and without IMDQ conjugation. **(D)** Cell viability of soluble IMDQ.

Flow Cytometry

RAW-Blue cells were seeded into a 24 well plate at a density of 250 000 cells/well (suspended in 0.90 mL of culture medium). The cells were incubated for 24 hours. Then, the cells were treated with 100 µL of a 10x concentrated sample solution (resulting in a total concentration of 10, 50 and 100 µg/mL). All samples were performed in triplicates (n=3). First the fluorescence spectra were measured, to ensure equal fluorescence for the different samples (Fig.S 16). After 24 hours of incubation at 37°C, the medium was removed. The cells washed with 1 mL PBS and 500 µL cell dissociation buffer (5 mM EDTA-solution pH = 7.4) and then incubated at 37°C for 30 minutes. The cells were detached by pipetting and the cell suspension was transferred into Eppendorf tubes. After centrifugation (300 g, 10 minutes, 4°C), the supernatant was removed and the pellets were stored on ice. Before measuring, the pellets were resuspended in 200-900 µL of PBS to achieve desirable cell counts (~100-200 events/sec).

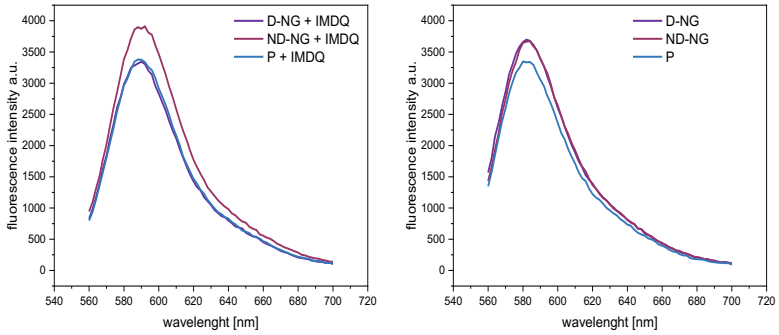

Fig.S 16: Fluorescence emission spectra of D-NG, ND-NG and P, conjugated to IMDQ, before FACS measurements (left). Fluorescence spectra of D-NG, ND-NG, and P without IMDQ before FACS measurements (right).

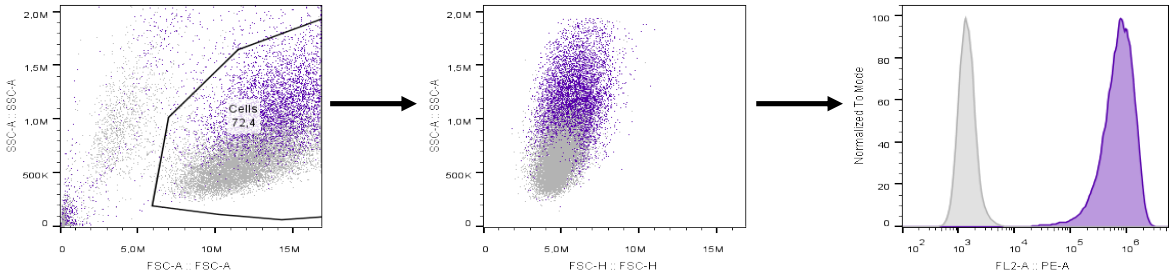

Fig.S 17: Gating strategy for flow cytometric analysis. Here, the gating strategy is exemplified for the samples D-NG + IMDQ (purple) and the PBS control (grey).

Flow cytometry: Nanogel Uptake

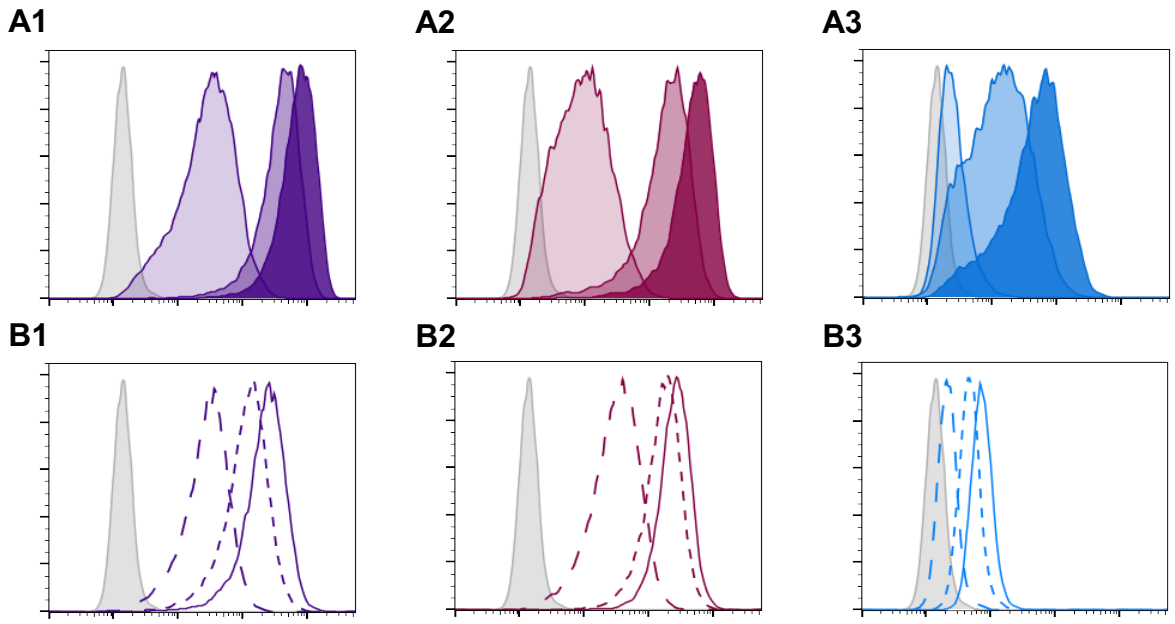

Fig.S 18: Cells were incubated with increasing amounts of nanogels (10, 50 and 100 µg/mL). Here, the histograms for the nanogels with IMDQ and without IMDQ are shown. **A1)** Histograms of **D-NG + IMDQ**. **A2)** Histograms of **ND-NG + IMDQ**. **A3)** Histograms of **P + IMDQ**. **B1)** Histograms of empty **D-NG**. **B2)** Histograms of empty N**D-NG**. **B1)** Histograms of empty **P**.

Flow cytometry: FRET measurement

For that purpose, nanogel particles were prepared from polymers covalently modifed with either with Cy3-dye only or Cy5-dye only. The differently labeled particles were mixed equimolar and crosslinked with either the ketal-containing bisamine or a ether containing bisamine to yield degradable and non-degradable particles.

RAW-Blue cells were then seeded into a 24 well plate at a density of 250 000 cells/well (suspended in 0.90 mL of culture medium). The cells were incubated for 4 hours. Then, the cells were treated with 100 µL of a 10x concentrated sample solution (resulting in a total concentration of 10, 50 and 100 µg/mL). All samples were performed in triplicates (n=3). First the fluorescence spectra were measured, to ensure equal fluorescence for the different samples (Fig.S 16). After 24 hours of incubation at 37°C, the medium was removed. The cells washed with 1 mL PBS and 500 µL cell dissociation buffer (5 mM EDTA-solution pH = 7.4) and then incubated at 37°C for 30 minutes. The cells were detached by pipetting and the cell suspension was transferred into Eppendorf tubes. After centrifugation (300 g, 10 minutes, 4°C), the supernatant was removed and the pellets were stored on ice. Before measuring, the pellets were resuspended in 200-900 µL of PBS to achieve desirable cell counts (~100-200 events/sec).

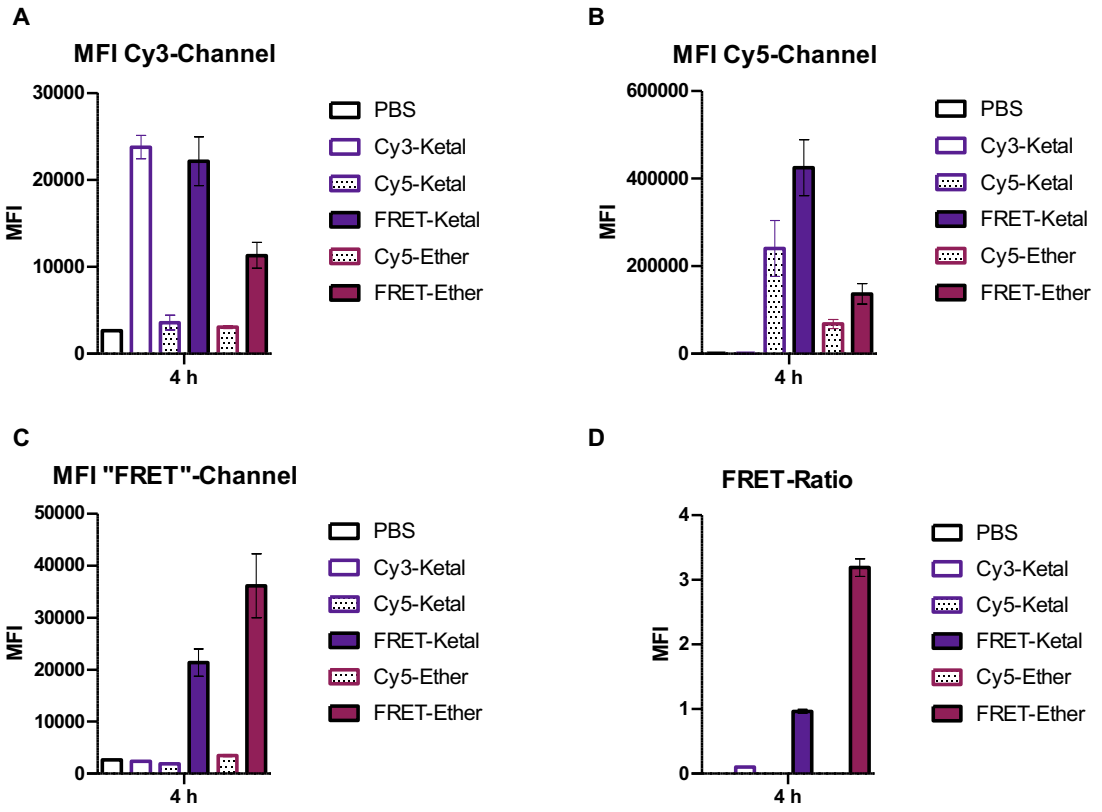

Fig.S 19: FRET ratio determination by flow cytometry. After 4 hours of incubation RAW-Blue macrophages were analyzed by flow cytometry and the mean fluorescence intensity (MFI) of a Cy3-Channel (A) upon excitation at 488 nm and the mean fluorescence intensity (MFI) of a Cy5-Channel (B) upon excitation at 633 nm can be dertermined. Moreover, the mean fluorescence intensity (MFI) for a FRET emission upon excitation at 488 nm can be recorded by the “FRET”-Channel (C). A FRET-Ratio can be derived by dividing the MFII of the “FRET”-Channel by the MFI of the Cy3-Channel (D). The FRET emission is higher for the ether-containing nanogel than for the ketal containing particle resulting in a three-fold higher FRET-Ratio, indicating degradation of the ketal containing nanogel.

8. Literature

[1] F. Sinner, M. R. Buchmeiser, *Macromolecules* **2000**, *33*, 5777.
[2] D. D. Manning, L. E. Strong, X. Hu, P. J. Beck, L. L. Kiessling, *Tetrahedron* **1997**, *53*, 11937.
[3] C. M. Schueller, D. D. Manning, L. L. Kiessling, *Tetrahedron Letters* **1996**, *37*, 8853.
[4] S. H. Jung, J.-W. Lee, H.-J. Kim, *Supramolecular Chemistry* **2016**, *28*, 634.
[5] P. Ahlers, H. Frisch, P. Besenius, *Polym. Chem.* **2015**, *6*, 7245.
[6] W. H. Binder, C. Kluger, M. Josipovic, C. J. Straif, G. Friedbacher, *Macromolecules* **2006**, *39*, 8092.
[7] M. Adams, V. Richmond, D. Smith, Y. Wang, F. Fan, A. P. Sokolov, D. A. Waldow, *Polymer* **2017**, *116*, 218.
[8] J. A. Love, J. P. Morgan, T. M. Trnka, R. H. Grubbs, *Angewandte Chemie* **2002**, *114*, 4207.
[9] R. Herrmann, M. Rennhak, A. Reller, *Beilstein Journal of Nanotechnology* **2014**, *5*, 2413.

9. NMR Spectra

9.1 Small Molecules

7-oxanorbornene-2-carboxylic acid

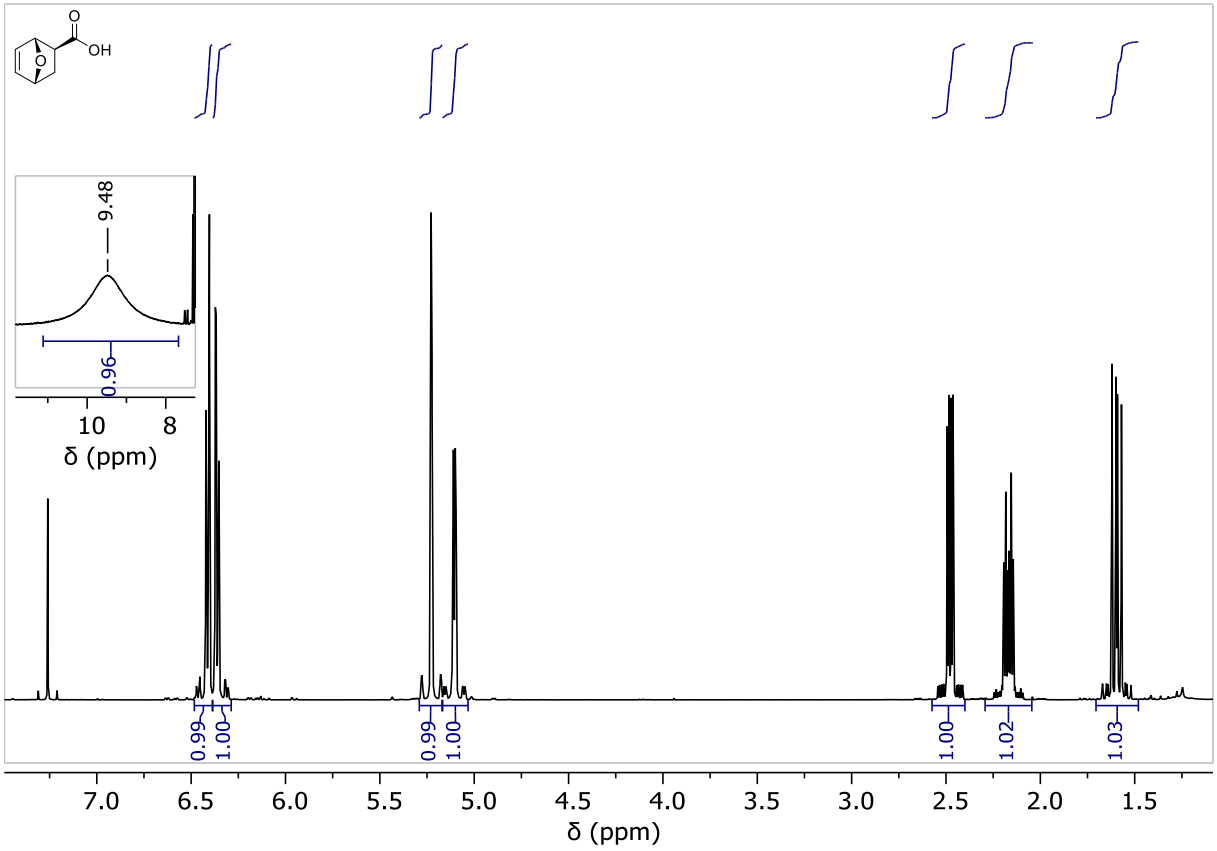

Fig.S 20: ^{1}H-NMR of the oxanorbornene carboxylic acid

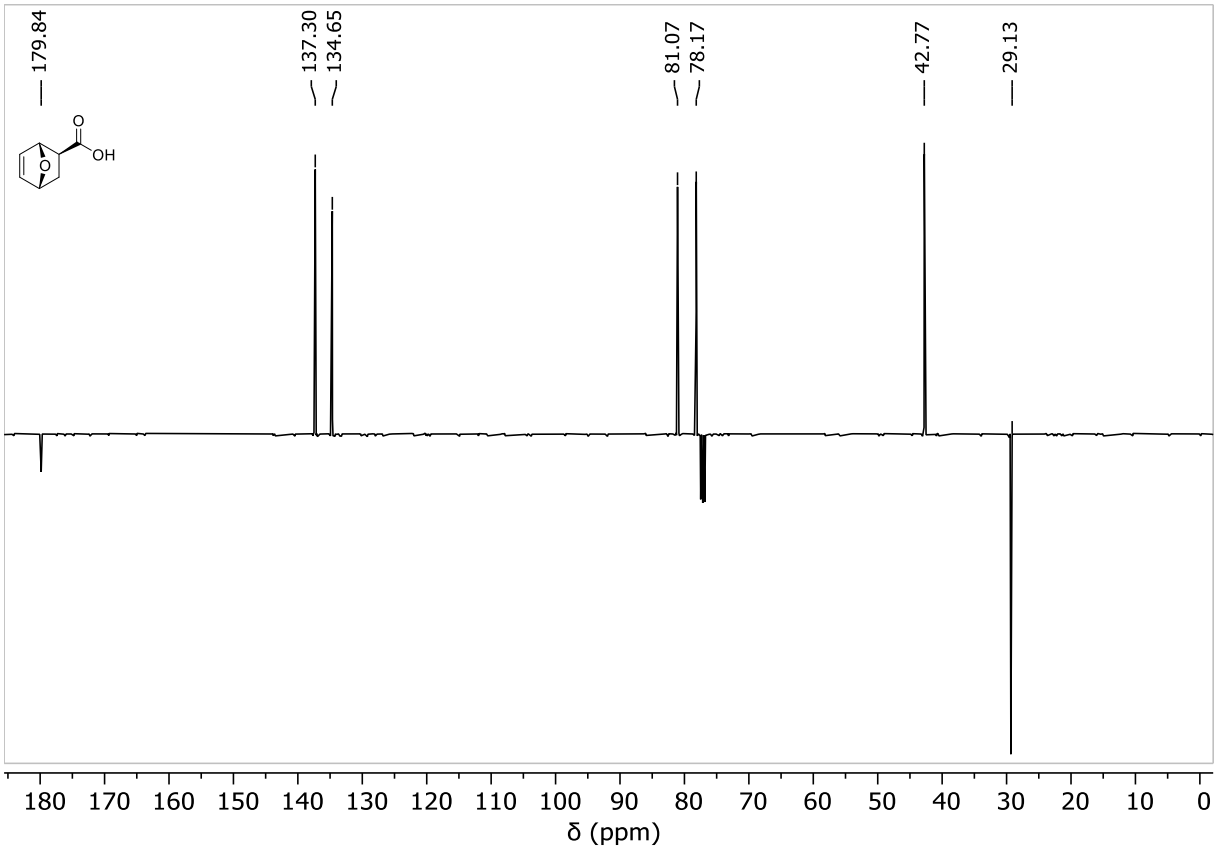

Fig.S 21: ^{13}C-NMR of the oxanorbornene carboxylic acid.

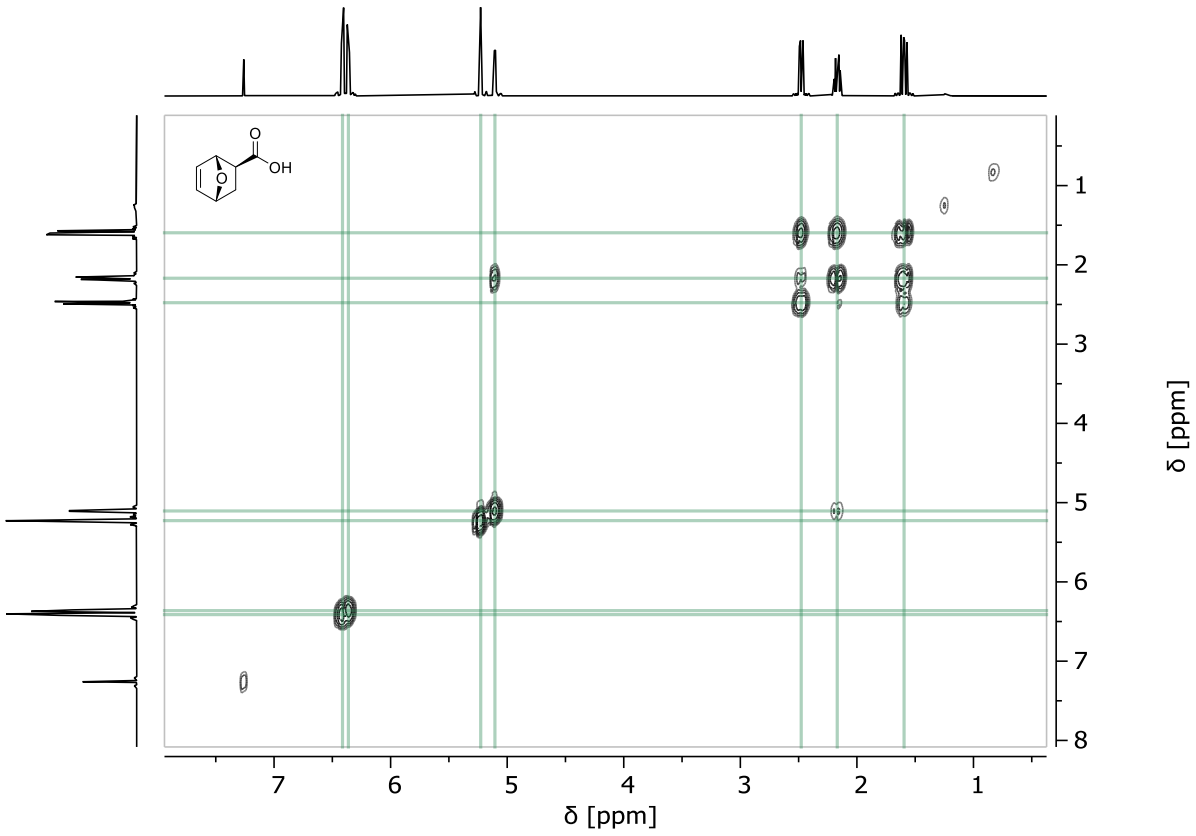

Fig.S 22: COSY-NMR of the oxanorbornene carboxylic acid.

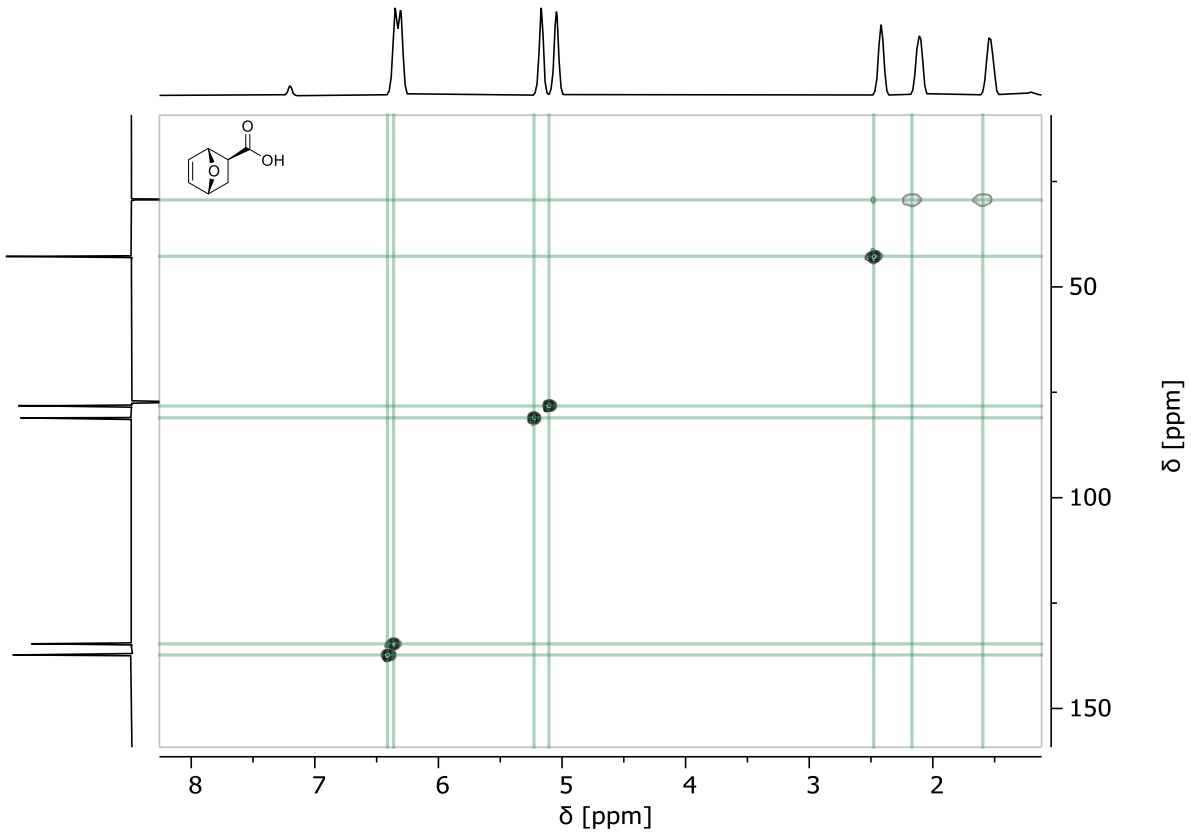

Fig.S 23: HSQC-spectrum of the oxanorbornene carboxylic acid.

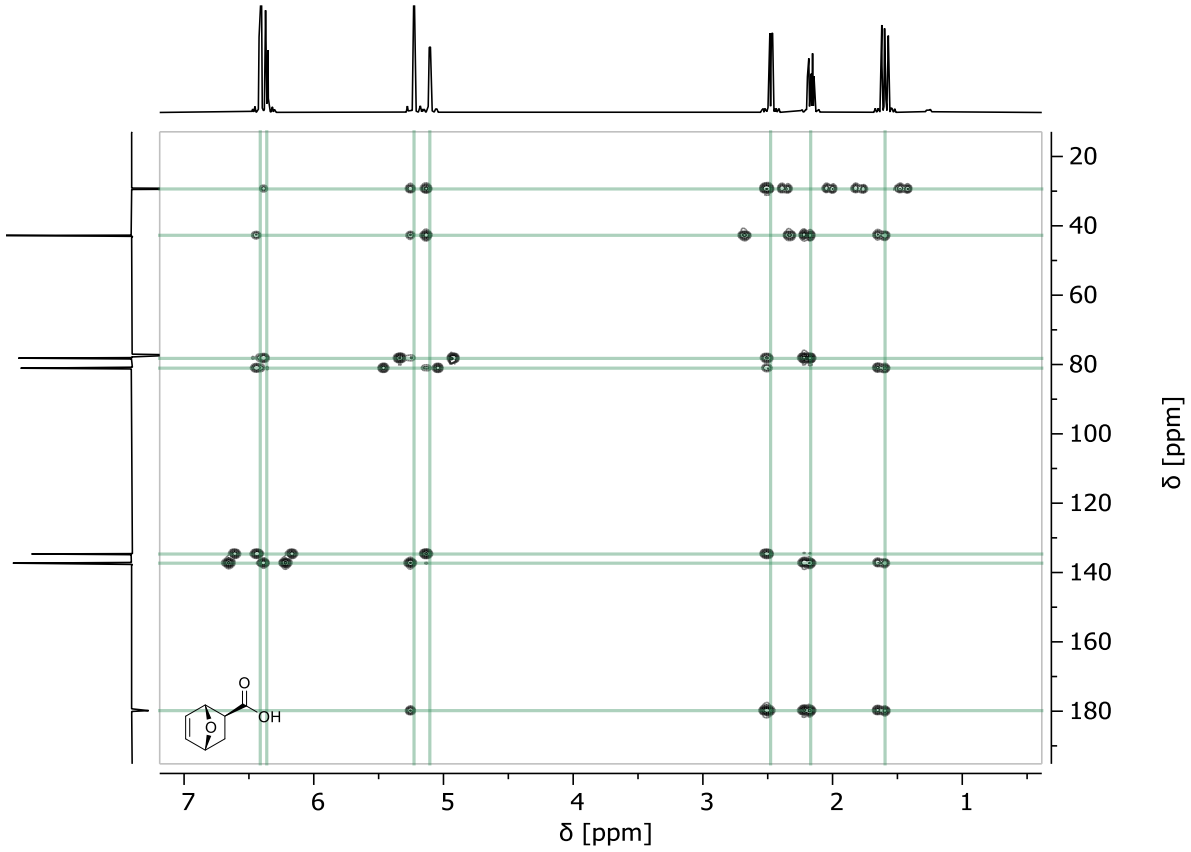

Fig.S 24: HMBC-spectrum of the oxanorbornene carboxylic acid.

7-oxanorbornene-2-carboxylic acid pentafluorophenyl ester

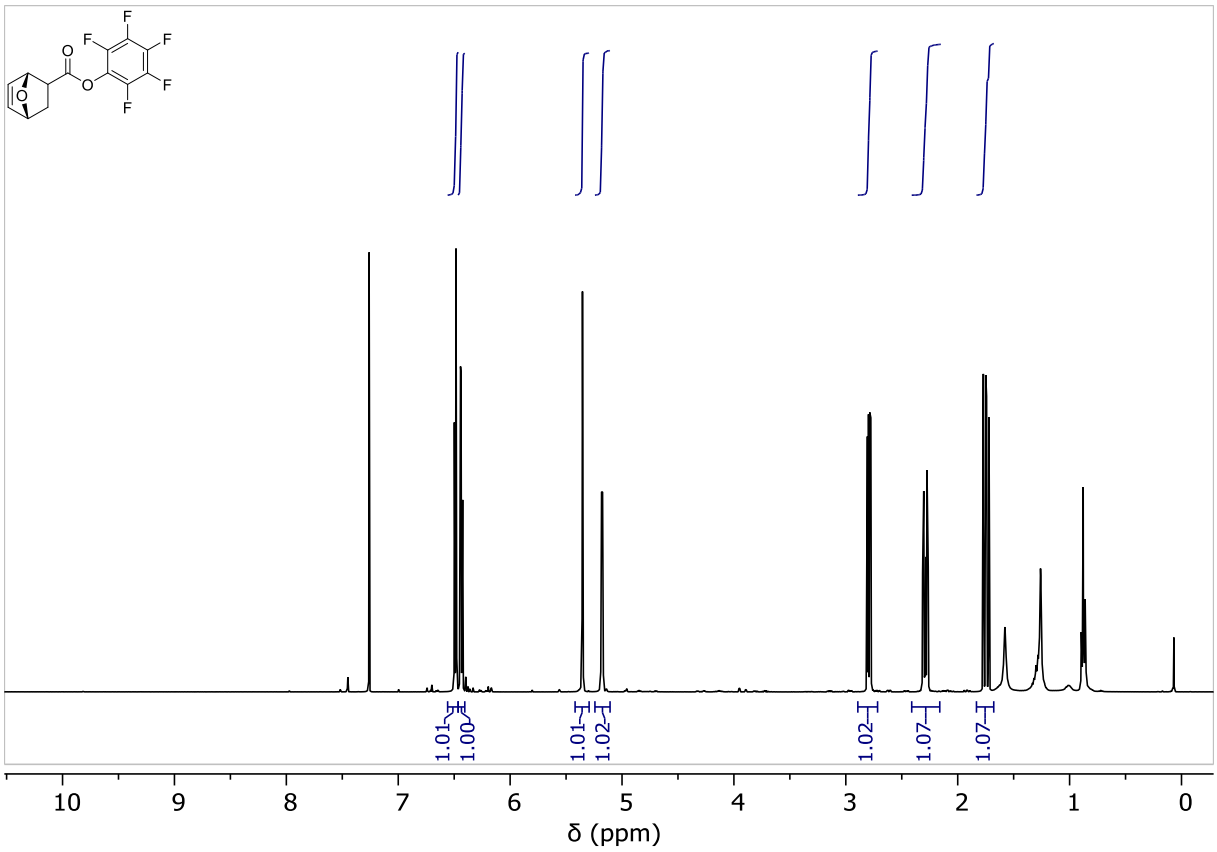

Fig.S 25: ^{1}H-NMR of the 7-oxabicyclo[2.2.1] hept-5-ene-exo-2-carboxylic acid pentafluorophenyl ester.

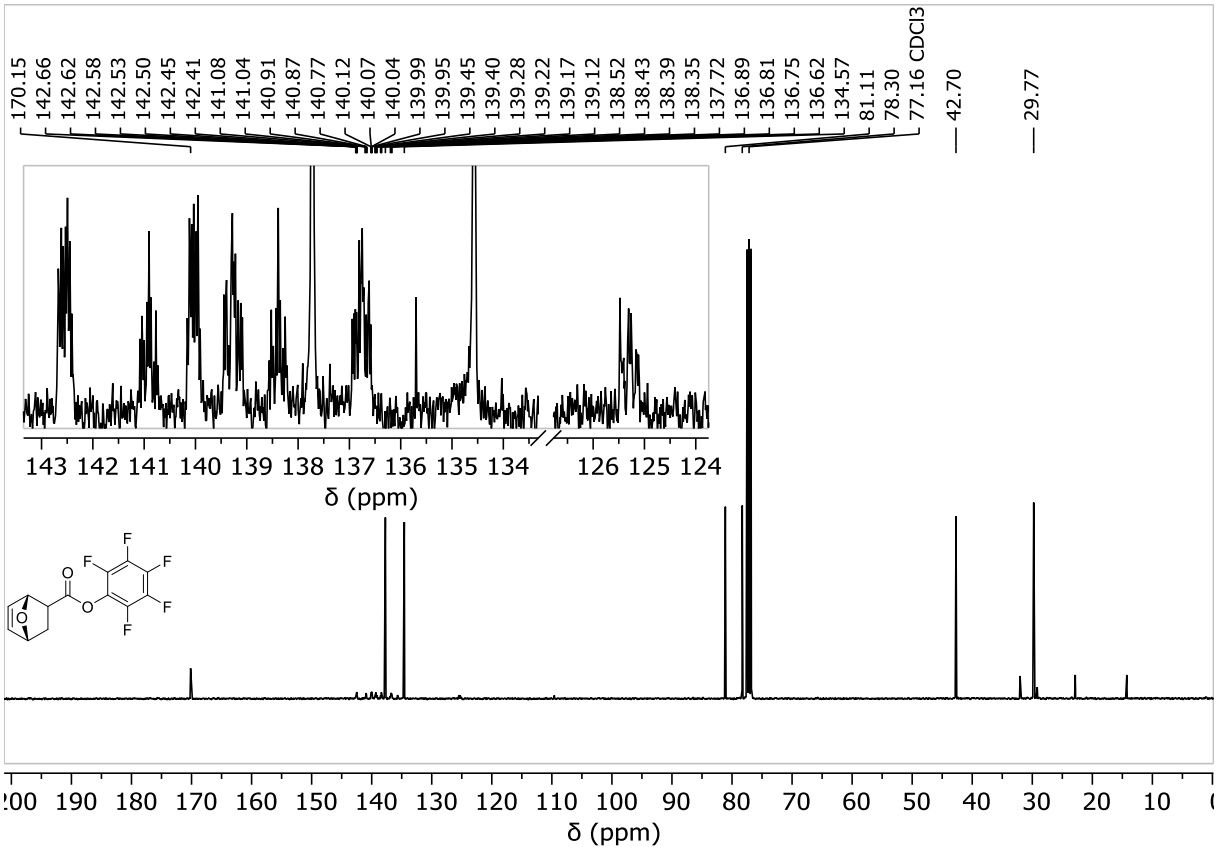

Fig.S 26: ^{13}C-NMR of 7-oxabicyclo[2.2.1] hept-5-ene-exo-2-carboxylic acid pentafluorophenyl ester.

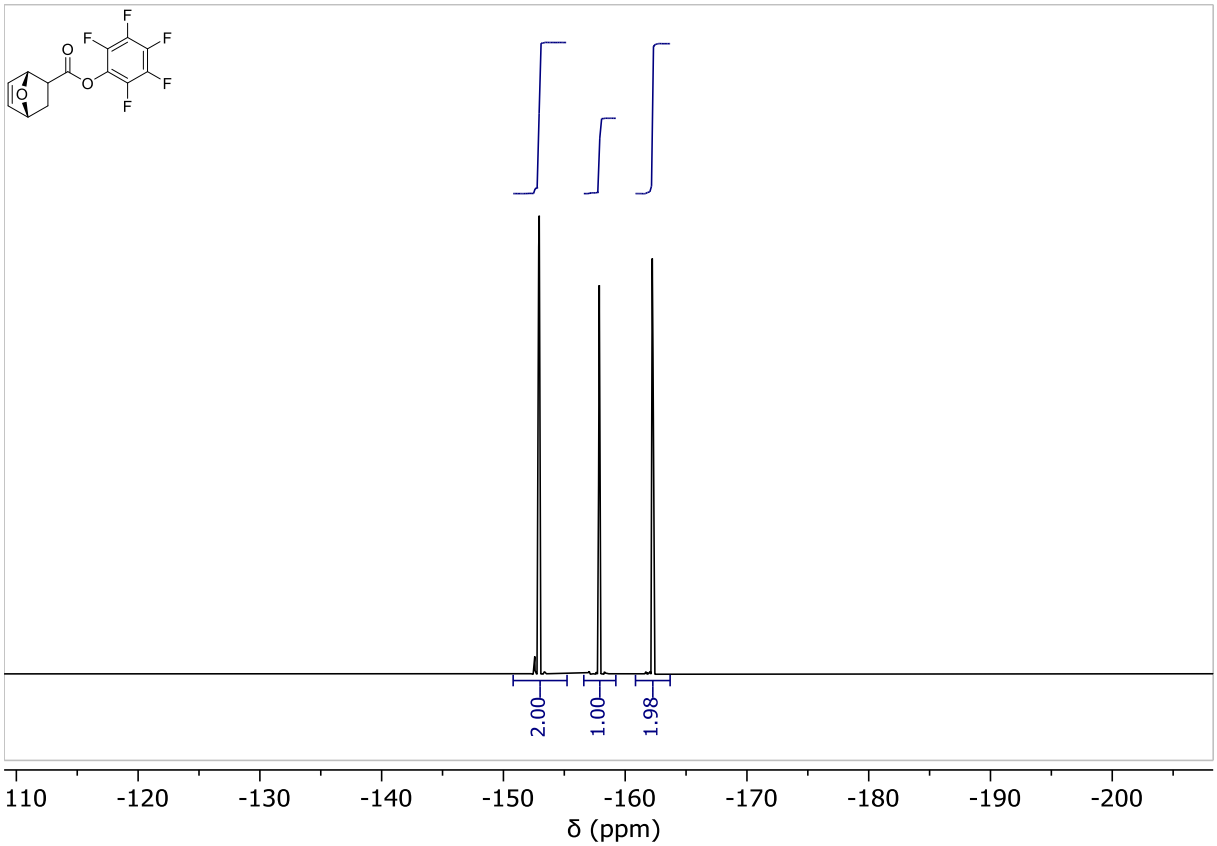

Fig.S 27: ^{19}F-NMR of 7-oxabicyclo[2.2.1] hept-5-ene-exo-2-carboxylic acid pentafluorophenyl ester.

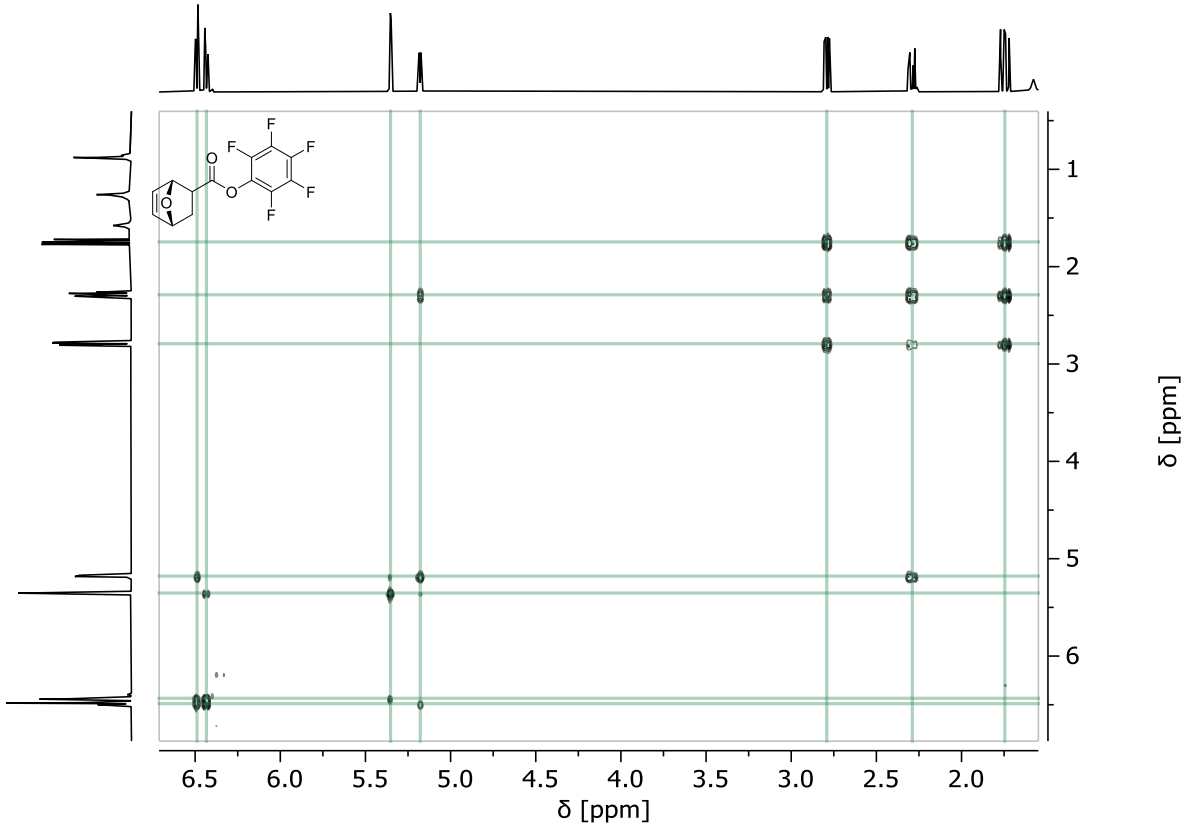

Fig.S 28: COSY-spectrum of 7-oxabicyclo[2.2.1] hept-5-ene-exo-2-carboxylic acid pentafluorophenyl ester.

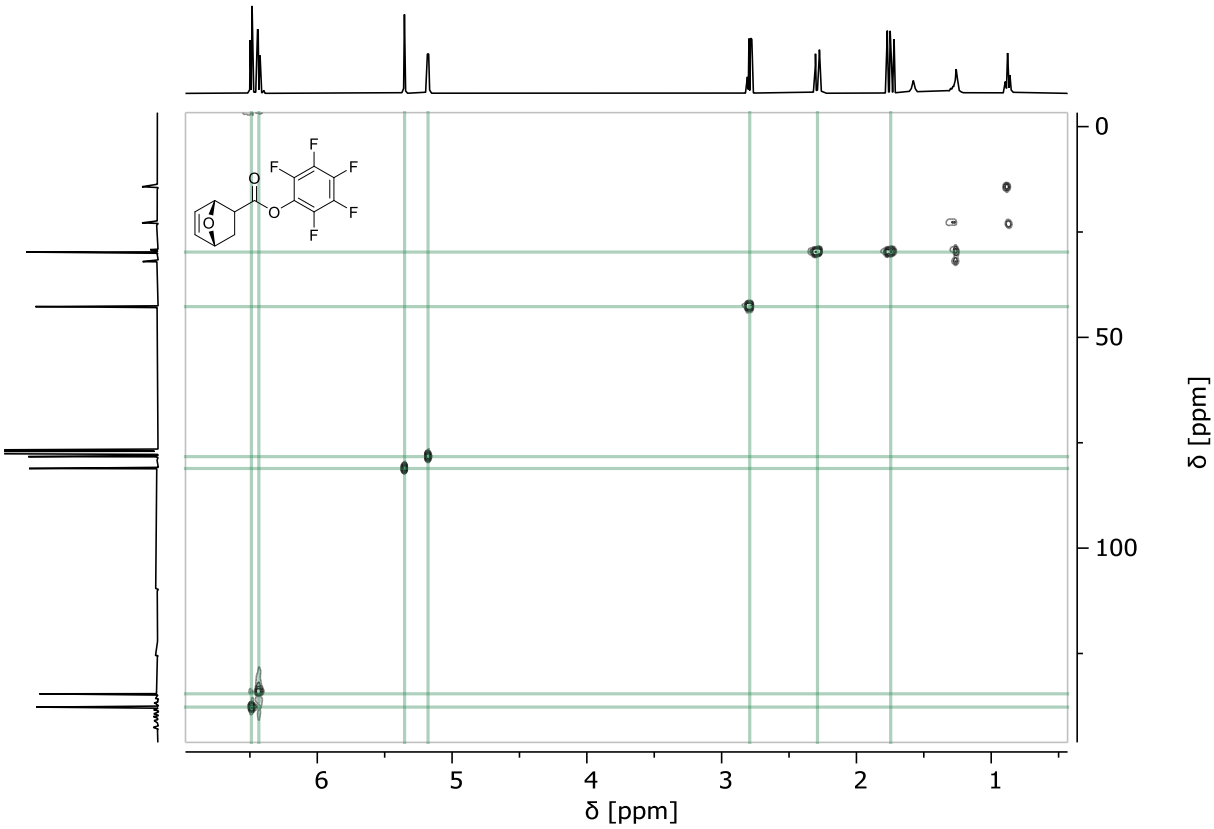

Fig.S 29: HSQC-spectrum of 7-oxabicyclo[2.2.1] hept-5-ene-exo-2-carboxylic acid pentafluorophenyl ester.

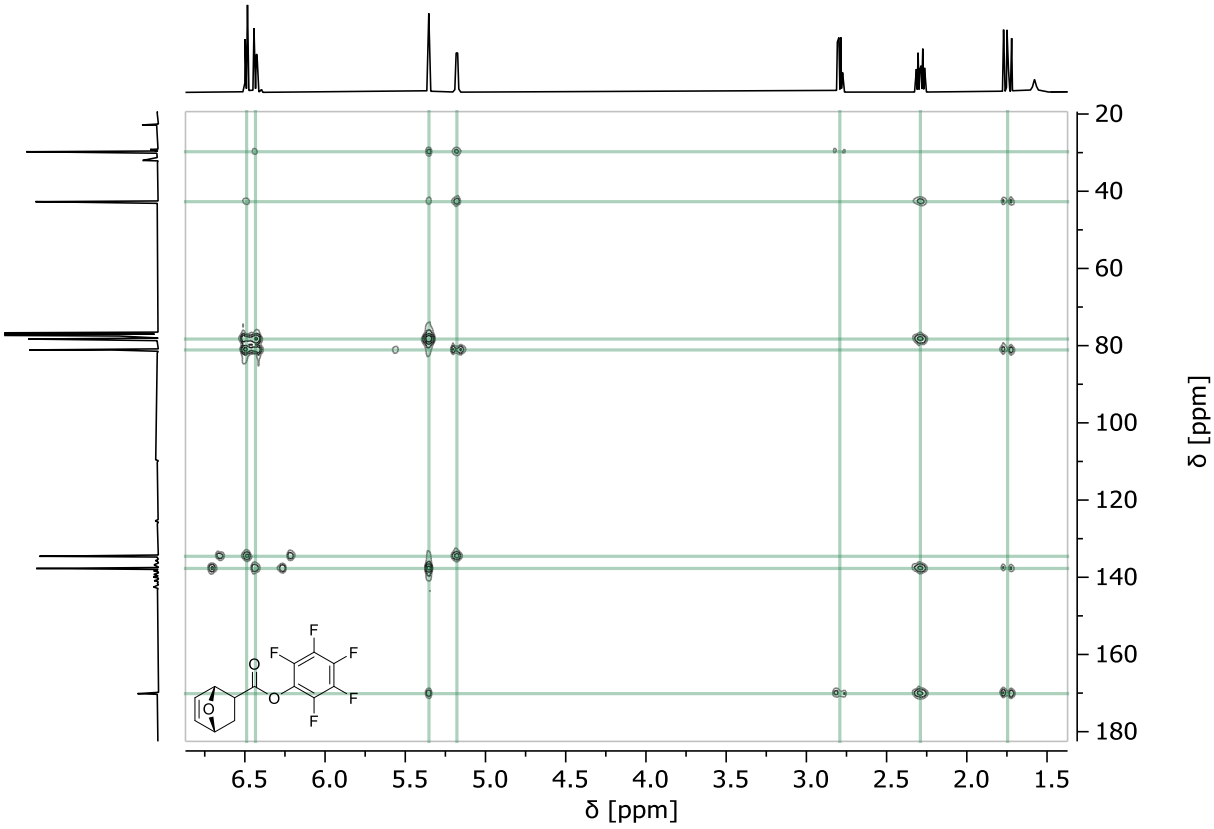

Fig.S 30: HMBC-spectrum of 7-oxabicyclo[2.2.1] hept-5-ene-exo-2-carboxylic acid pentafluorophenyl ester.

Triethylene glycol monomethyl tosylate

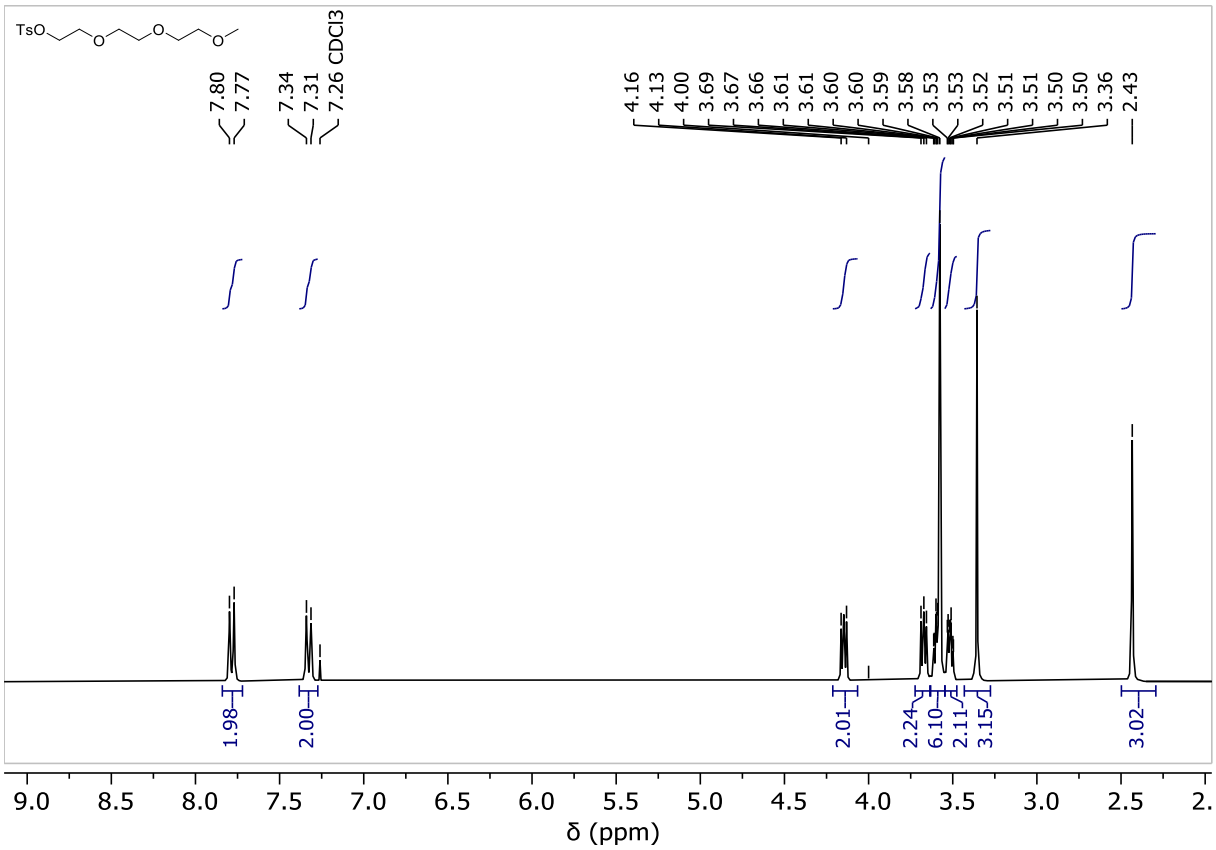

Fig.S 31: 1H-NMR of triethylene glycol monomethyl tosylate.

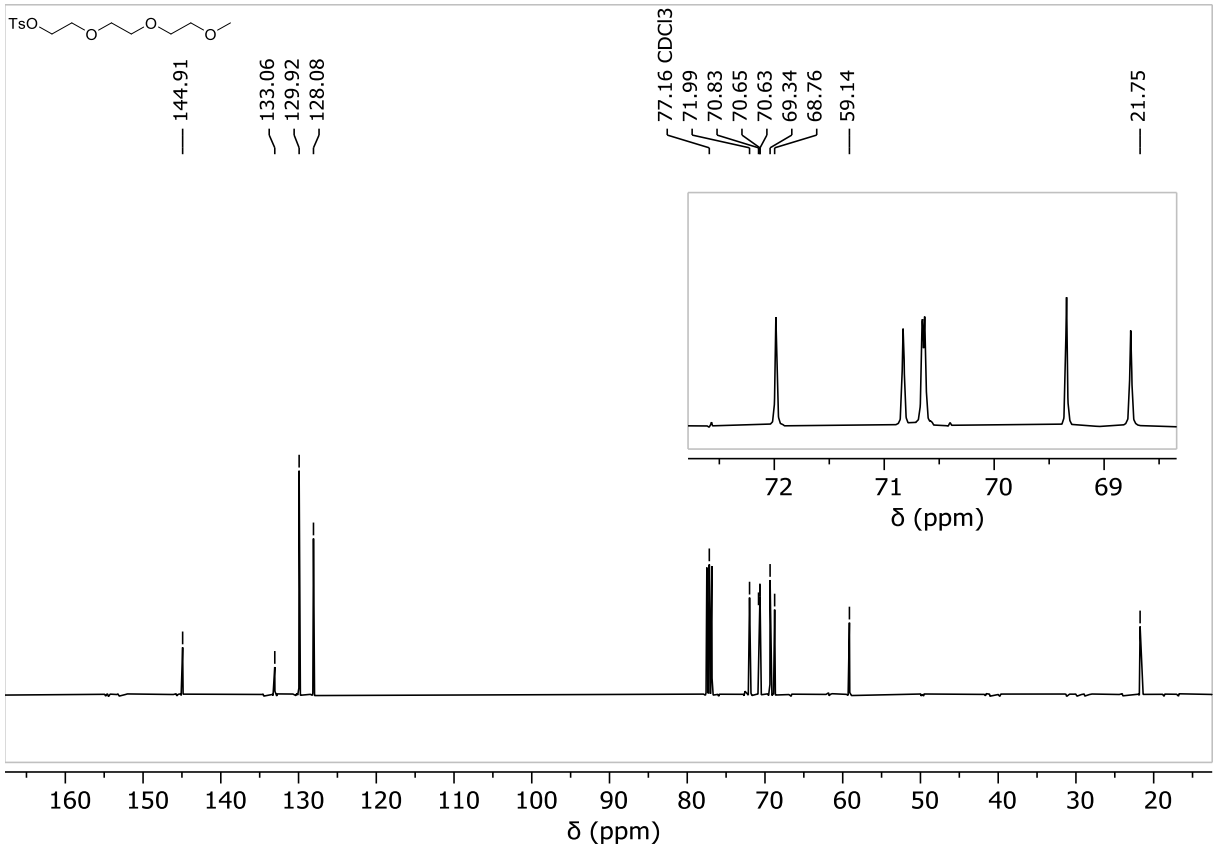

Fig.S 32: ^{1}H-NMR of triethylene glycol monomethyl tosylate.

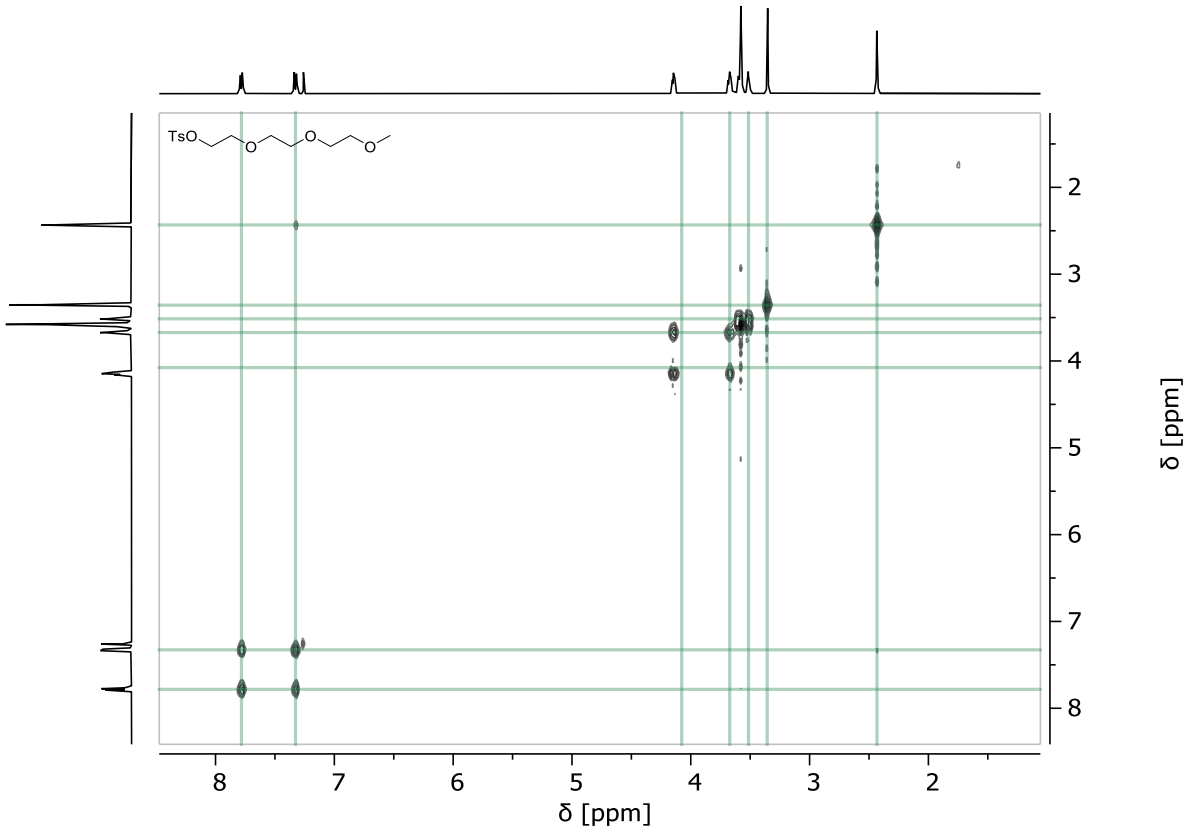

Fig.S 33: COSY-spectrum of triethylene glycol monomethyl tosylate.

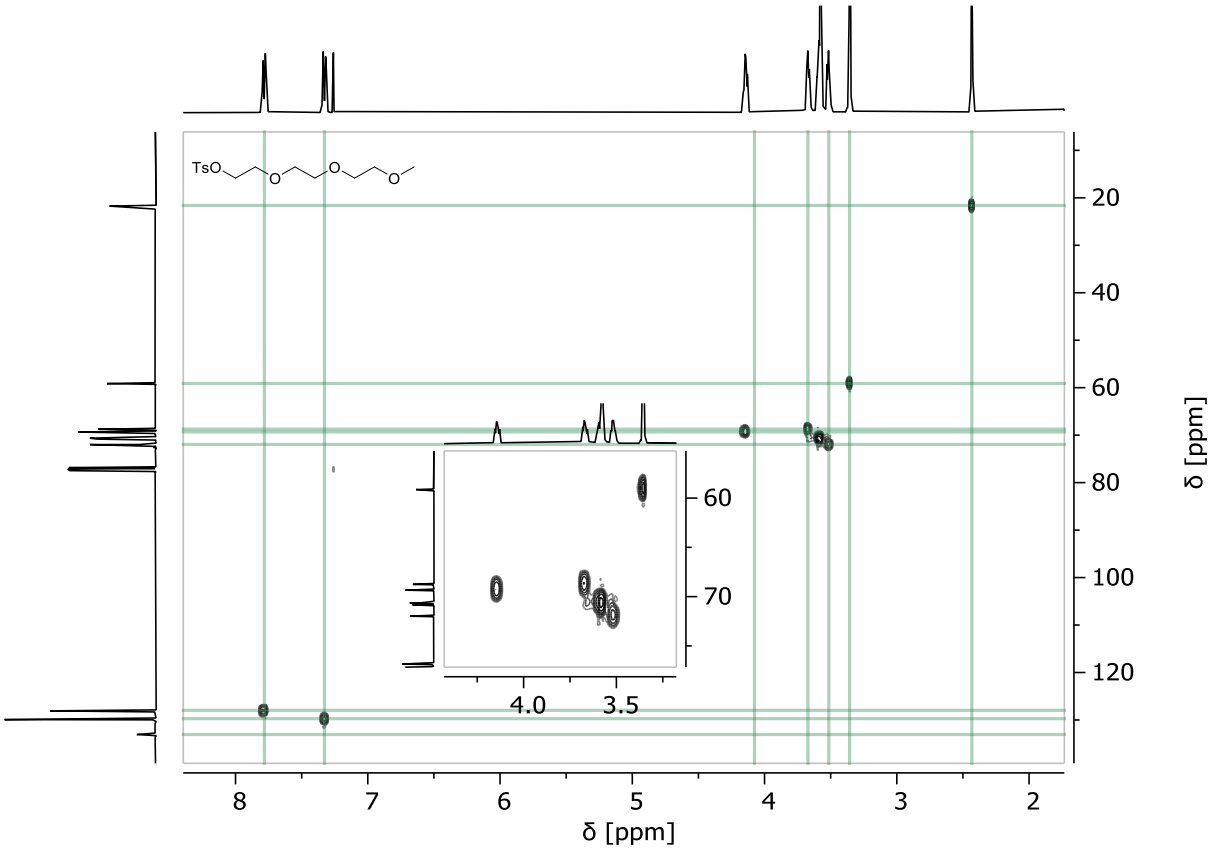

Fig.S 34: HSQC-spectrum of triethylene glycol monomethyl tosylate.

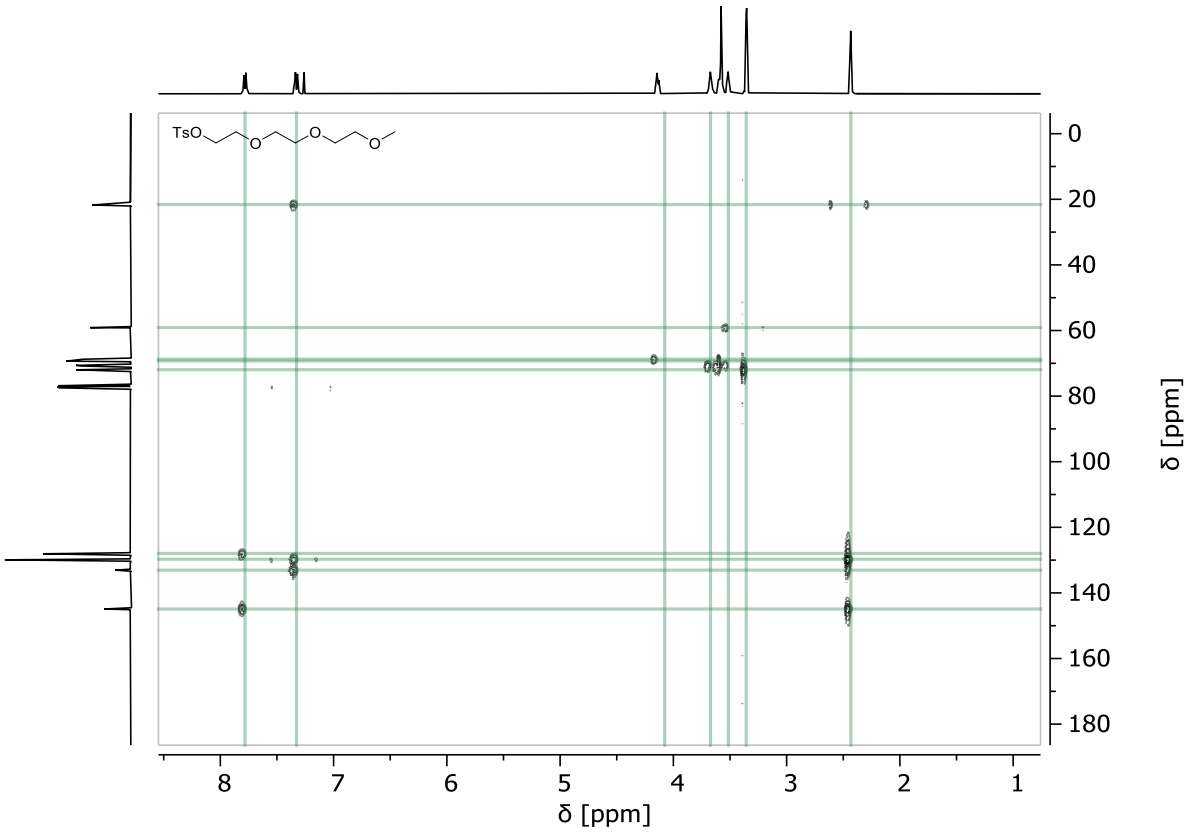

Fig.S 35: HMBC-spectrum of triethylene glycol monomethyl tosylate.

Methoxy triethylene glycol azide

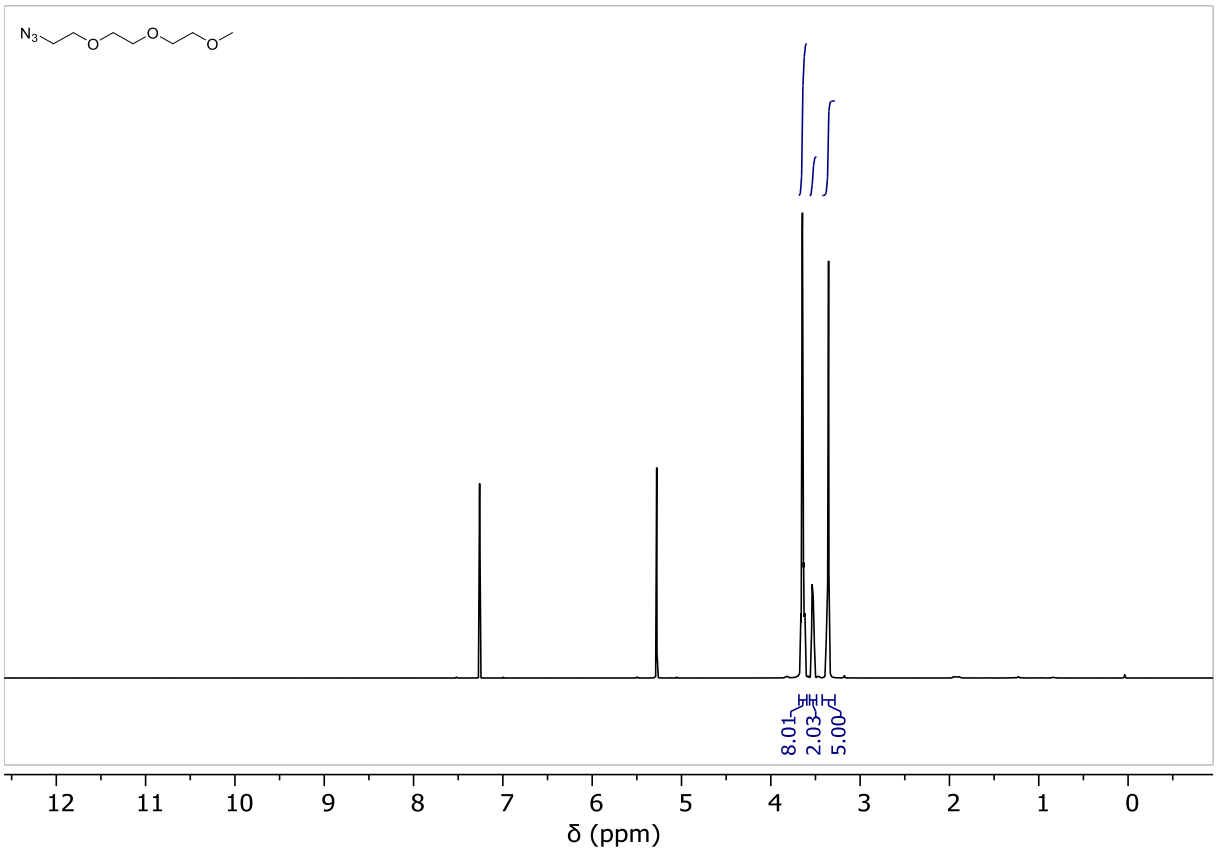

Fig.S 36: ^{1}H-NMR of triethylene glycol monomethyl azide

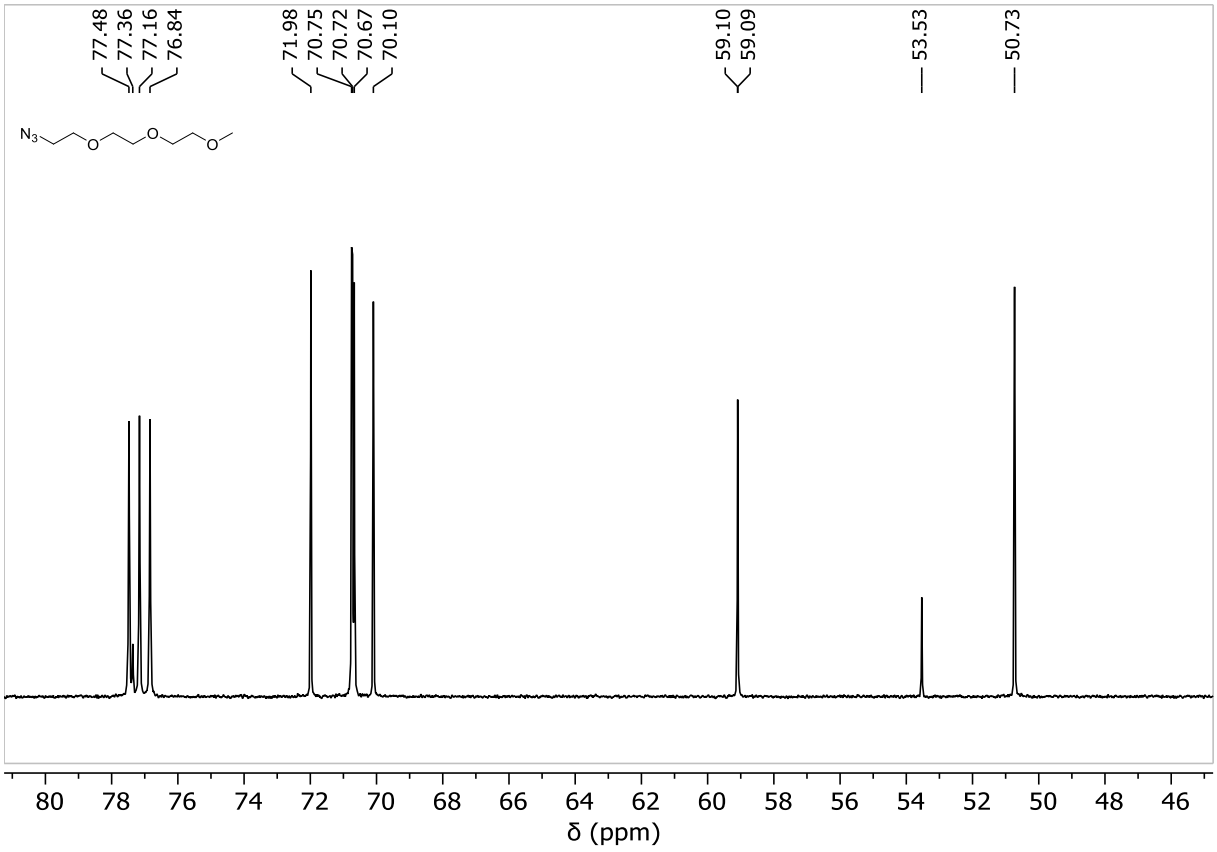

Fig.S 37: ^{13}C-NMR of triethylene glycol monomethyl azide.

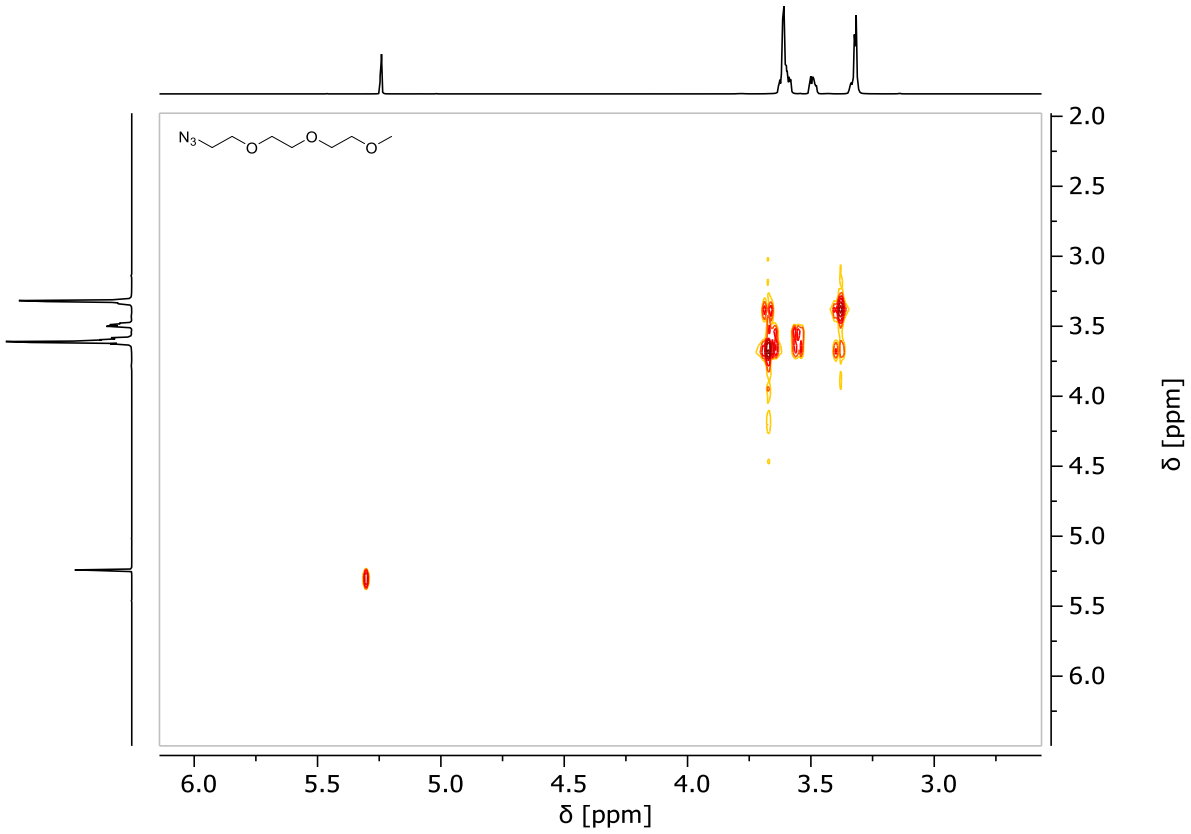

Fig.S 38: COSY-spectrum of triethylene glycol monomethyl azide.

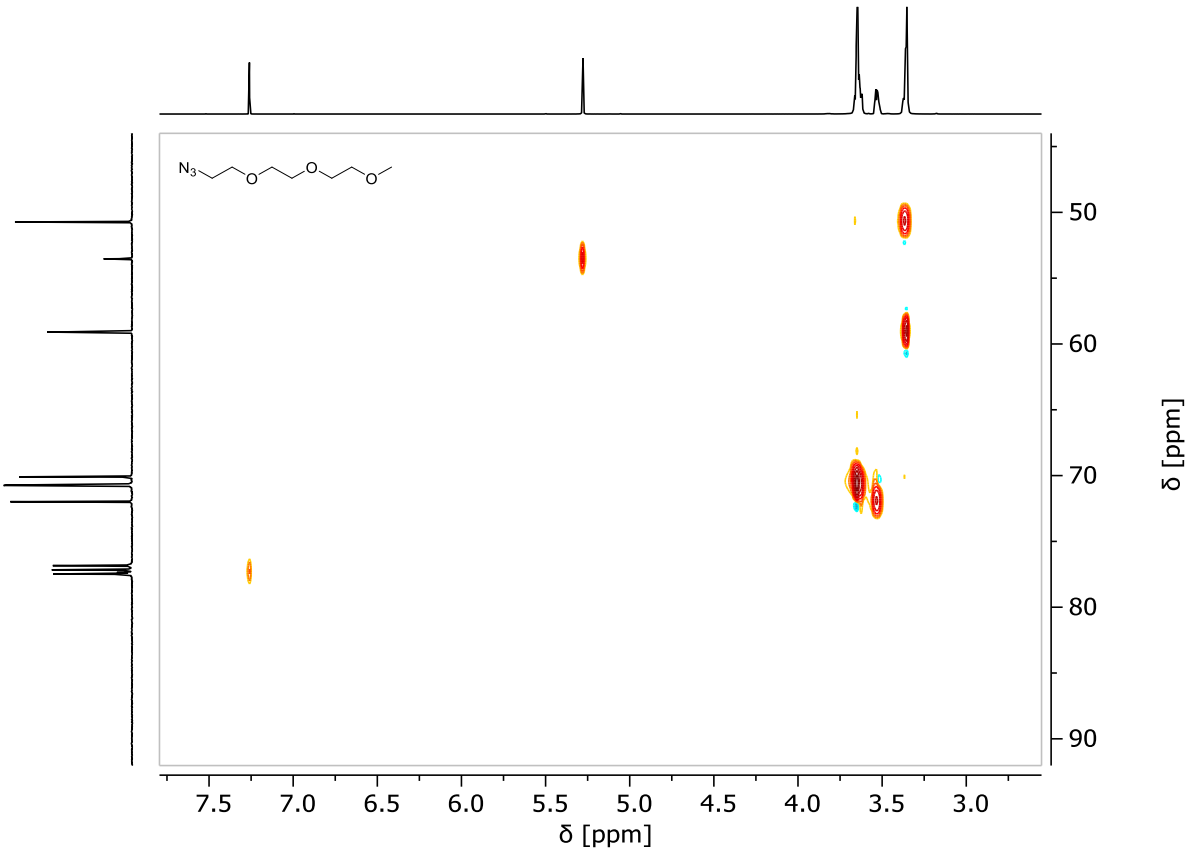

Fig.S 39: HSQC-spectrum of triethylene glycol monomethyl azide.

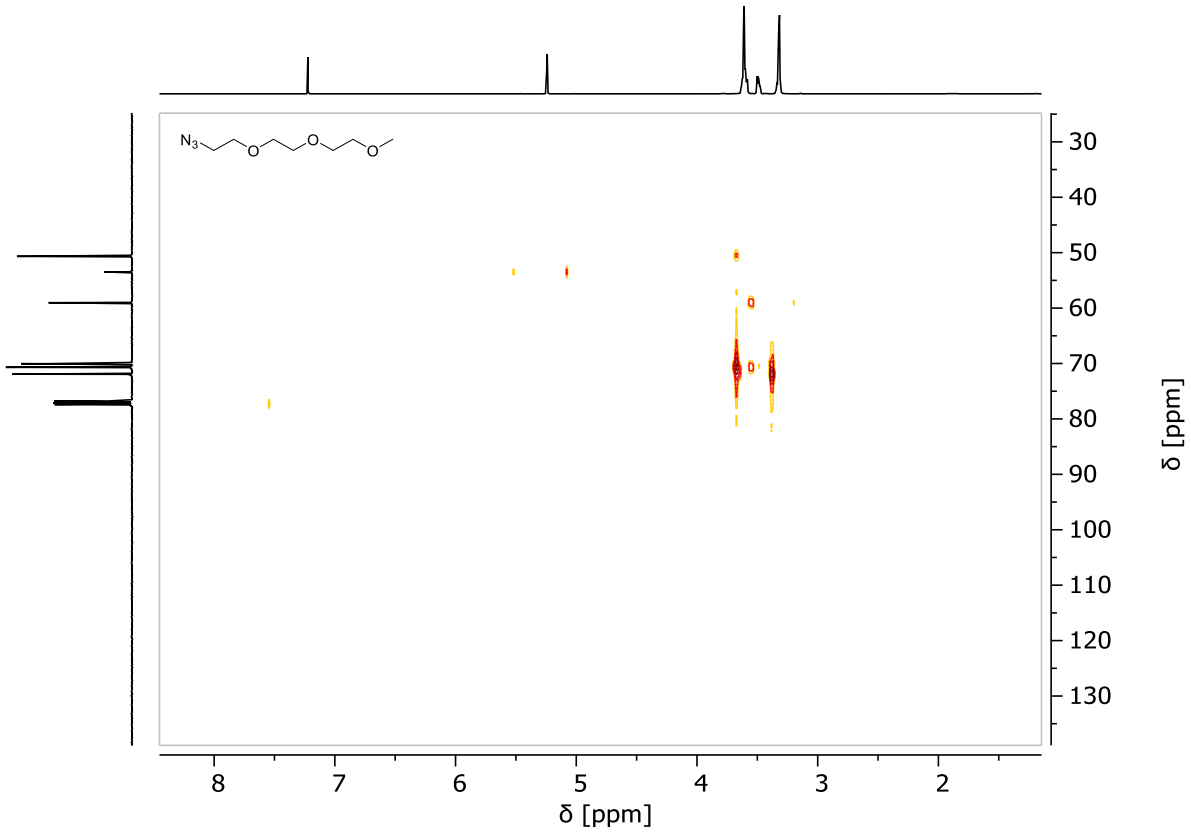

Fig.S 40: HMBC-spectrum of triethylene glycol monomethyl azide.

2-(2-(2-Methoxyethoxy)ethoxy) ethanamine

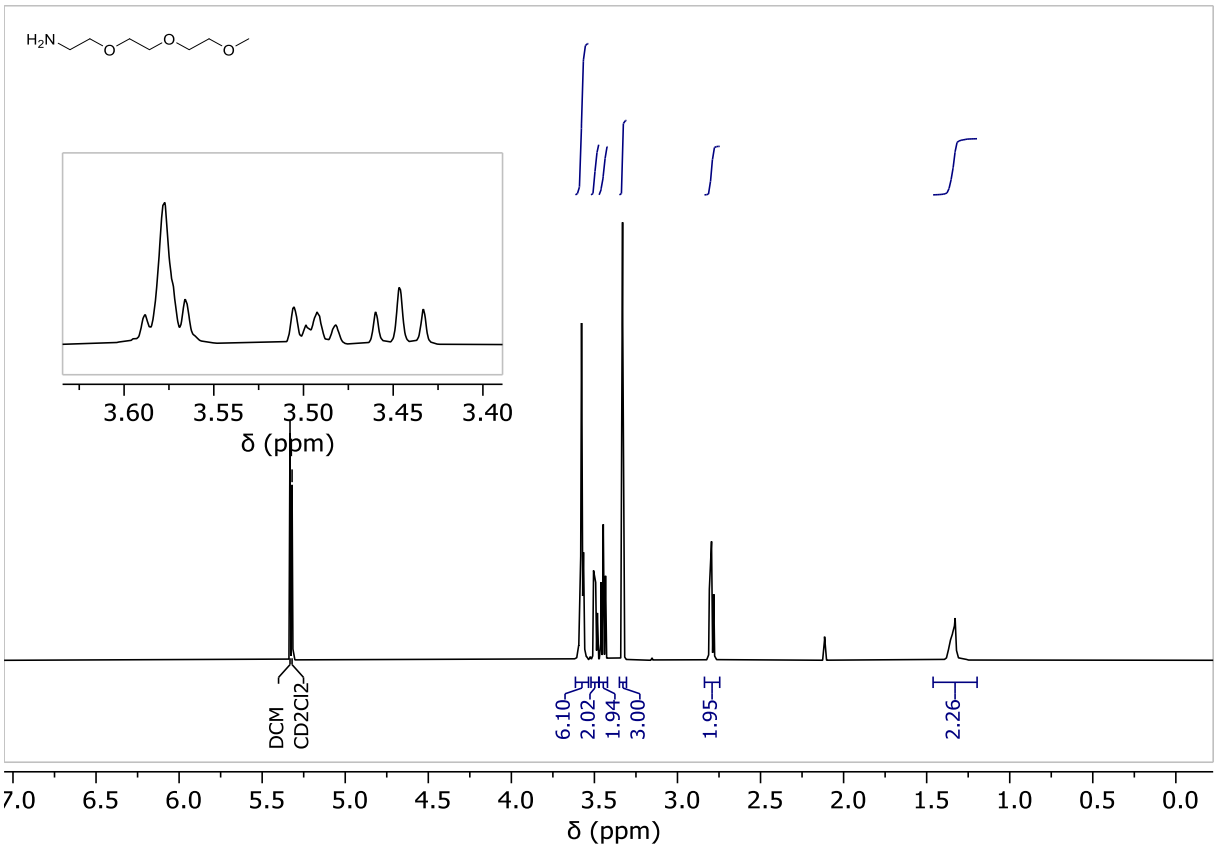

Fig.S 41: ^{1}H-NMR of 2-(2-(2-Methoxyethoxy)ethoxy) ethanamine.

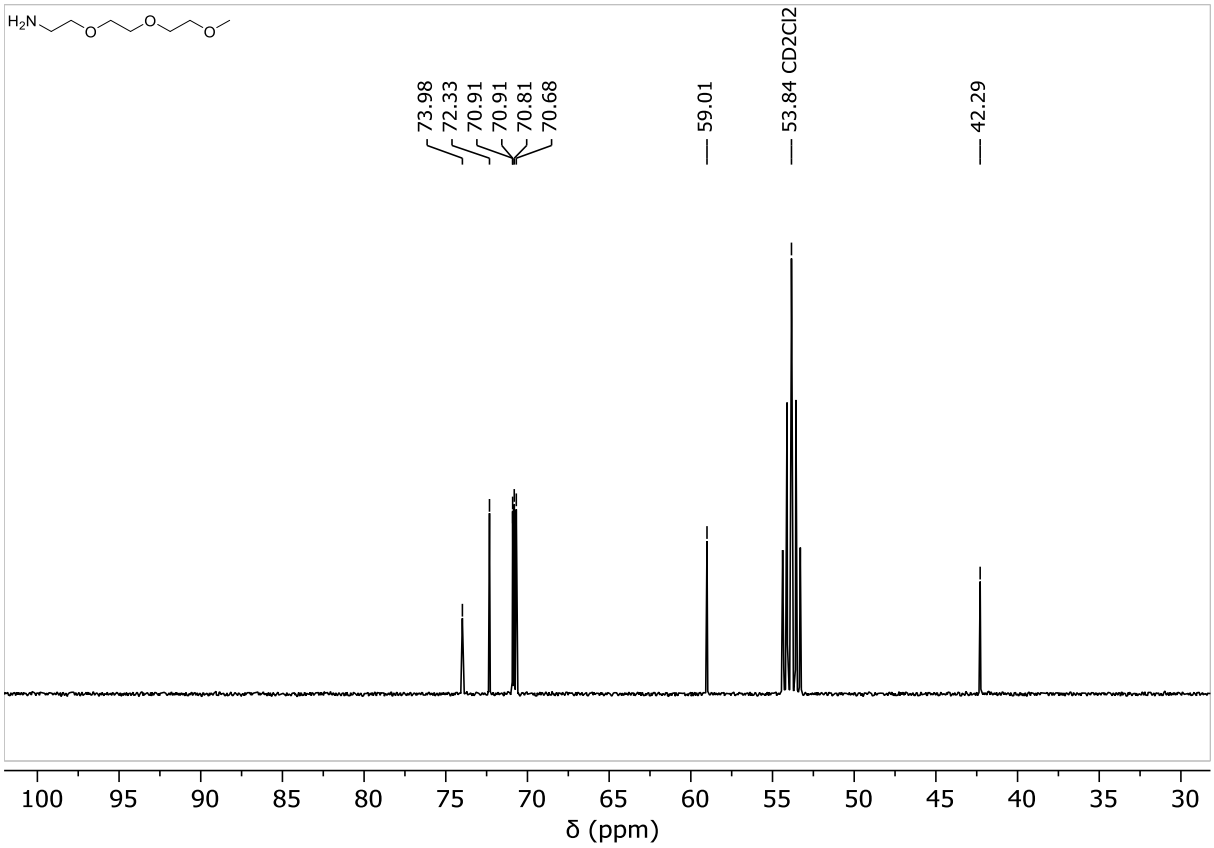

Fig.S 42: ^{13}C-NMR of 2-(2-(2-Methoxyethoxy)ethoxy) ethanamine.

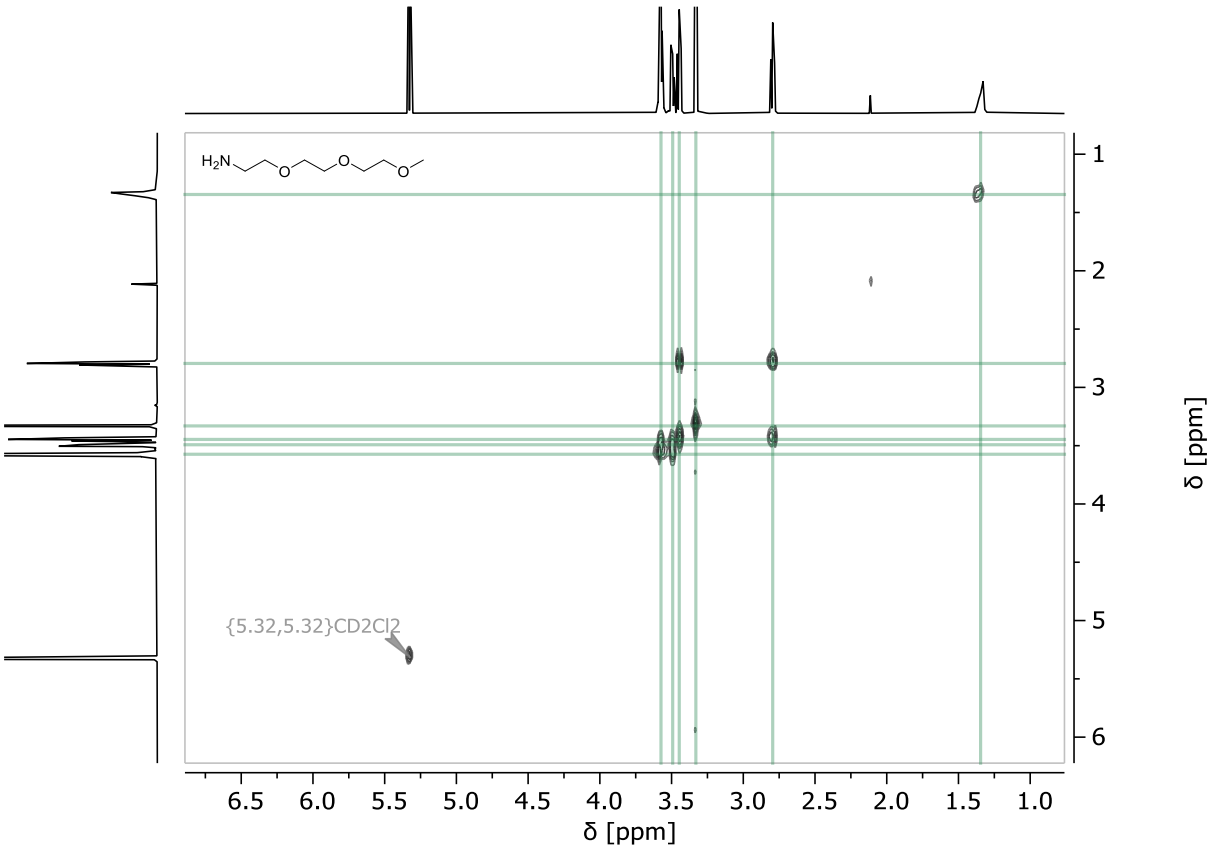

Fig.S 43: COSY-spectrum of 2-(2-(2-Methoxyethoxy)ethoxy) ethanamine.

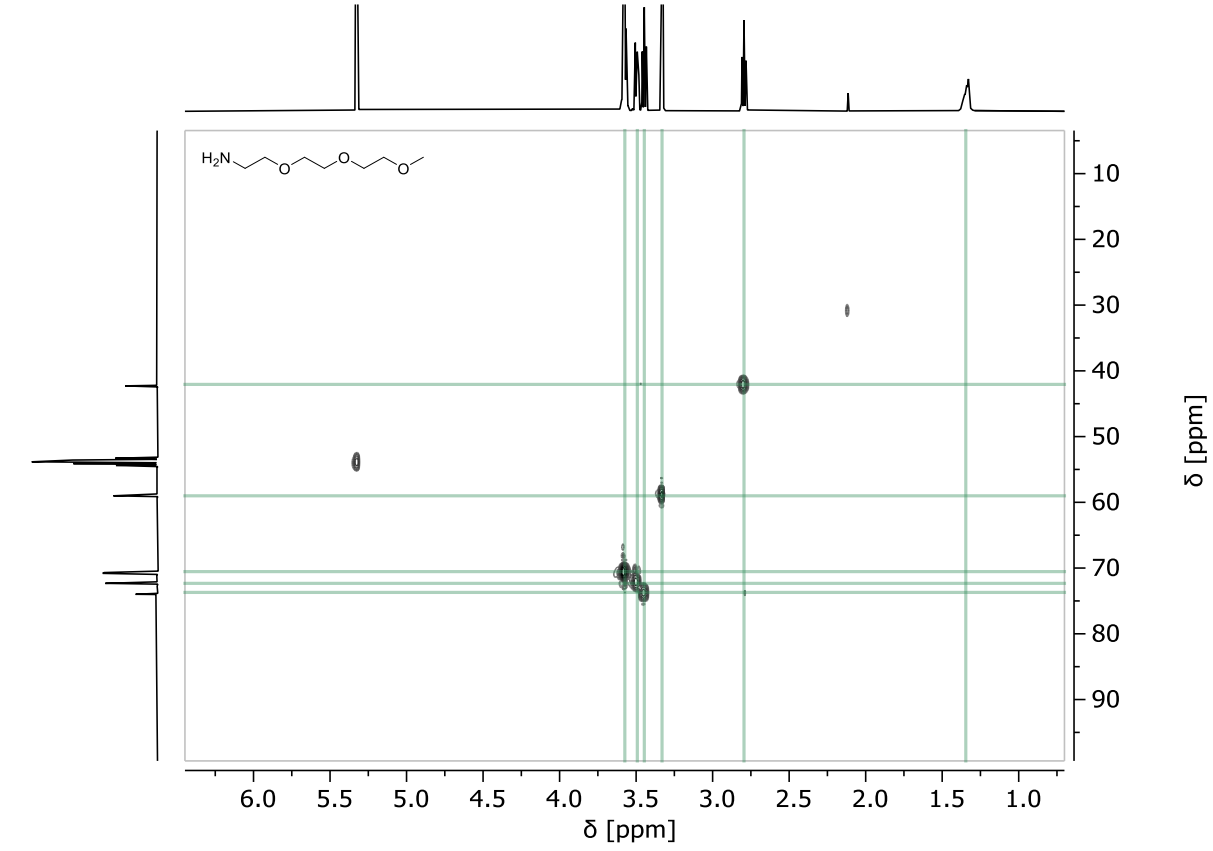

Fig.S 44: HSQC-spectrum of 2-(2-(2-Methoxyethoxy)ethoxy) ethanamine.

7-Oxanorbornene-2,3-exo-dicarboximide

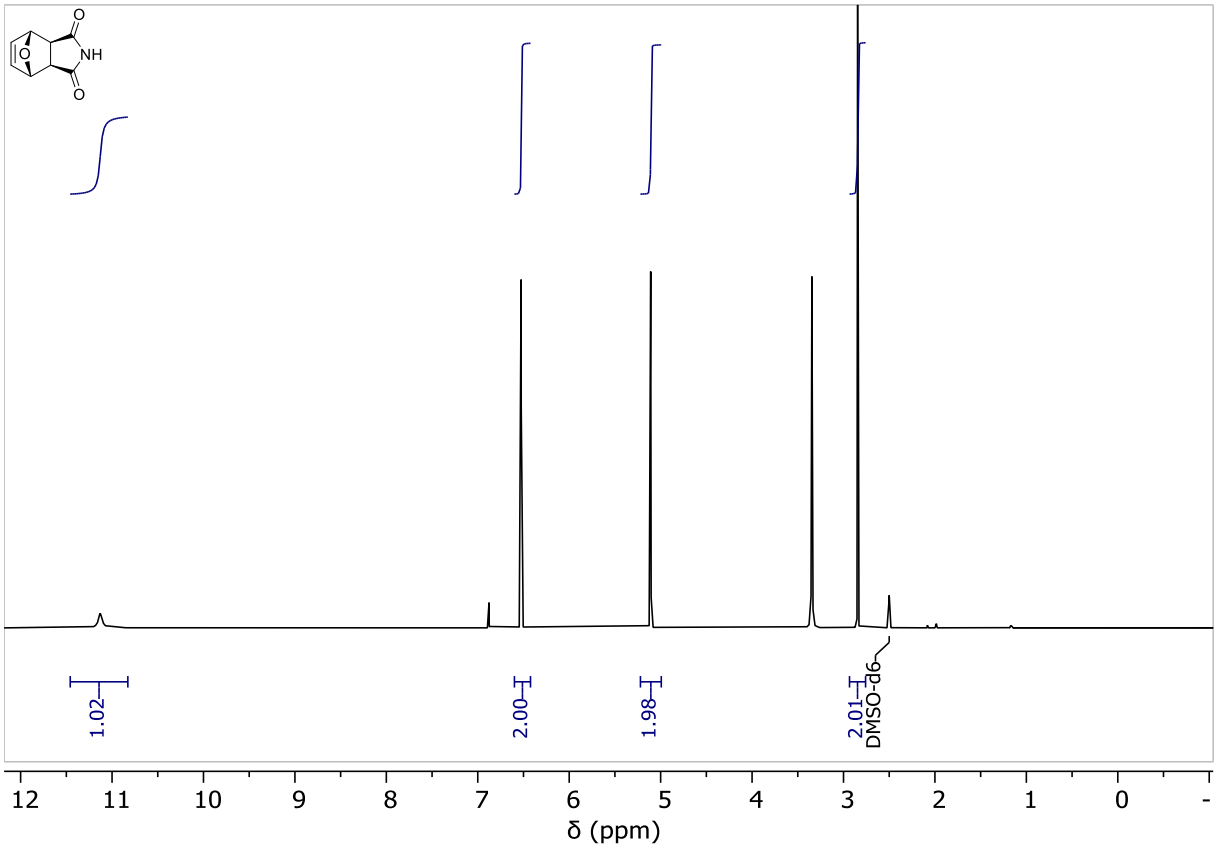

Fig.S 45: ^{1}H-NMR of 7-oxanorbornene-2,3-*exo*-dicarboximide.

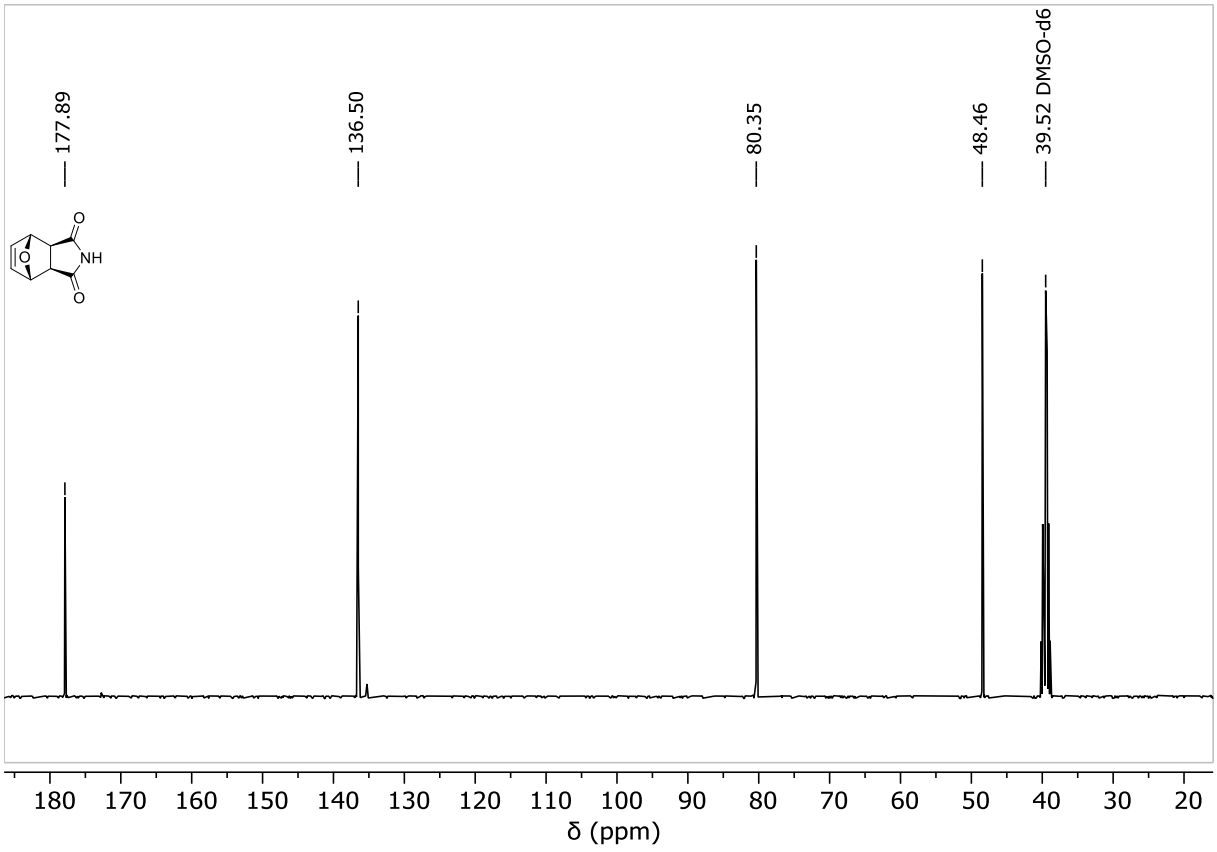

Fig.S 46: ^{13}C-NMR of 7-oxanorbornene-2,3-*exo*-dicarboximide.

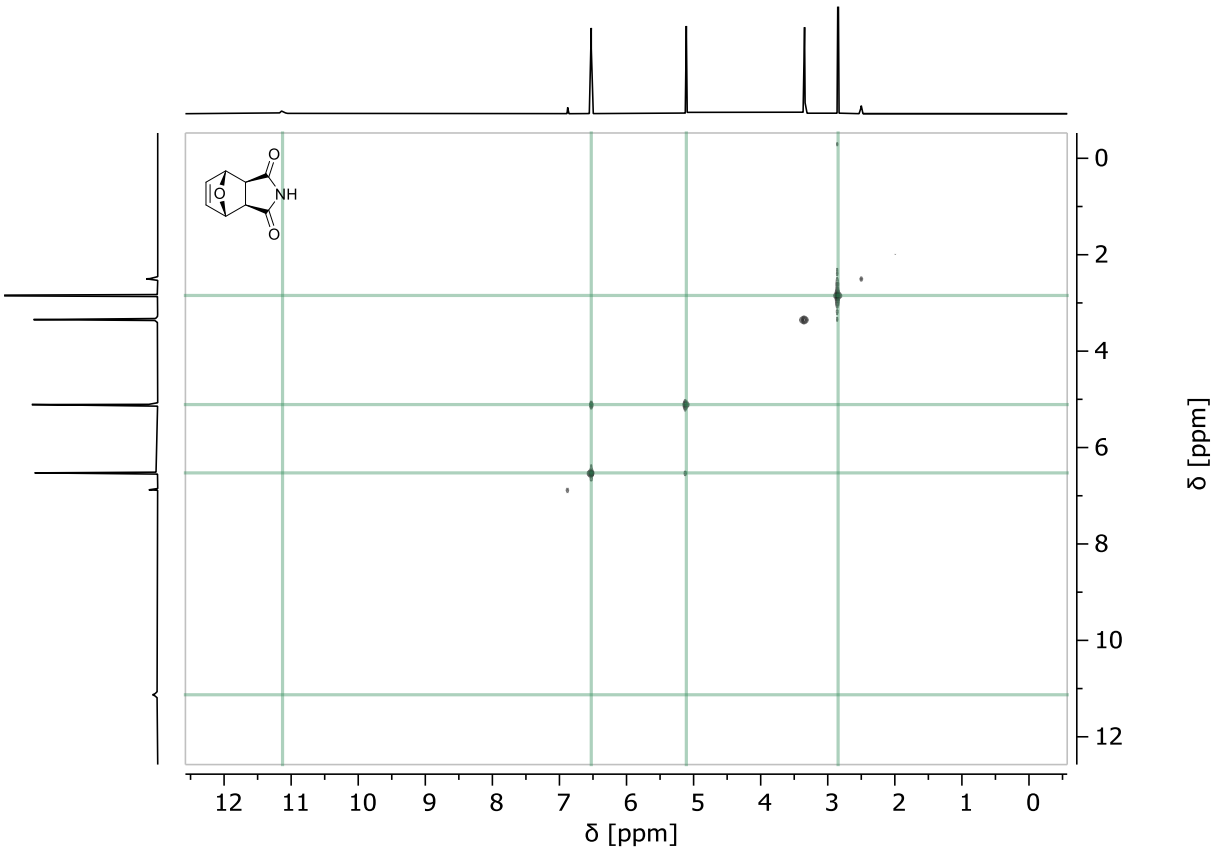

Fig.S 47: COSY-spectrum of 7-oxanorbornene-2,3-*exo*-dicarboximide.

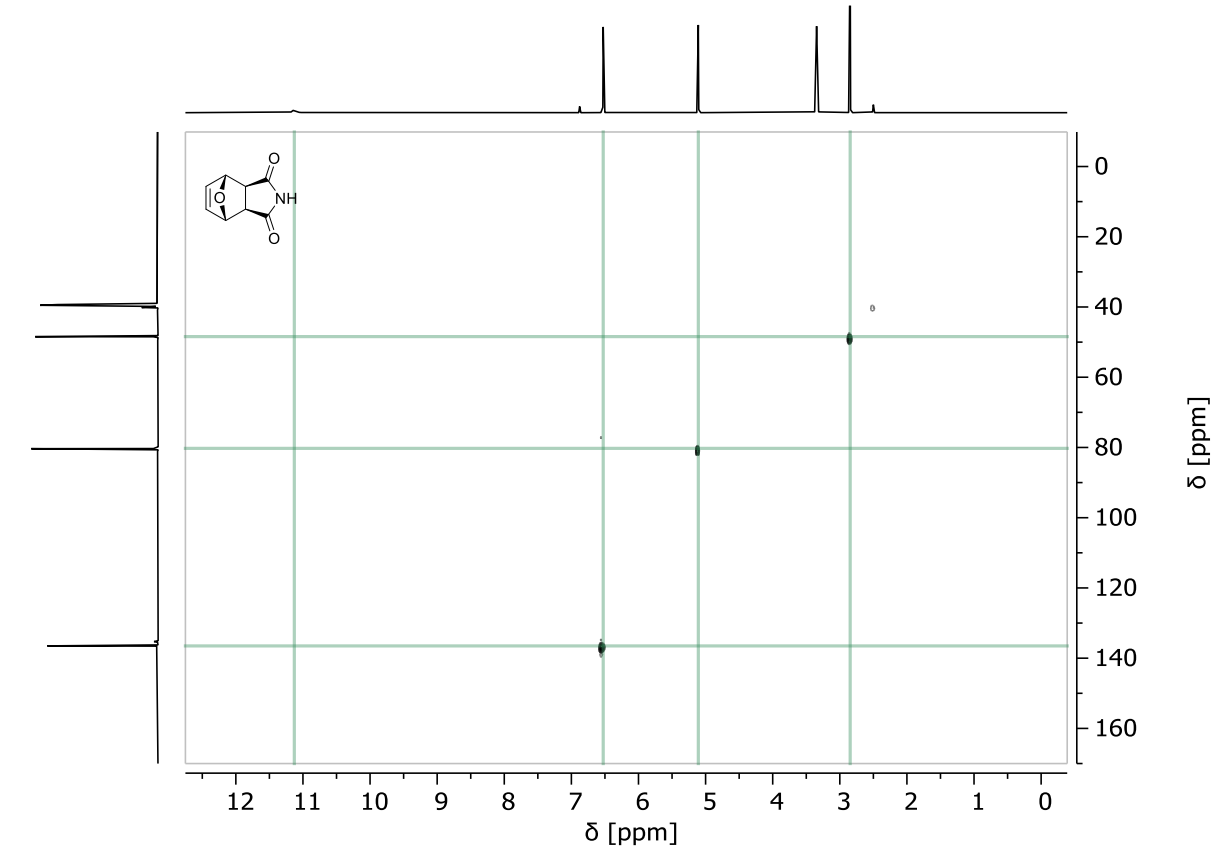

Fig.S 48: HSQC-spectrum-NMR of 7-oxanorbornene-2,3-*exo*-dicarboximide.

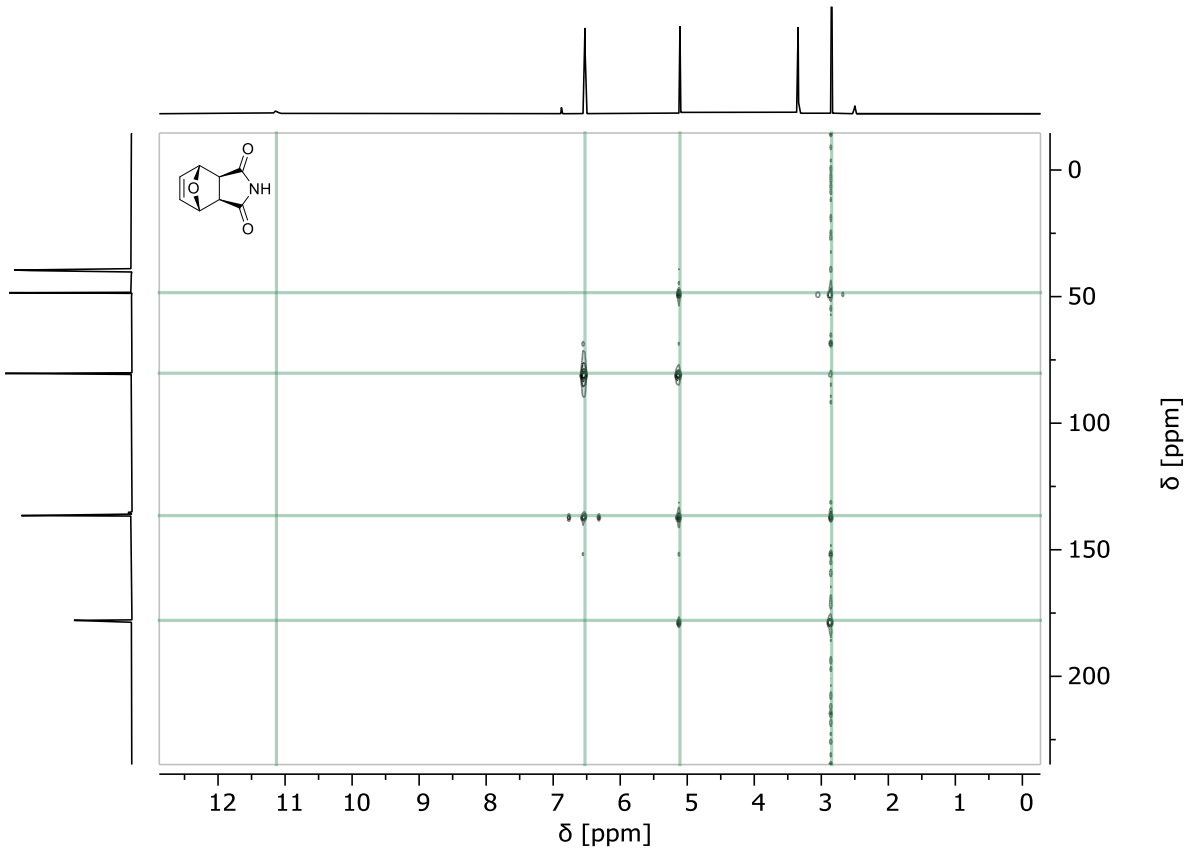

Fig.S 49: HMBC-spectrum of 7-oxanorbornene-2,3-*exo*-dicarboximide.

N-(triethylene glycol)-7-oxanorborn-5-ene-2,3-dicarboximide

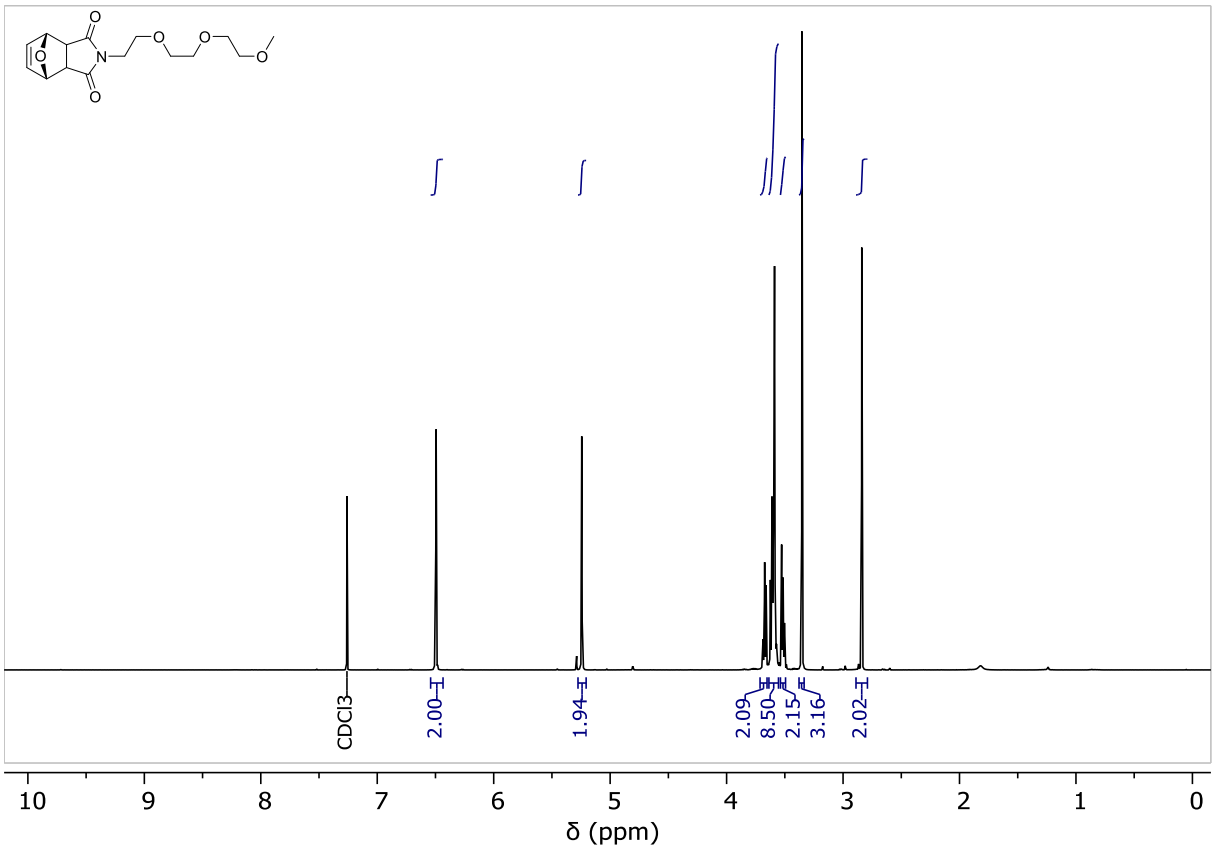

Fig.S 50: ^{1}H-NMR of *N*-(triethylene glycol)-7-oxanorborn-5-ene-2,3-dicarboximide.

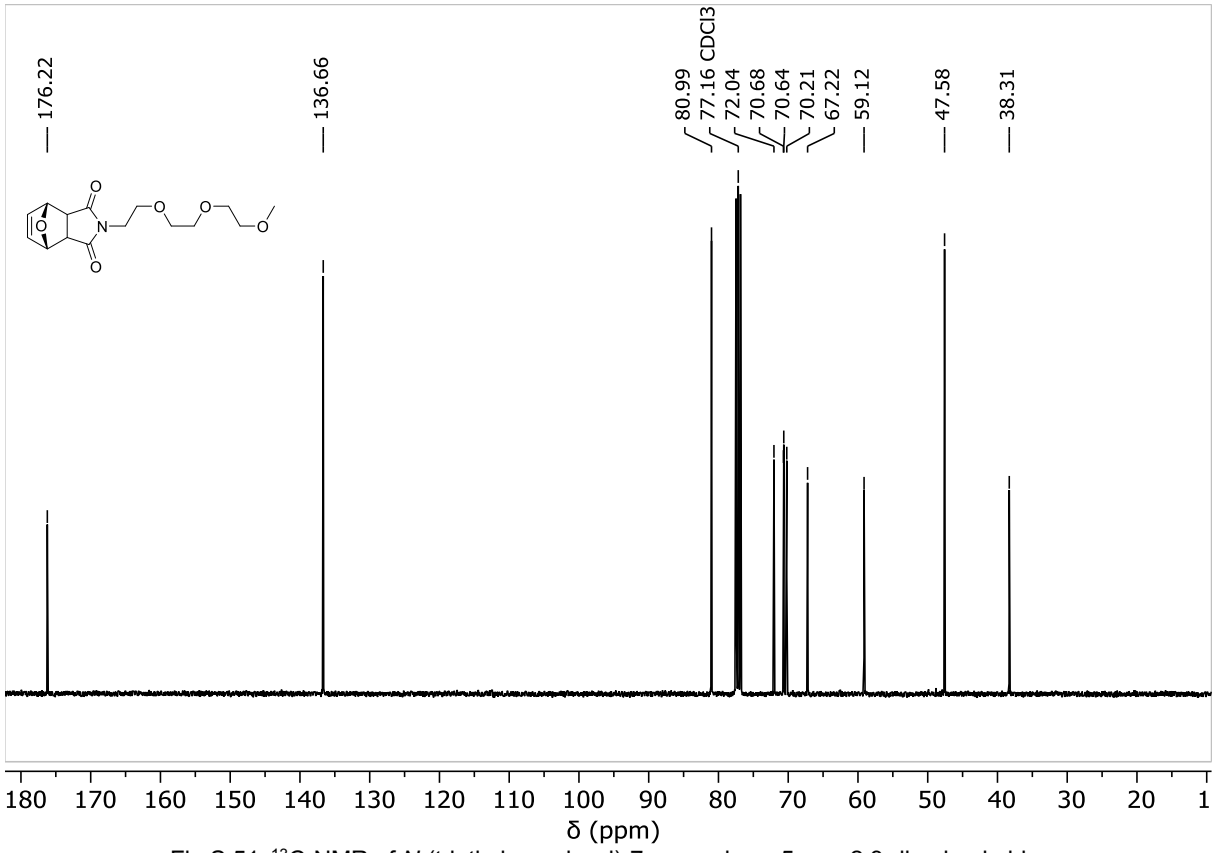

Fig.S 51: ^{13}C-NMR of *N*-(triethylene glycol)-7-oxanorborn-5-ene-2,3-dicarboximide.

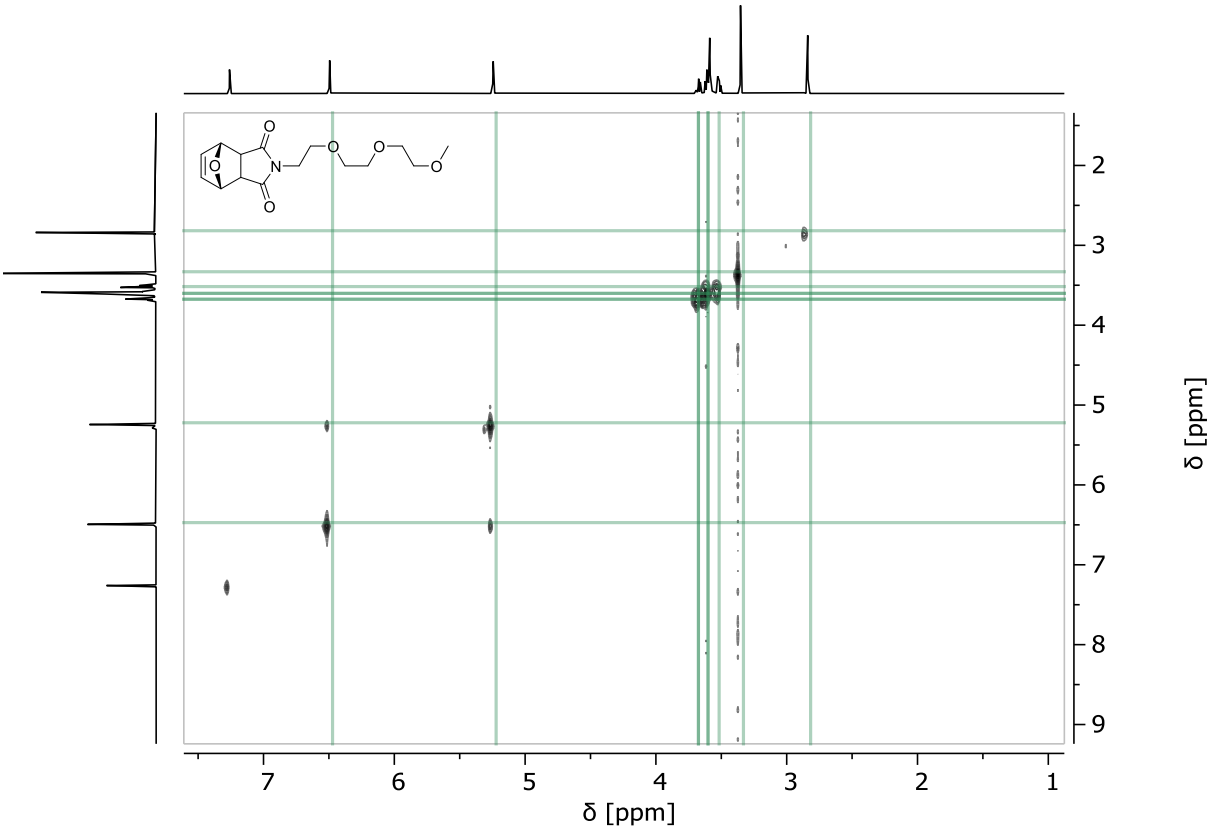

Fig.S 52: COSY-spectrum of *N*-(triethylene glycol)-7-oxanorborn-5-ene-2,3-dicarboximide.

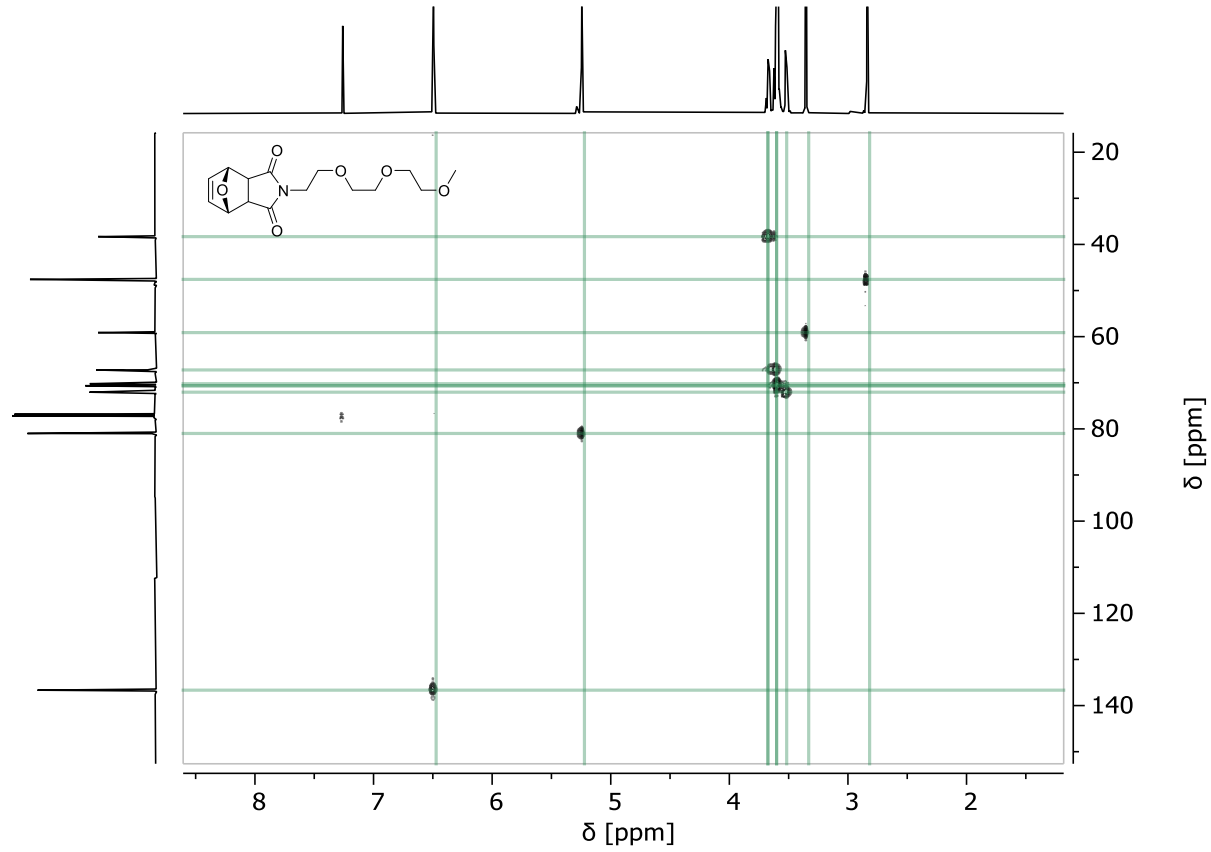

Fig.S 53: HSQC spectrum of *N*-(triethylene glycol)-7-oxanorborn-5-ene-2,3-dicarboximide.

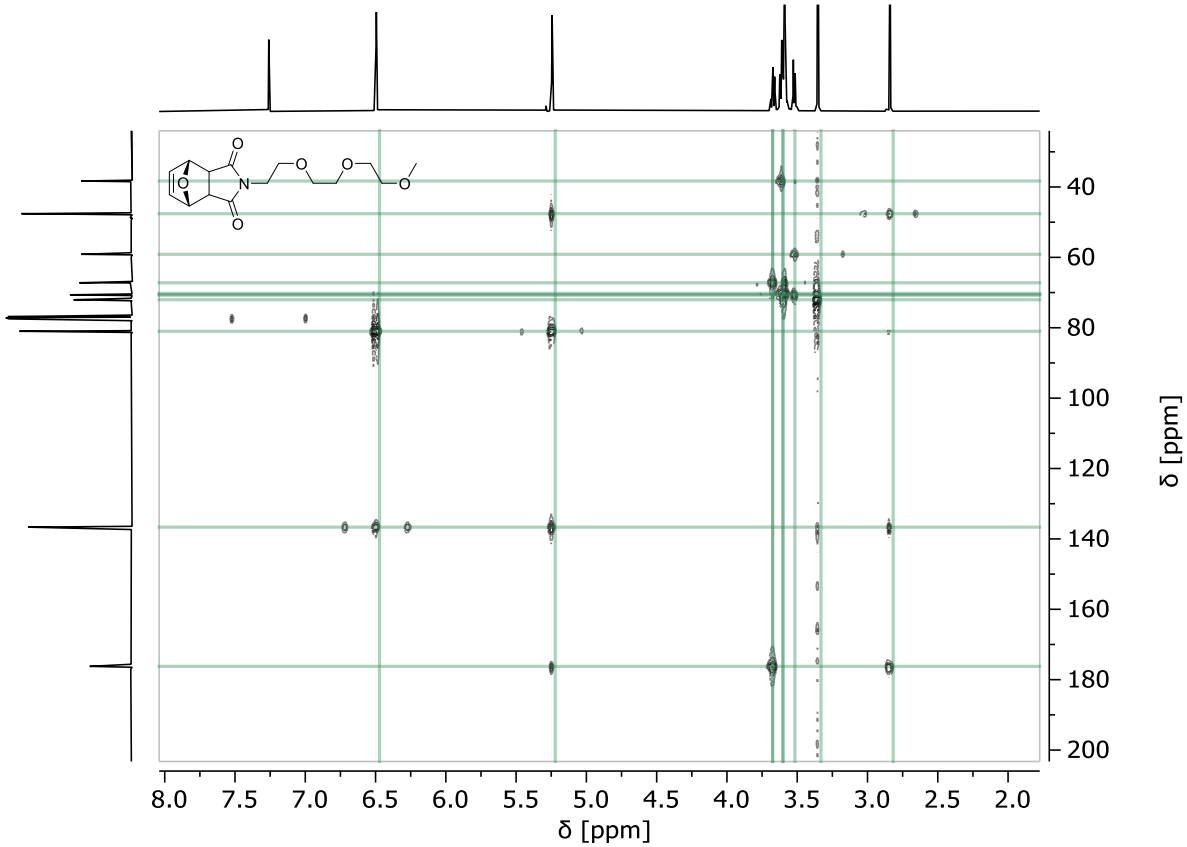

Fig.S 54: HMBC spectrum of *N*-(triethylene glycol)-7-oxanorborn-5-ene-2,3-dicarboximide.

9.2 Polymers

Homopolymers of ONB-Pfp

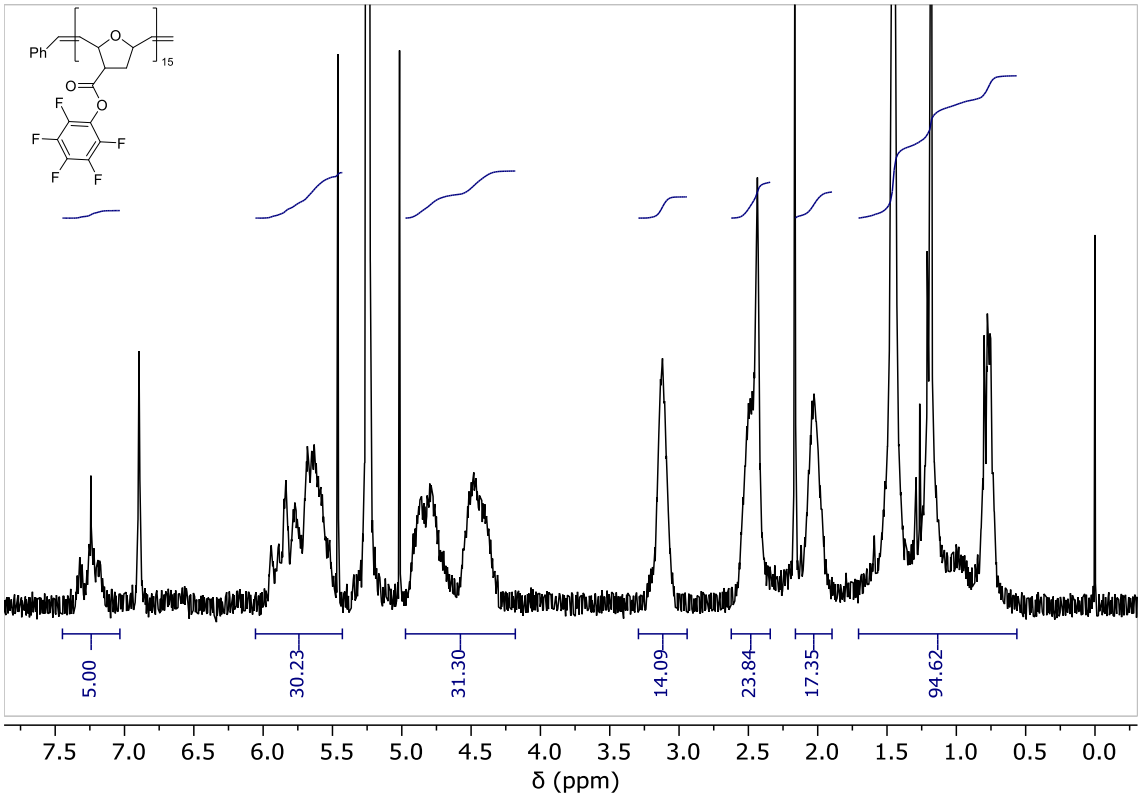

Fig.S 55:[1]H NMR of the Homopolymer P(ONB-PFP)-15.

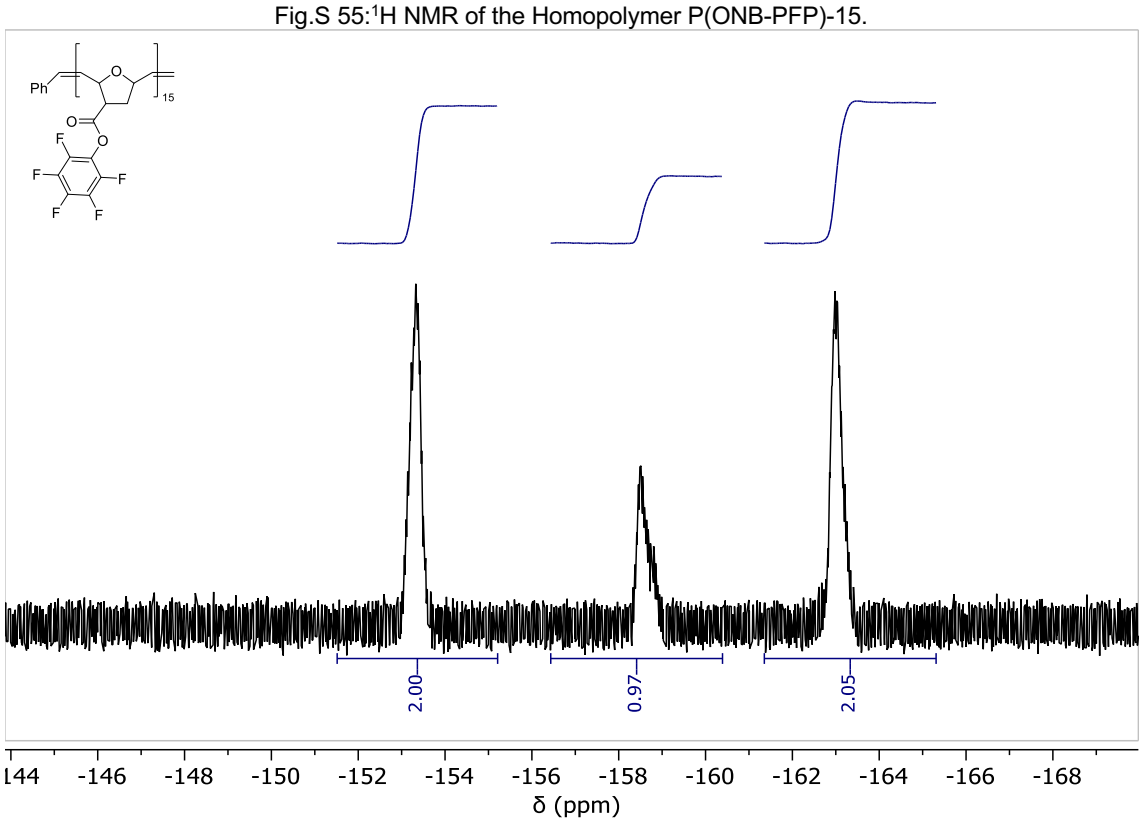

Fig.S 56: [19]F NMR of the Homopolymer P(ONB-PFP)-15.

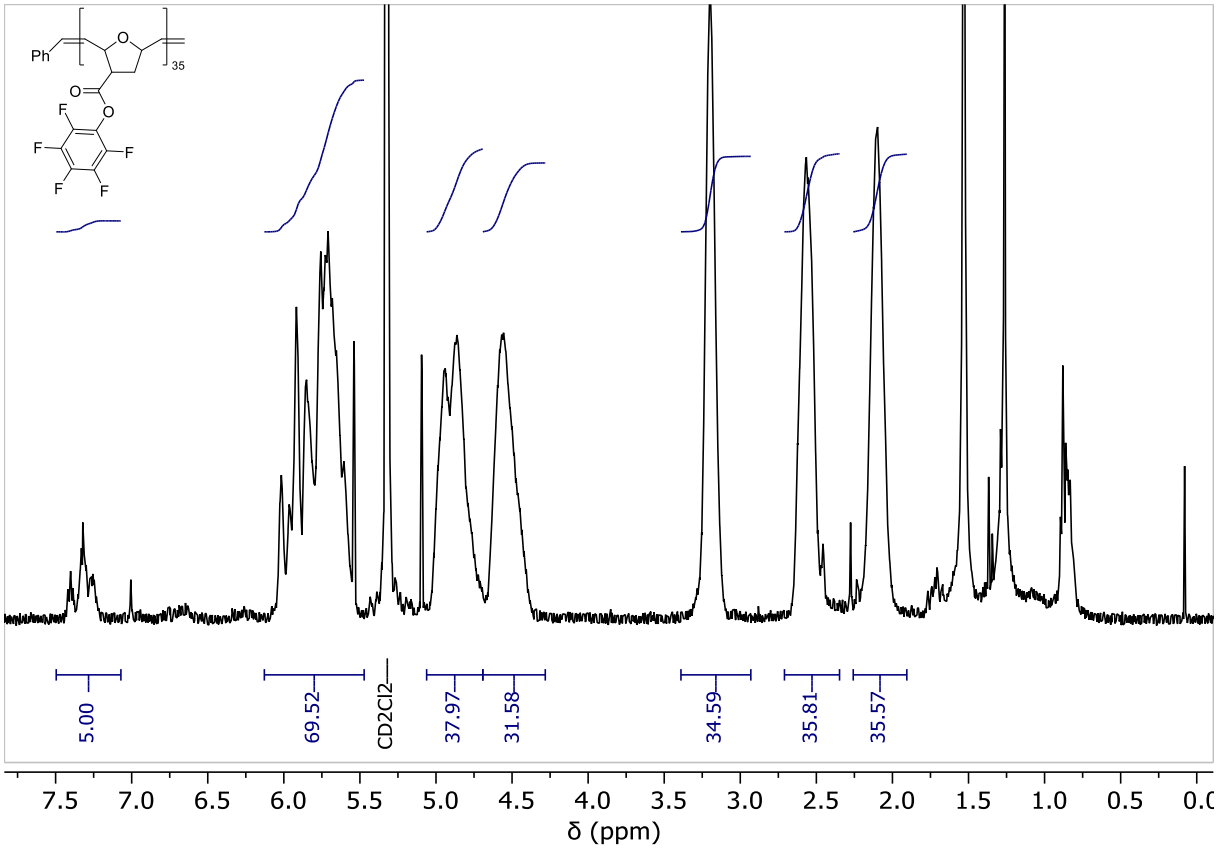

Fig.S 57: ^{1}H NMR of the Homopolymer P(ONB-PFP)-35.

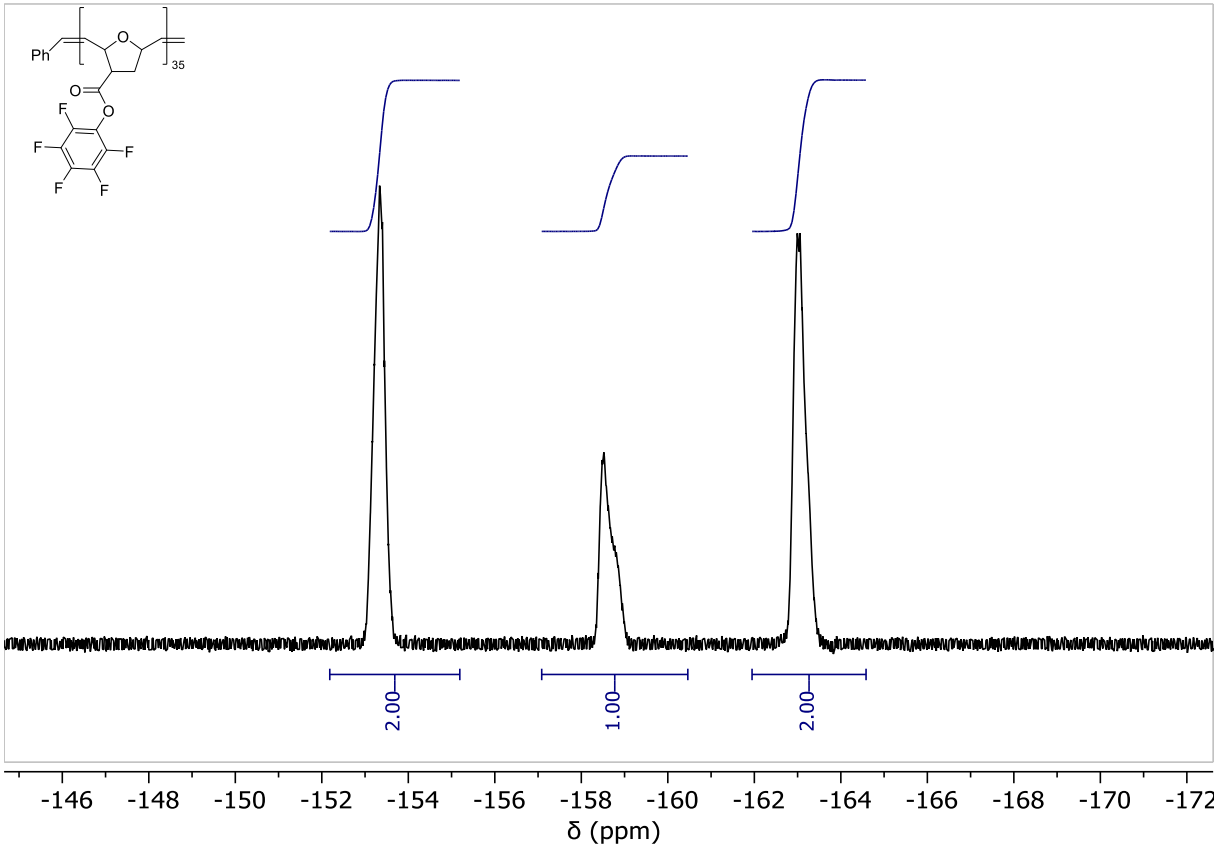

Fig.S 58: ^{19}F NMR of the Homopolymer P(ONB-PFP)-35.

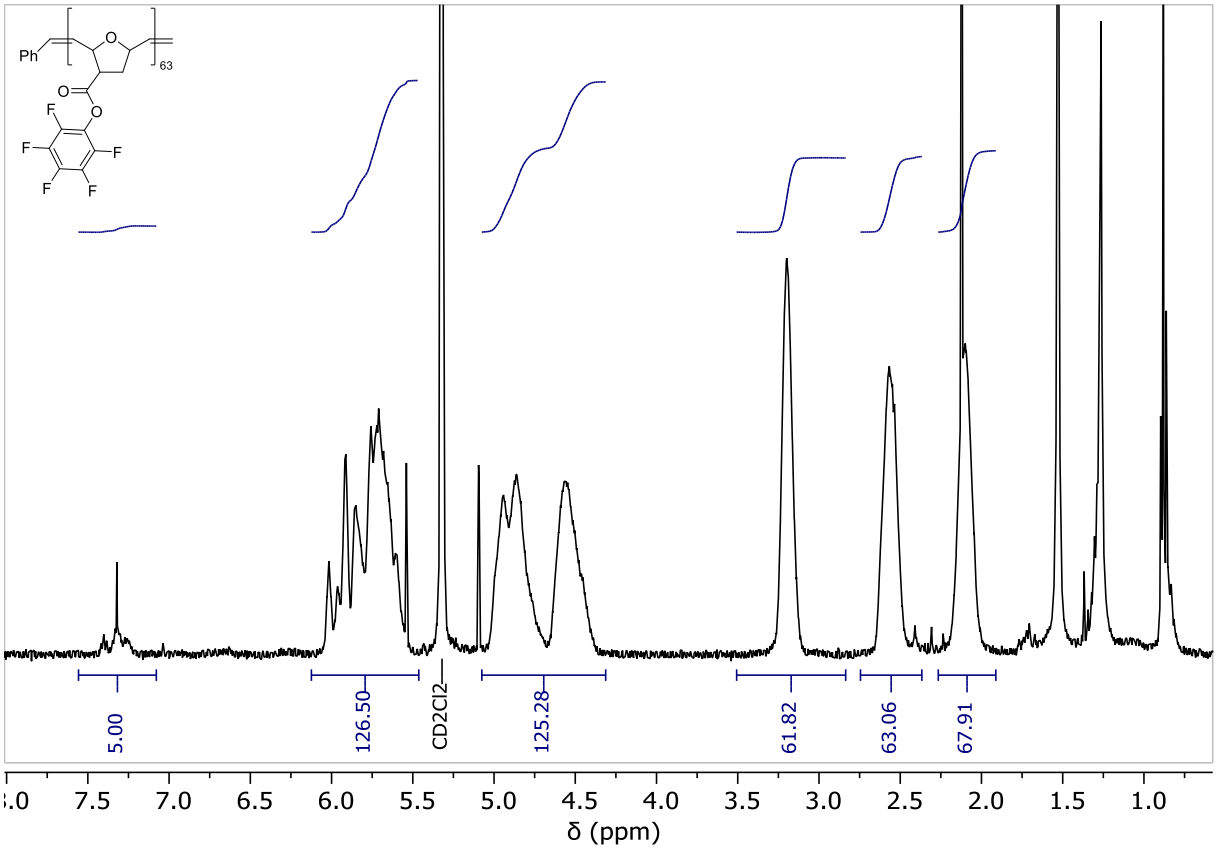

Fig.S 59: ^{1}H NMR of the Homopolymer P(ONB-PFP)-63.

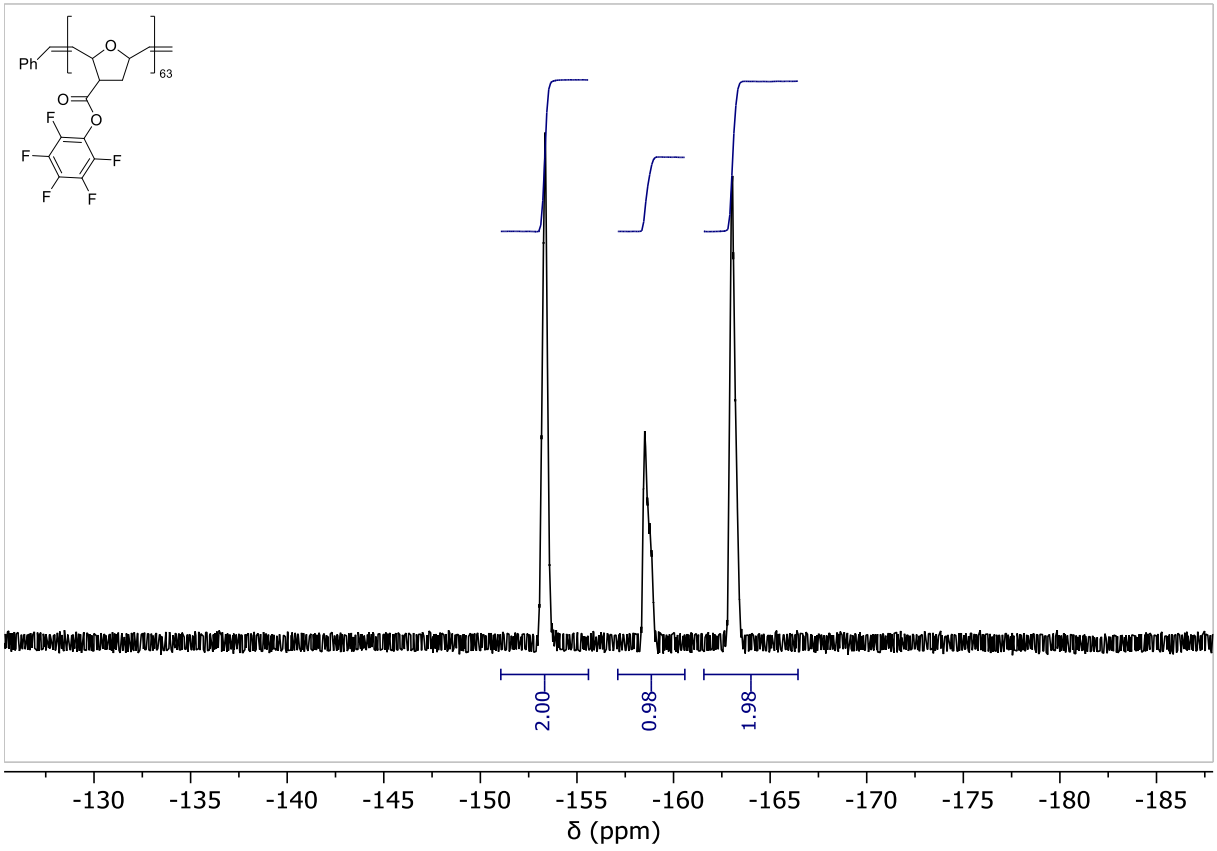

Fig.S 60: ^{19}F NMR of the Homopolymer P(ONB-PFP)-63.

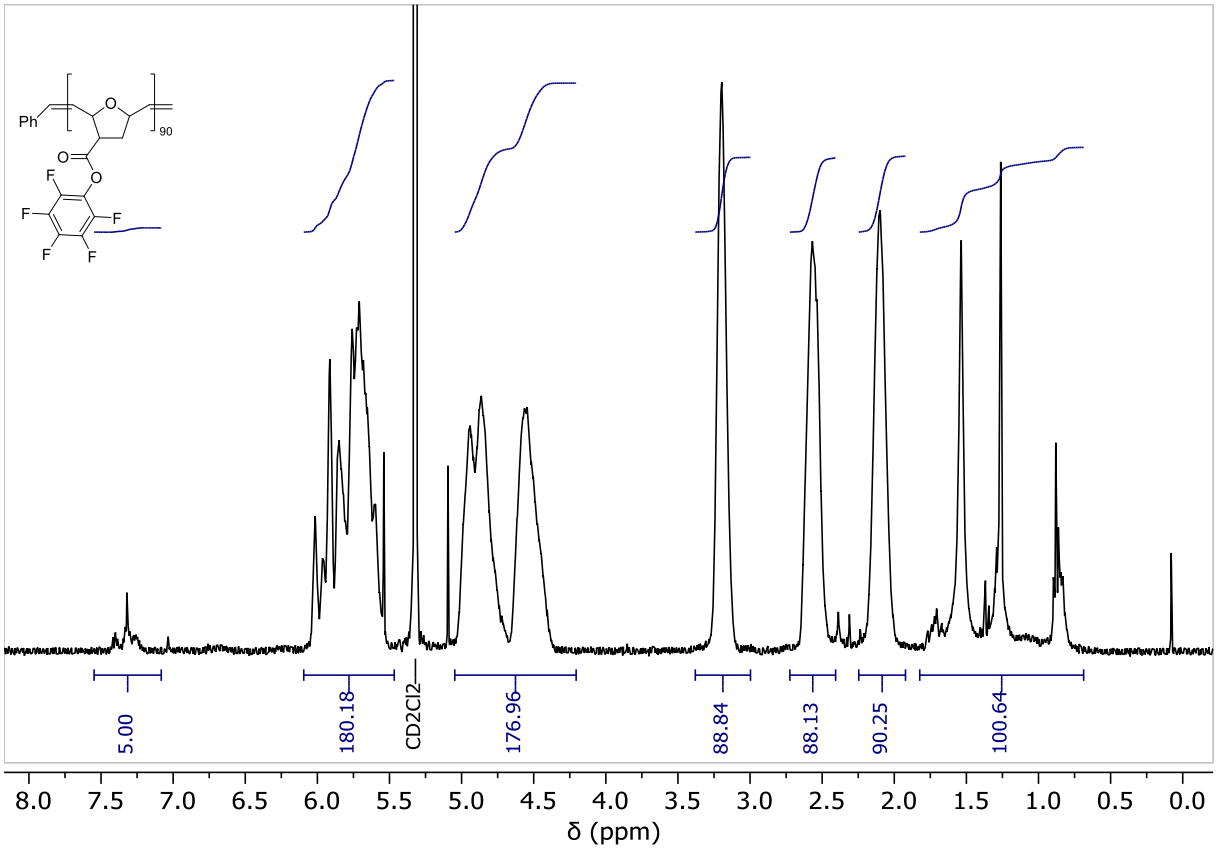

Fig.S 61: ^{1}H NMR of the Homopolymer P(ONB-PFP)-15.

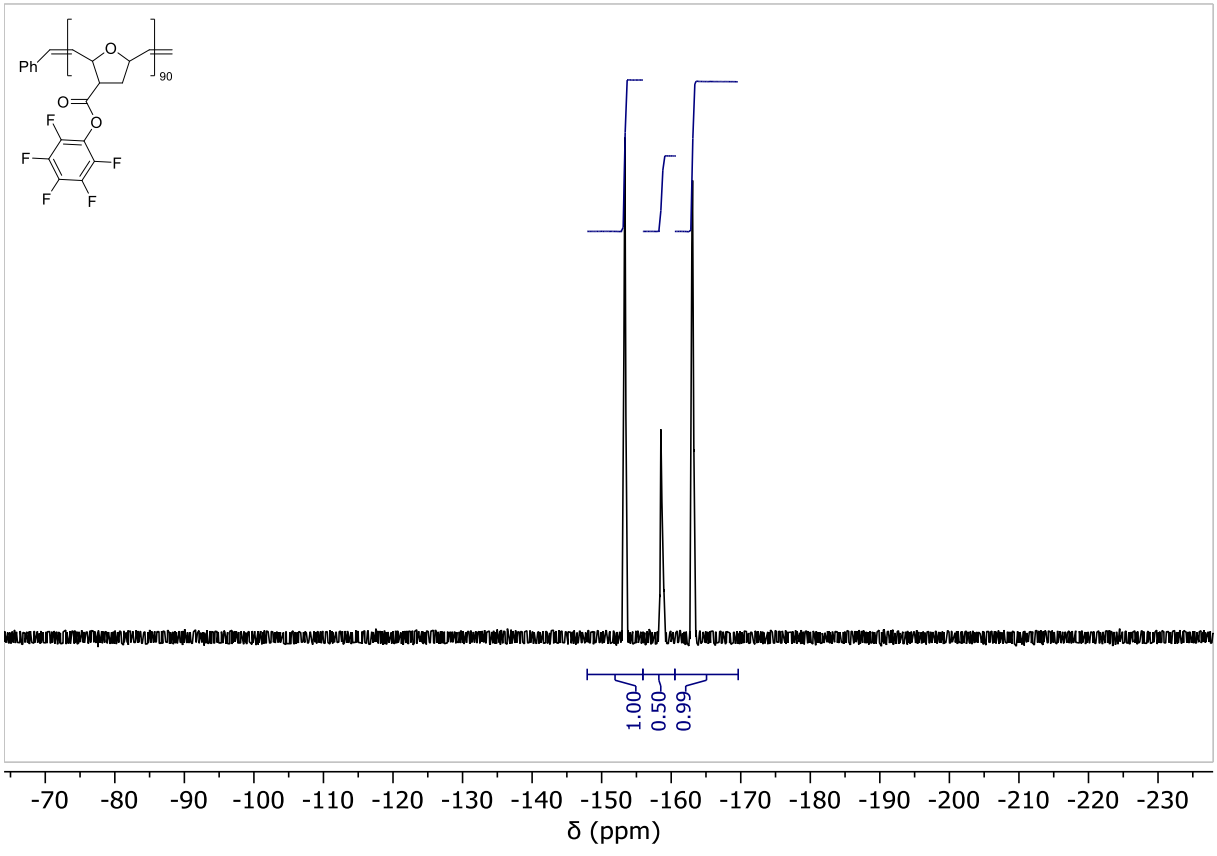

Fig.S 62: ^{19}F NMR of the Homopolymer P(ONB-PFP)-90.

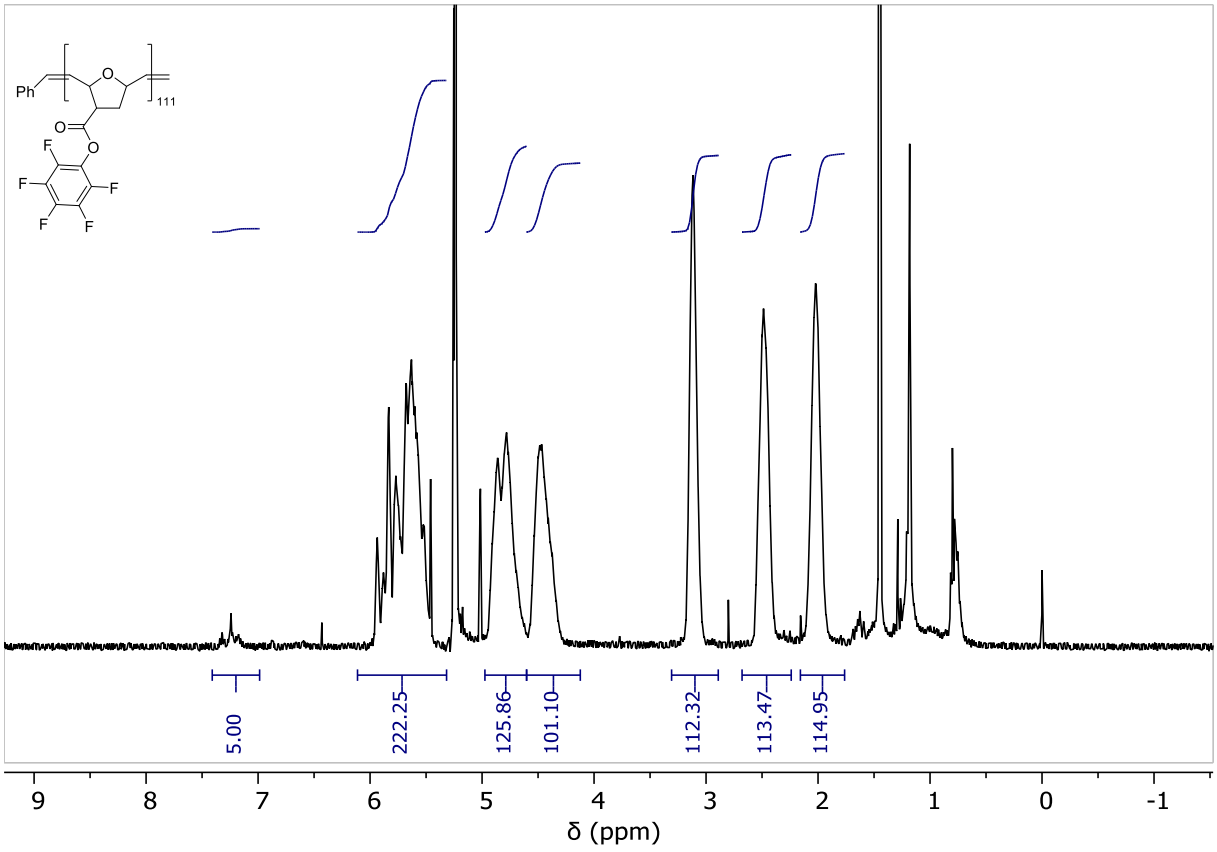

Fig.S 63: ^{1}H NMR of the Homopolymer P(ONB-PFP)-111.

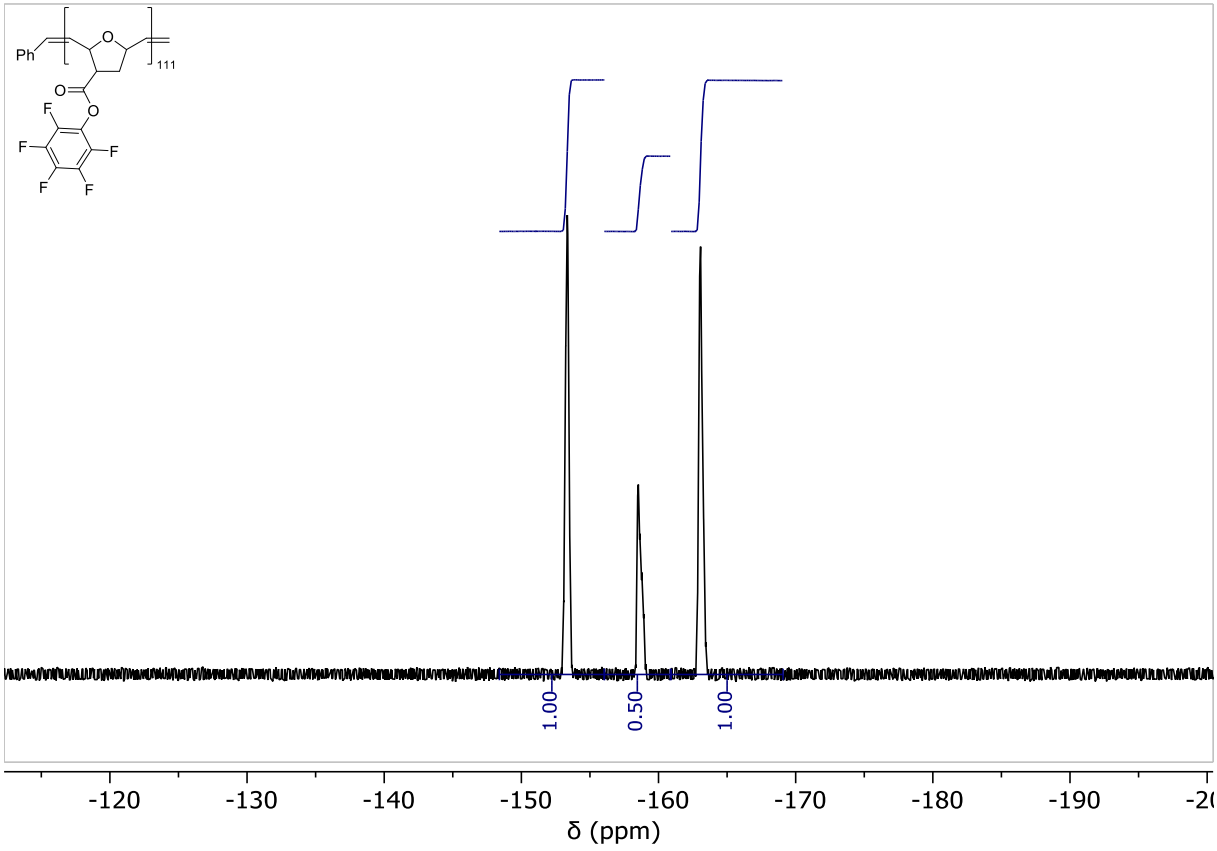

Fig.S 64: ^{19}F NMR of the Homopolymer P(ONB-PFP)-111.

Homopolymers of ONB-TEG

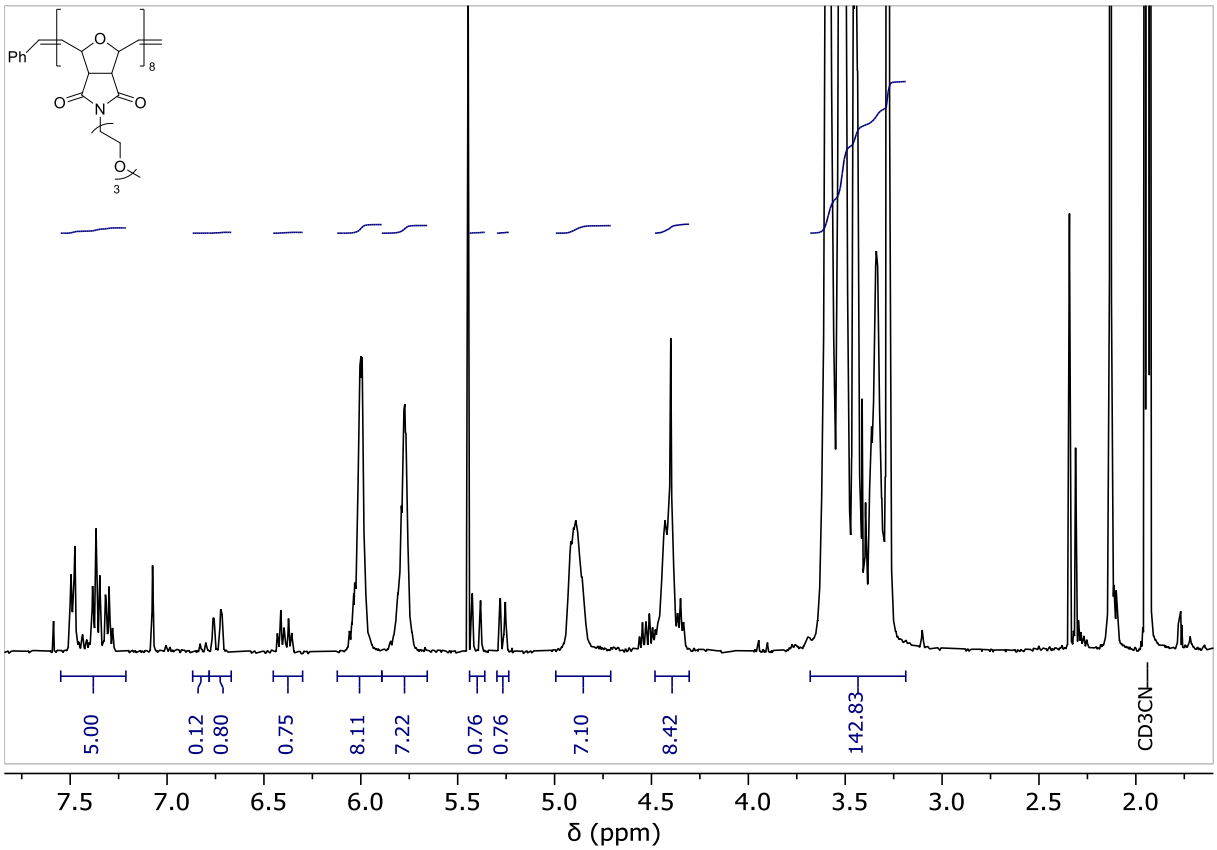

Fig.S 65: ^{1}H NMR of the Homopolymer P(ONB-TEG)-8.

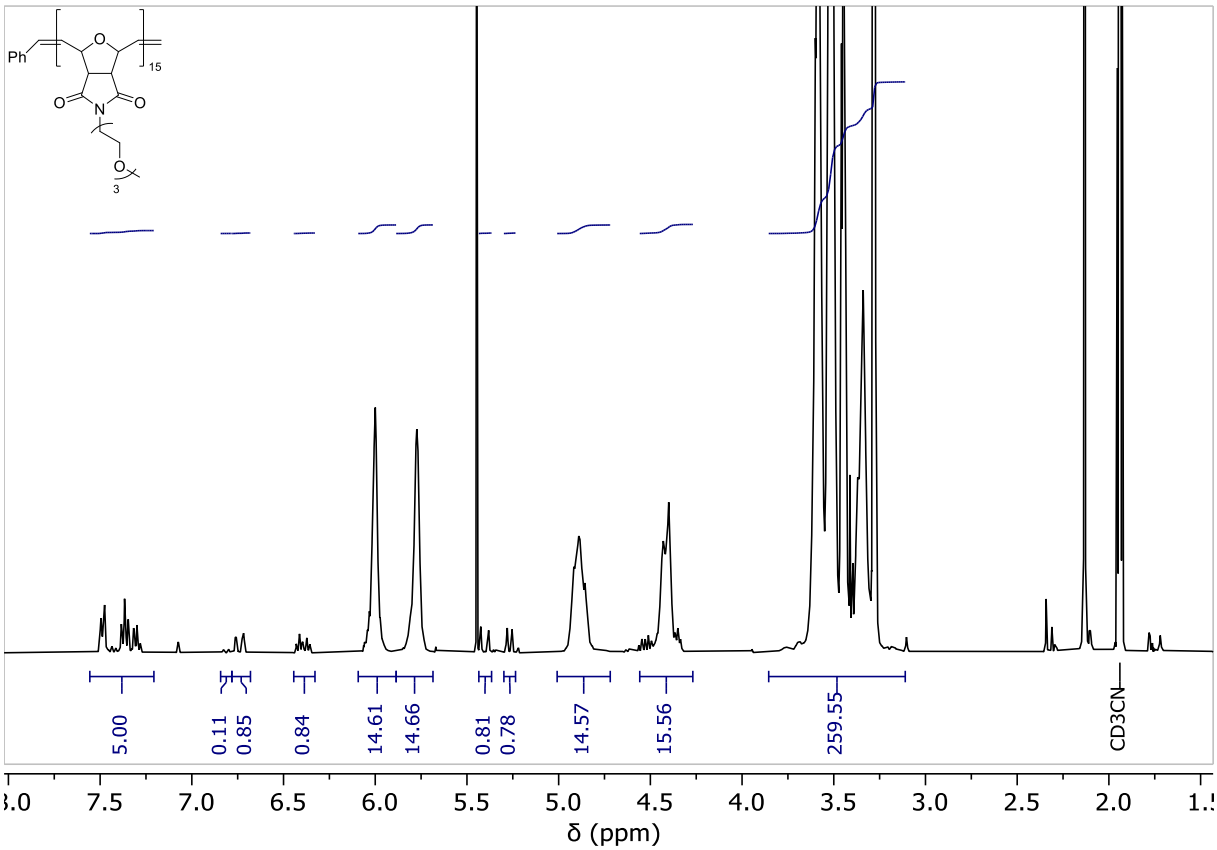

Fig.S 66: ^{1}H NMR of the Homopolymer P(ONB-TEG)-15.

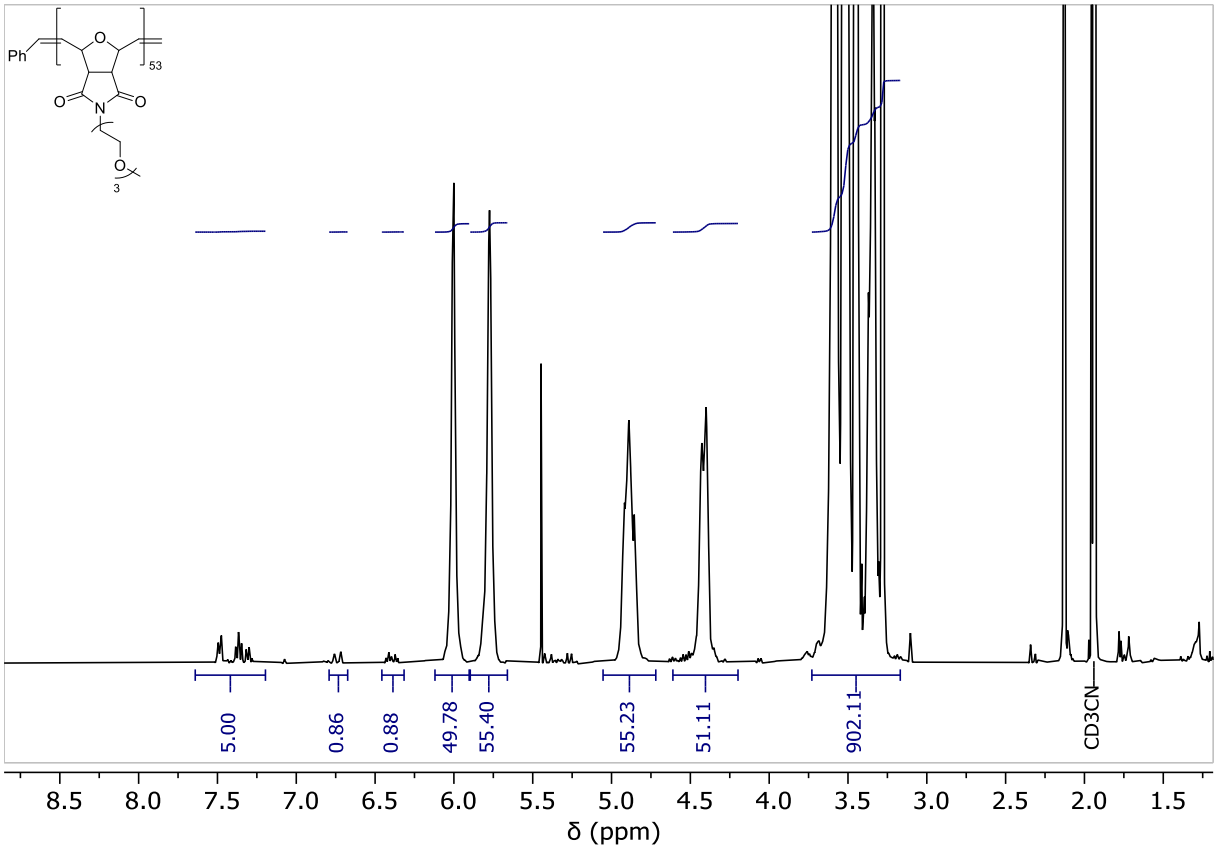

Fig.S 67: ^{1}H NMR of the Homopolymer P(ONB-TEG)-53.

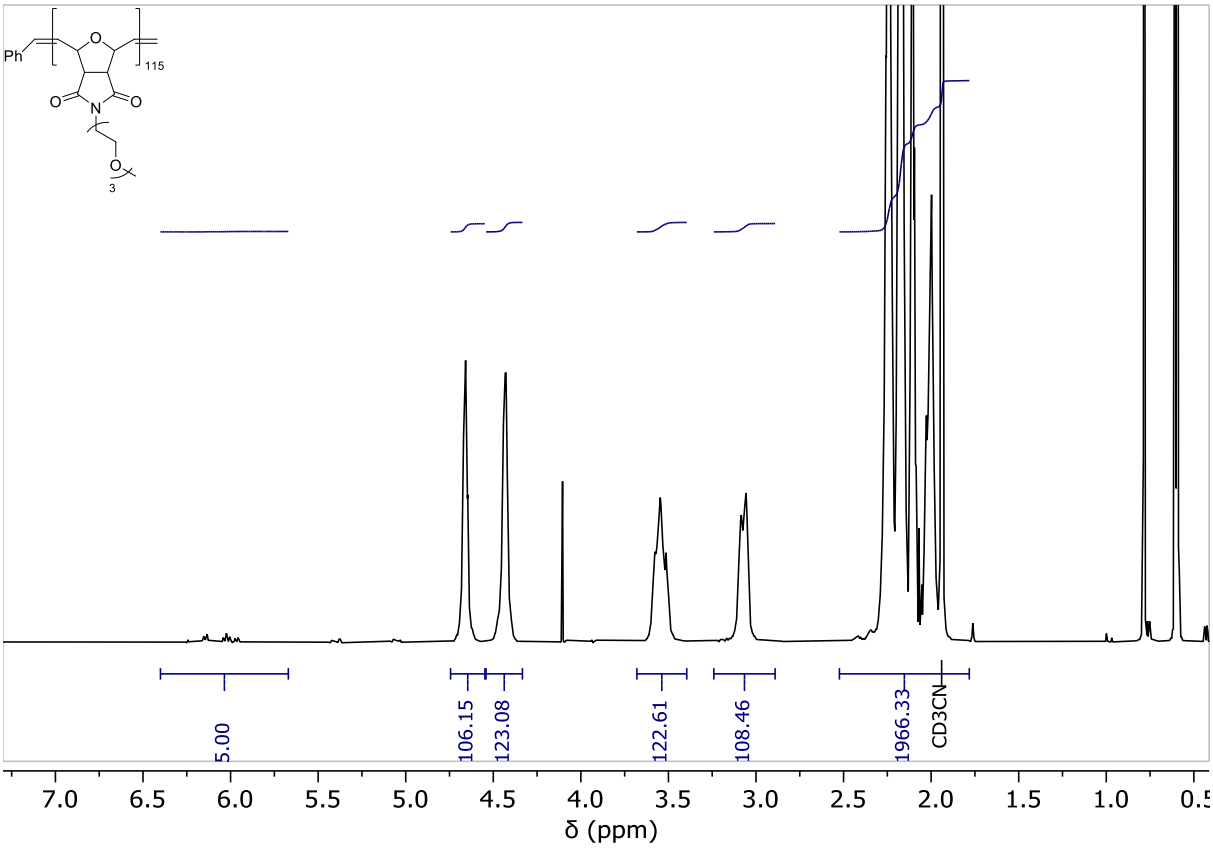

Fig.S 68: ^{1}H NMR of the Homopolymer P(ONB-TEG)-115.

Block Copolymers

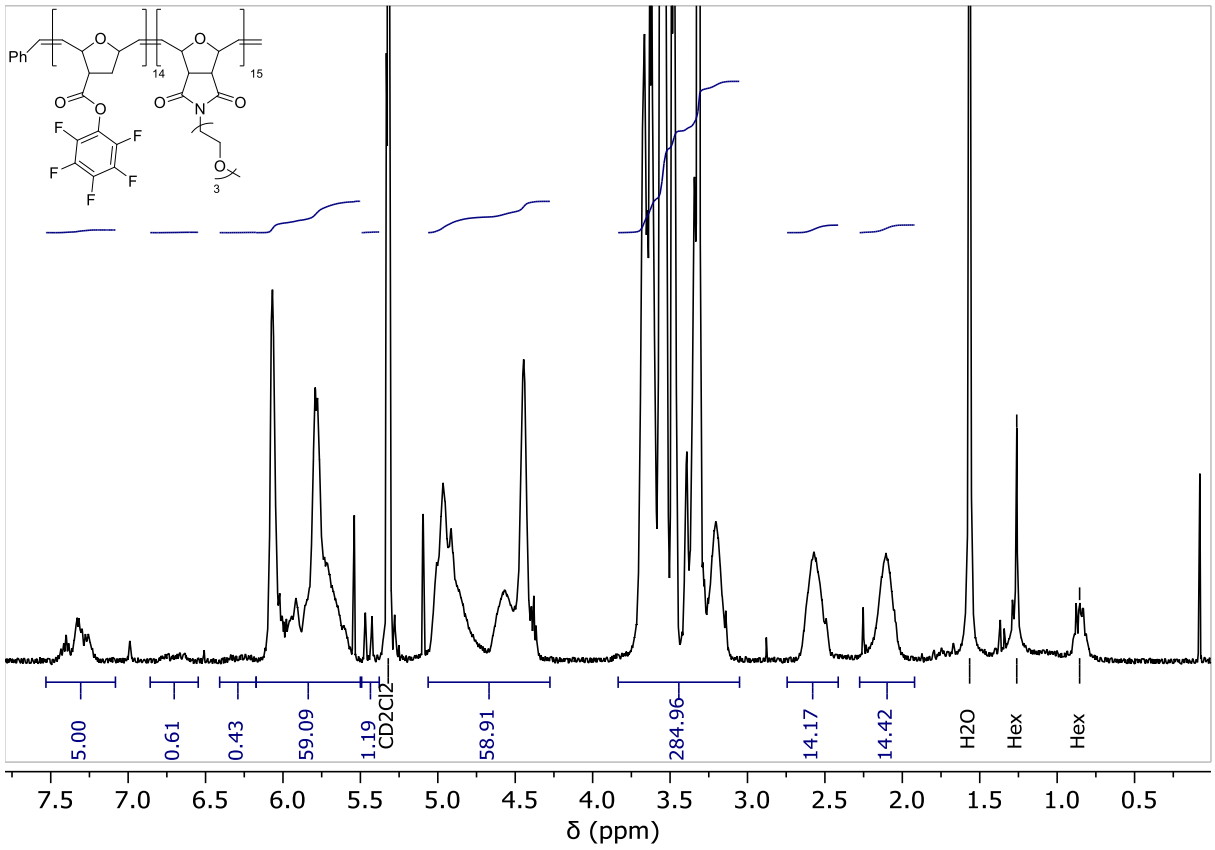

Fig.S 69: ^{1}H NMR of the block copolymer BP-1.

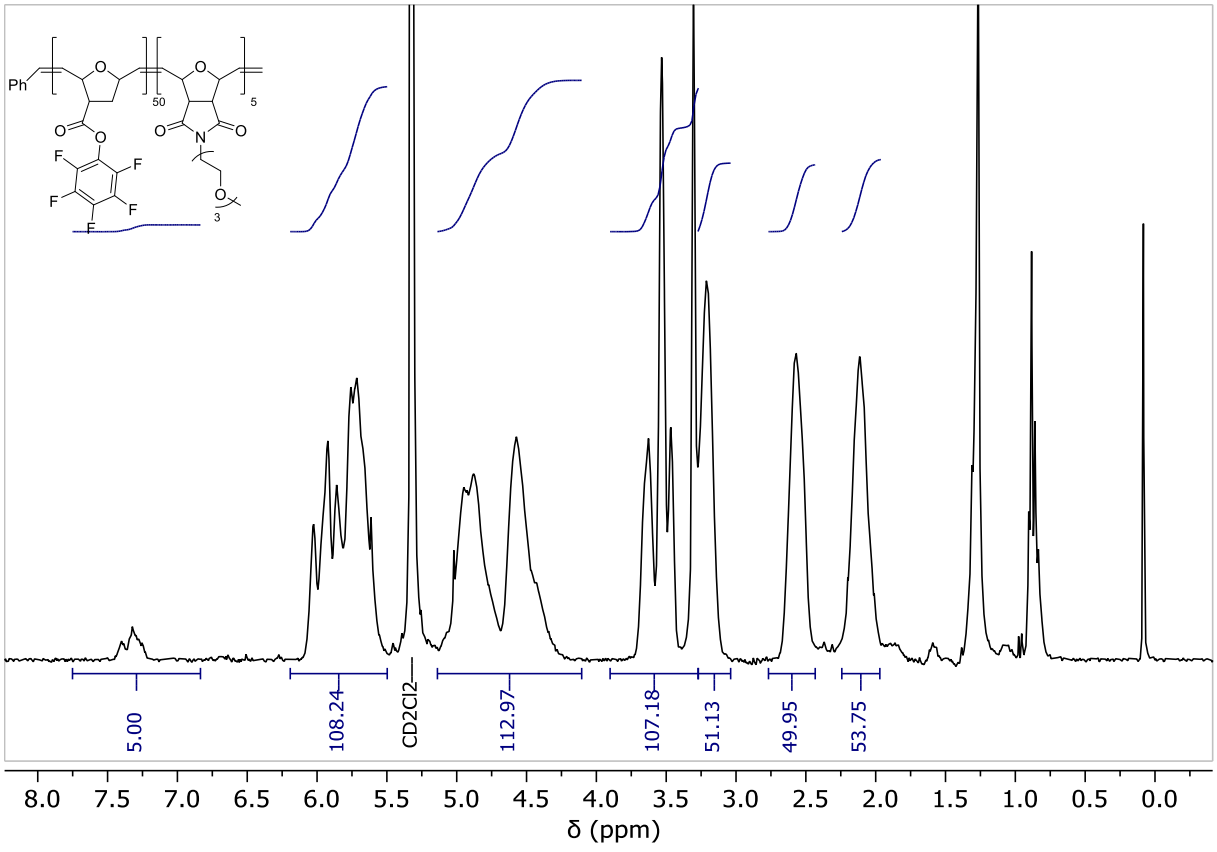

Fig.S 70: ^{1}H NMR of the block copolymer BP-2.

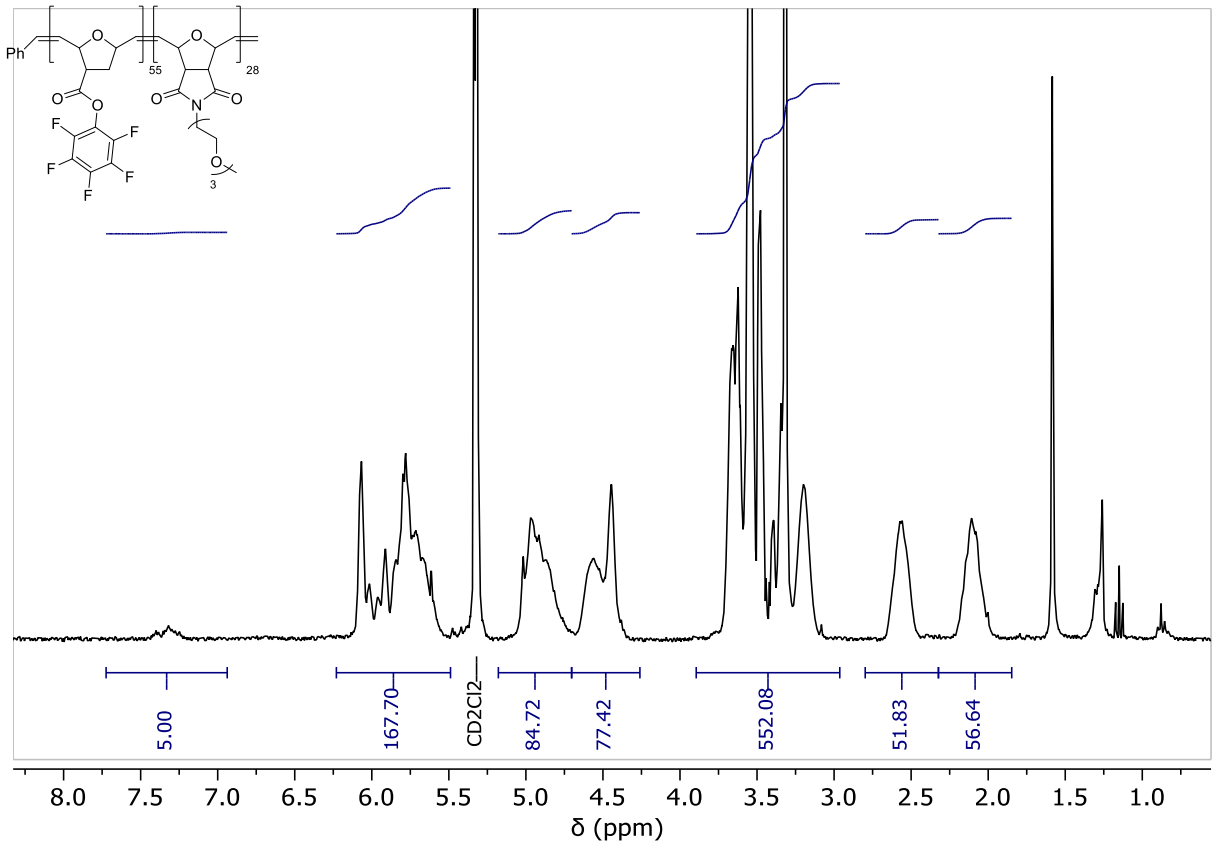

Fig.S 71: ^{1}H NMR of the block copolymer BP-3.

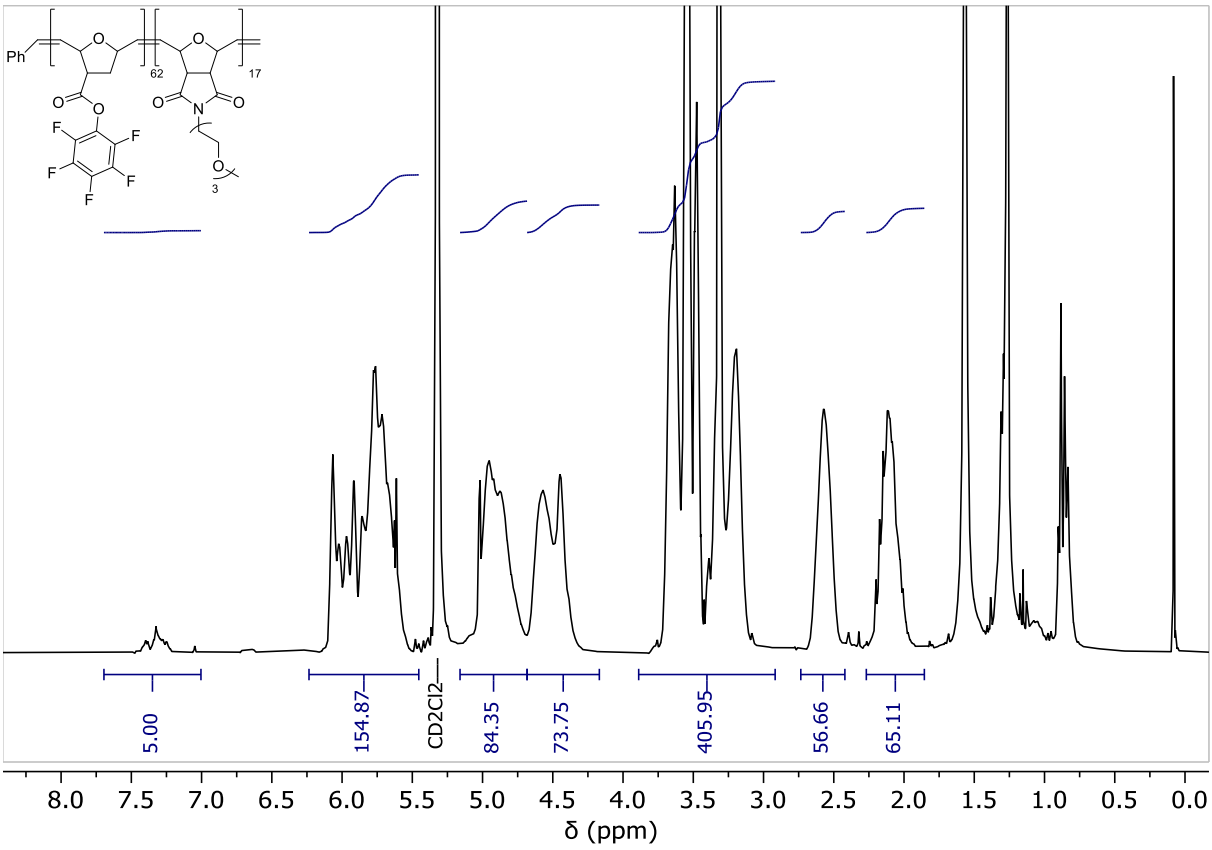

Fig.S 72: ^{1}H NMR of the block copolymer BP-4.

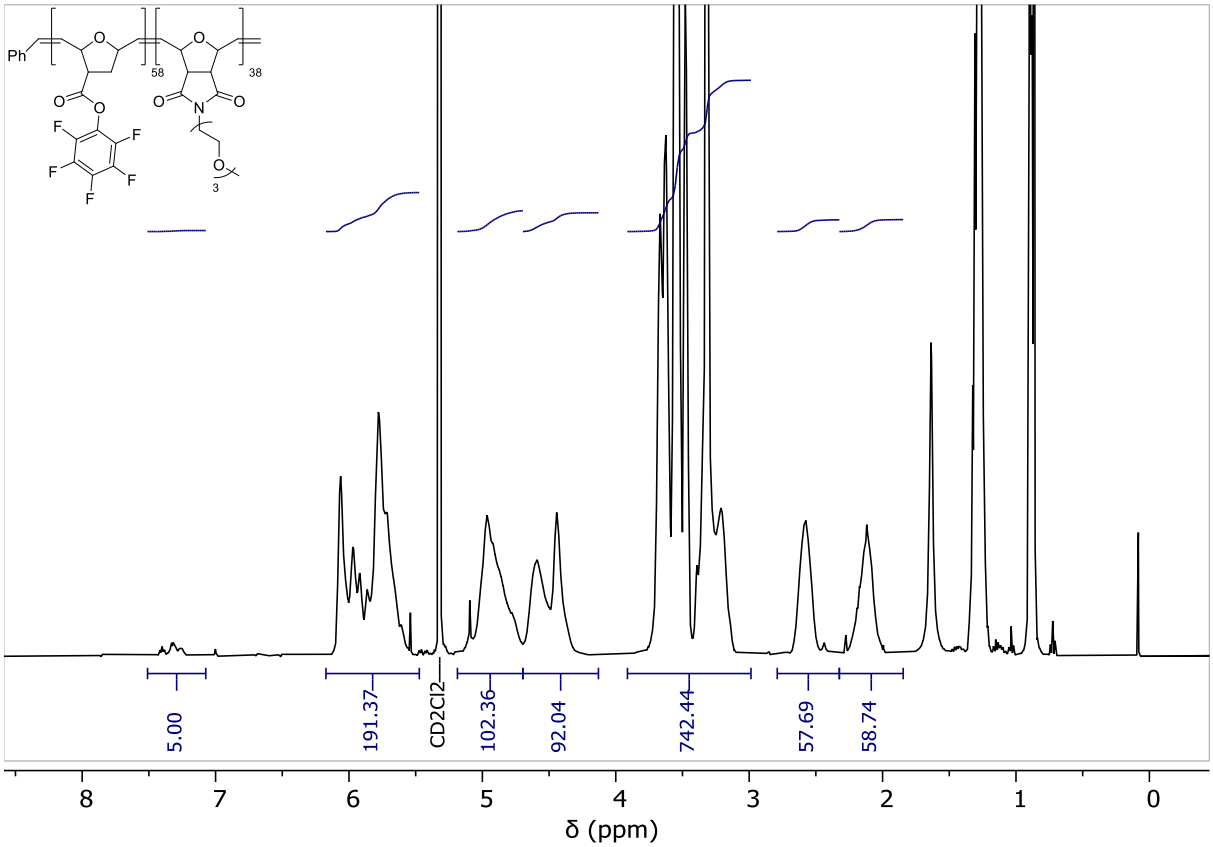

Fig.S 73: ^{1}H NMR of the block copolymer BP-5.

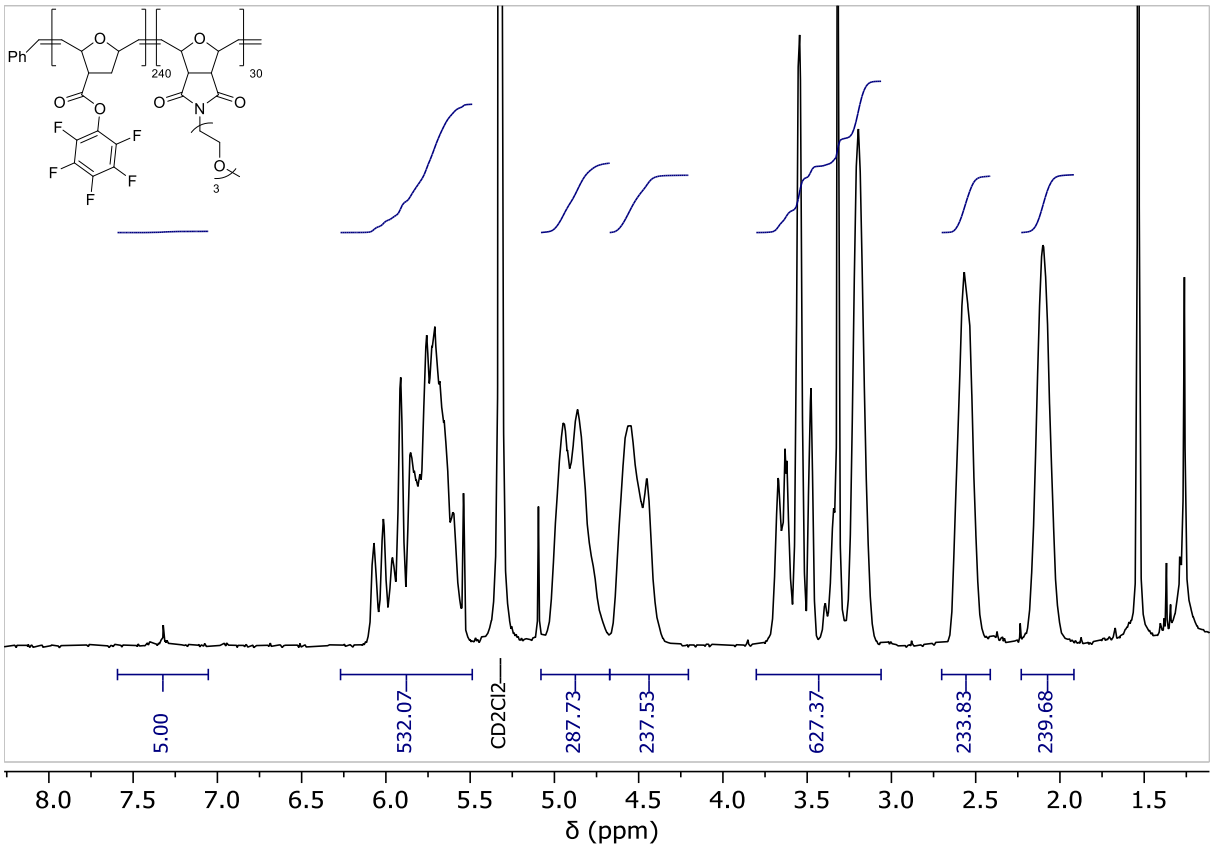

Fig.S 74: ^{1}H NMR of the block copolymer BP-6.